

AD-A089 375

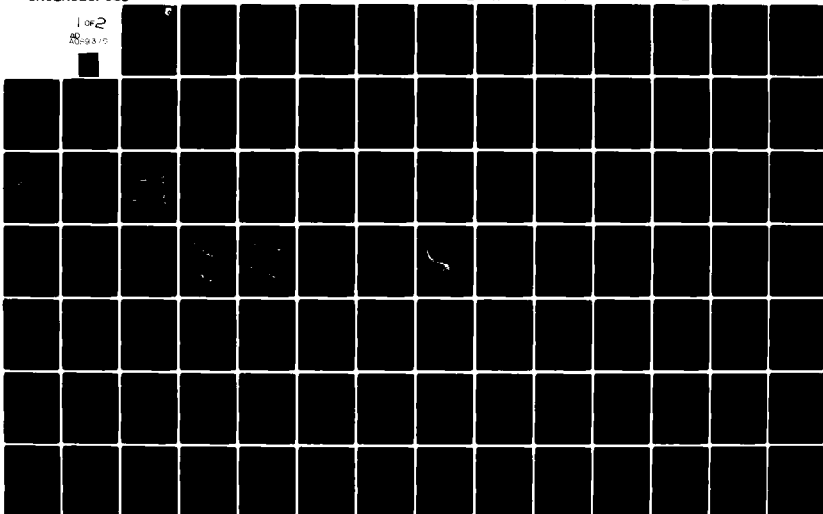
FLORIDA UNIV GAINESVILLE DEPT OF CHEMISTRY F/G 21/2
TEMPORAL AND SPATIAL TEMPERATURE MEASUREMENTS OF COMBUSTION FLA--ETC(U)
MAY 80 J O WINEFORDNER F33615-78-C-2038

UNCLASSIFIED

AFWAL-TR-80-2045

NL

1 of 2
AD-A089 375

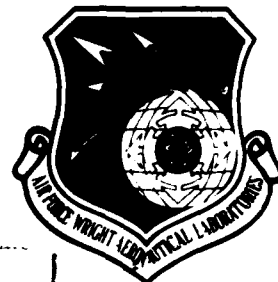


18

AFWAL-TR-80-2045

19

2



6

TEMPORAL AND SPATIAL TEMPERATURE MEASUREMENTS OF COMBUSTION FLAMES.

AD A089375

10

JAMES D. WINEFORDNER

Department of Chemistry
University of Florida
Gainesville FL 32611

11 May 1980

12 165

Technical Report AFWAL-TR-80-2045

9

Final Report, 1 Jun 1979 to 29 Feb 1980

15

F32015-78-C-1/38

16

2301

17

S1

DDC FILE COPY

Approved for public release; distribution unlimited

AERO PROPULSION LABORATORY
AIR FORCE WRIGHT AERONAUTICAL LABORATORIES
AIR FORCE SYSTEMS COMMAND
WRIGHT-PATTERSON AIR FORCE BASE, OHIO 45433

80 9 23 018

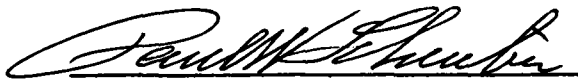
400478

NOTICE

When Government drawings, specifications, or other data are used for any purpose other than in connection with a definitely related Government procurement operation, the United States Government thereby incurs no responsibility nor any obligation whatsoever; and the fact that the government may have formulated, furnished, or in any way supplied the said drawings, specifications, or other data, is not to be regarded by implication or otherwise as in any manner licensing the holder or any other person or corporation, or conveying any rights or permission to manufacture use, or sell any patented invention that may in any way be related thereto.

This report has been reviewed by the Office of Public Affairs (ASD/PA) and is releasable to the National Technical Information Service (NTIS). At NTIS, it will be available to the general public, including foreign nations.

This technical report has been reviewed and is approved for publication.

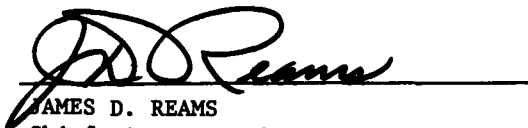


PAUL W. SCHREIBER
Project Engineer



ROBERT R. BARTHELEMY
Chief, Energy Conversion Branch
Aerospace Power Division

FOR THE COMMANDER



JAMES D. REAMS
Chief, Aerospace Power Division
Aero Propulsion Laboratory

"If your address has changed, if you wish to be removed from our mailing list, or if the addressee is no longer employed by your organization please notify AFWAL/POOC-3 W-PAFB, OH 45433 to help us maintain a current mailing list".

Copies of this report should not be returned unless return is required by security considerations, contractual obligations, or notice on a specific document.

SECURITY CLASSIFICATION OF THIS PAGE (When Data Entered)

REPORT DOCUMENTATION PAGE		READ INSTRUCTIONS BEFORE COMPLETING FORM
1. REPORT NUMBER AFWAL-TR-80-2045	2. GOVT ACCESSION NO. AD-A089375	3. RECIPIENT'S CATALOG NUMBER
4. TITLE (and Subtitle) TEMPORAL AND SPATIAL TEMPERATURE MEASUREMENTS OF COMBUSTION FLAMES		5. TYPE OF REPORT & PERIOD COVERED Final June 1, 1978 to February 29, 1980.
		6. PERFORMING ORG. REPORT NUMBER
7. AUTHOR(s) James D. Winefordner		8. CONTRACT OR GRANT NUMBER(s) F33615-78-C-2038
9. PERFORMING ORGANIZATION NAME AND ADDRESS University of Florida Department of Chemistry Gainesville, FL 32611		10. PROGRAM ELEMENT, PROJECT, TASK AREA & WORK UNIT NUMBERS 2301S102
11. CONTROLLING OFFICE NAME AND ADDRESS Propulsion Laboratory Air Force Wright Aeronautical Laboratories Air Force Systems Command		12. REPORT DATE February 27, 1980
14. MONITORING AGENCY NAME & ADDRESS (if different from Controlling Office) Wright Patterson Air Force Base, OH 45433		13. NUMBER OF PAGES
		15. SECURITY CLASS. (of this report) UNCLASSIFIED
		15a. DECLASSIFICATION/DOWNGRADING SCHEDULE
16. DISTRIBUTION STATEMENT (of this Report) Approved for public release; distribution unlimited.		
17. DISTRIBUTION STATEMENT (of the abstract entered in Block 20, if different from Report)		
18. SUPPLEMENTARY NOTES		
19. KEY WORDS (Continue on reverse side if necessary and identify by block number) Combustion Diagnostics Molecular Gases Spatial Flame Temperatures Real Time Flame Temperatures Saturated Fluorescence		
20. ABSTRACT (Continue on reverse side if necessary and identify by block number) Five methods have been developed theoretically from steady state rate theory and four have been verified experimentally for the measurement of spatial flame temperatures. All of the methods have potential use on a "single" pulse (time period less than 1 μ s) basis for the measurements of flame temperatures. All of the methods involve the use of one or two closely spaced (in time) dye laser pulses to excited atomic fluorescence of probe atoms.		

DD FORM 1473
1 JAN 73

SECURITY CLASSIFICATION OF THIS PAGE (When Data Entered)

(e.g., Tl, In, Ga, etc.) introduced as an aerosol into the flames. Several experimental difficulties have resulted in initial barriers to the measurement of flame temperatures in hydrocarbon flames as well as the use of an available SIT detector for height profiles of flame temperatures. Other studies have included the theoretical development and experimental implementation of absolute concentration measurements of atom probes in flames as well as a study of saturation broadening of atomic lines.

FOREWORD

This report was prepared by James D. Winefordner of the Department of Chemistry of the University of Florida, Gainesville, FL 32611 for the research under Contract AF-F33615-78-C-2038 for Propulsion Laboratory, Air Force Wright Aeronautical Laboratories, Air Force Systems Command, Wright Patterson Air Force Base, OH 45433. The report covers work performed during the period June 1, 1980 to February 29, 1980, "Temporal and Spatial Temperature Measurements of Combustion Flames" under the technical direction of Paul W. Schreiber, Energy Conversion Branch, Aerospace Power Division, Aero Propulsion Laboratory, Air Force Wright Aeronautical Laboratories, Wright Patterson Air Force Base, OH 45433.

Acknowledgements are gratefully made to Mr. Art Grant, Machine Shop, University of Florida, who built burners and optical mounts used in the completion of these experiments. The technical assistance of Paul Schreiber is especially recognized.

Credit is also given to the Environmental Protection Agency who partially funded this research work through the Intraagency Agreement IAG-780-F0236 (U.S. Environmental Protection Agency, Industrial Environmental Research Lab) and to AFOSR who also partially supported this work through a separate research contract-AF-AFOSR-F44620-78-C-0005.

Advertisement Fee	
Rate	✓
Time	8
Unit	8
Total \$	
By _____	
Date _____	
Printed Name _____	
Address _____ City _____ State _____ Zip _____	
A	Amount paid/or Special

TABLE OF CONTENTS

<u>SECTION</u>		<u>PAGE</u>
I	INTRODUCTION	1
II	THEORY OF FLAME TEMPERATURE METHODS	3
	1. Method 1. Linear Two Line Method	3
	2. Method 2. Saturation Two Line Method With Sequential Pumping	6
	3. Method 3. Saturation Two Line Method With Simultaneous Pumping	8
	4. Method 4. Saturation Two Line Method With Peak Detection	9
	5. Method 5. Laser Excitation of Probe Thermal Excitation-Emission Method	10
III	THEORY OF ABSOLUTE NUMBER DENSITY AND QUANTUM EFFICIENCY DETERMINATION	12
IV	EXPERIMENTAL SYSTEM AND TECHNIQUES	16
	1. Results on Flame Temperature Measurements	22
V	CONCLUSIONS	39
	1. Summary of Studies Completed	39
	2. Summary of Studies To Be Completed	40
VI	MISCELLANEOUS ITEMS	42
REFERENCES		44
APPENDIX A	STEADY STATE ATOMIC FLUORESCENCE RADIANCE EXPRESSIONS FOR CONTINUUM EXCITATION	45
APPENDIX A1	STEADY STATE APPROACH TO CONCENTRATION EXPRESSIONS	62
APPENDIX A2	SATURATION SPECTRAL IRRADIANCE, E_V^S	64
APPENDIX B	FIVE LASER EXCITED FLUORESCENCE METHODS TO MEASURE SPATIAL FLAME TEMPERATURES PART I. THEORETICAL BASIS	66
APPENDIX C	THERMALLY ASSISTED FLUORESCENCE. A NEW TECHNIQUE FOR LOCAL FLAME TEMPERATURE MEASUREMENT	95
APPENDIX D	A THEORETICAL AND EXPERIMENTAL APPROACH TO LASER SATURATION BROADENING IN FLAMES	127

LIST OF FIGURES

Figure		Page
1	Energy Level Diagram and First Order Rate Constants for Activation-Deactivation of a Three Level Tl-Like Atom.	4
2	Atomic Term Diagrams for B, Al, Ga, In, and Tl.	5
3	Instrumental Setup for Laser Excited Fluorescence Flame Temperature Measurement Methods	17
4	Fluorescence Excitation Spectra Obtained by Scanning Laser Wavelength for Tl for Two Excitation Lines	19
5	Fluorescence Radiance, B_F , in $W\ cm^{-2}\ sr^{-1}$, vs Laser Flux Φ_L , $W\ cm^{-2}$ for Several Flames and Several Fluorescence Transitions	30
6	Fluorescence Radiance, B_F , in $W\ cm^{-2}\ sr^{-1}$, Vs Laser Flux Φ_L , in $W\ cm^{-2}$; For Laser Excited Fluorescence, $B_{F_{3 \rightarrow 2/1 \rightarrow 3}}$ (curve a) and For Laser Excited Thermally Assisted Emission, $B_{F_{4 \rightarrow 1/1 \rightarrow 3}}$ (curve b). The Laser Excitation Bandpass is $0.24 \pm 0.02\ \text{\AA}$.	
7	Temporal Scan of Tl Fluorescence Response $B_{F_{3 \rightarrow 2/1 \rightarrow 3}}$ (curve a) and $B_{F_{3 \rightarrow 2/2 \rightarrow 3}}$ (curve b) for $H_2/O_2/Ar$ Flame (2/1/4)	34
7b	Temporal Scan of Tl Fluorescence Response $B_{F_{3 \rightarrow 2/1 \rightarrow 3}}$ (curve a) and $B_{F_{3 \rightarrow 2/2 \rightarrow 3}}$ (curve b) for $H_2/O_2/N_2$ Flame (2/1/4)	35
8	Temporal Scan of Tl Fluorescence $B_{F_{3 \rightarrow 2/1 \rightarrow 3}}$ (curve a) and Thermally Excited Emission $B_{F_{4 \rightarrow 1/1 \rightarrow 3}}$ for $H_2/O_2/N_2$ Flame (2/1/4). Maximum photomultiplier current kept constant with neutral density filters.	38
Appendices		
1A	a. Two Level Atomic System with Radiational, A, and Radiationless, k. Rate Constants.	61

Figure	LIST OF FIGURES (Con't)	Page
1A	b. Three Level Case I(e.g., Na) Atomic System with Radiational, A, and Radiationless, k, Rate Constants (k_{13} , k_{12} , $A_{32} \approx 0$)	61
	c. Three Level Case II (e.g., Tl) Atomic System With Radiational, A, and Radiationless, k, Rate Constants (k_{13} , k_{23} , $A_{21} \approx 0$).	61
1B	Energy Level Diagram of 3-Level Tl-Like Atom With Activation (Solid Lines) and Deactivation (Dashed Lines) Rate Constants Shown (see text for Definition)	91
2B	Hypothetical Fluorescence Temporal Waveform Produced With a Rectangular Excitation Pulse (t_{ex} long).	92
3B	Hypothetical Fluorescence Temporal Waveform Produced by Excitation with $2 \rightarrow 3$ to Saturate the $3 \rightarrow 1$ Fluorescence and then While $2 \rightarrow 3$ Excitation Occurs, Excitation Occurs Simultaneously at $2 \rightarrow 3$ and $1 \rightarrow 3$ to Saturate the $3 \rightarrow 1$ Fluorescence.	93
4B	Energy Level Diagram of Multi-Level Atom, e.g., Tl, with Activation (Solid Lines) and Deactivation (Dashed Lines) Rate Constants Shown (see text for definitions)	94
1C	Two-Level System, Showing Deviation from the Boltzmann Distribution	117
2C	Three-Level System Under Spectral Irradiances $E_{\nu 12}$ and Collisional Excitation of the 3rd Level	118
3C	The Population Ratio n_3/n_2 of a 3 Level System as Function of the Ratio Between Radiative and Collisional Excitation of the Level 2	119
4C	Four-Level System Under Spectral Irradiance $E_{\nu 12}$ and with Radiative and Collisional Coupling Among the Levels	120
5C	Experimental Set-Up for the Thermally Assisted Fluorescence Measurements	121
6C	Temporal Resolved Fluorescence Pulses of Tl	122
7C	Energy Scheme of In Showing the Transitions Observed	123

<u>Figure</u>	LIST OF FIGURES (Con't)	<u>Page</u>
8C	Typical Thermally Assisted Fluorescence Pulse (3257 \AA) as Recorded with our Apparatus	124
9C	Energy Scheme of Tl Showing the Transitions Observed	125
10C	Energy Scheme of Tl Showing the Transitions Observed	126
1D	Fluorescence Excitation Profiles for Indium in the $\text{Ar/O}_2/\text{H}_2$ flame	152
2D	Fluorescence Excitation Profiles for Sodium in the $\text{Ar/O}_2/\text{H}_2$ flame	153
3D	Fluorescence Excitation Profiles for Calcium in the $\text{N}_2/\text{O}_2/\text{H}_2$ flame	154
4D	Fluorescence Excitation Profiles for Strontium in the $\text{N}_2/\text{O}_2/\text{H}_2$ flame	155

LIST OF TABLES

<u>TABLE</u>		<u>PAGE</u>
I	PRELIMINARY FLAME TEMPERATURES VIA SEVERAL MEASUREMENT TECHNIQUES	23
II	EXPERIMENTAL CONDITIONS AND INFLUENCE OF SOURCE IRRADIANCE ON LINEAR TWO-LINE (METHOD 1), FLAME TEMPERATURES	24
III	EXPERIMENTAL CONDITIONS AND FLAME TEMPERATURES VIA THERMAL EXCITATION-EMISSION METHOD (METHOD 5)	26
IV	INFLUENCE OF LASER IRRADIANCE UPON THERMAL EXCITATION EMISSION (METHOD 5) FLAME TEMPERATURES	28
V	FLAME TEMPERATURES MEASURED BY SIMULTANEOUS SATURATION METHOD (METHOD 2) BY TWO APPROACHES	36

SECTION I

INTRODUCTION

This report describes the results of theoretical and experimental investigations of flame temperature methods based upon laser excited fluorescence measurements of inorganic probes introduced into the flame gases; these studies were conducted under USAF Contract F33615-78-C-2038.

The objective of this contract was to investigate the use of laser excited fluorescence for spatial/temporal temperature measurements. Development of such new combustion-diagnostic techniques is important to the Air Force in connection with the development and refinement of cleaner and more efficient jet engines.

Atomic fluorescence excited with a spectrally quasi-continuum source has been shown to be a reliable method of measuring flame temperatures.¹⁻⁷ In fact, it combines the advantages of optical methods, i.e., of not disturbing the combustion process, with the capability of providing spatially-resolved measurements, the last feature being common to all "scattering based methods", such as for example, the Raman method.⁸

The use of the laser as an excitation source for atomic fluorescence has the obvious advantage that spatial resolution can be significantly improved because of the low divergence of the beam coupled with its high spectral irradiance. The use of a pulsed laser/gated detector system also has the advantage of temporal resolution.

Moreover, as shown by Measures¹⁰ and Omenetto and Winefordner¹¹ if the laser irradiance is such that saturation of the excitation transition(s) can be achieved, then the temperature of the atomic system can be evaluated without the necessity of calibration of the electro-optical detection system and without measuring the laser power. However, as discussed below, other constraints are imposed on the method. The aim of this report is to give for the first time several means (5 different approaches) of calculating the temperatures of several H₂-based laboratory flames by laser excitation of a 3-level atomic probe, such as, In, Tl, Pb, etc., aspirated at a low concentration into the flame and excited simultaneously or sequentially with one or two laser beams.

SECTION II

THEORY OF FLAME TEMPERATURE METHODS

The theoretical steady state expressions have been derived by the use of the radiance expressions derived by Boutilier, et al¹². In Appendix A, (the Boutilier, et al paper¹²), more details are given. To facilitate the discussion, it will be assumed that the atomic probe introduced into the flame gases has 3 significant levels, where level 1 is the ground state, level 2 is the closely-spaced metastable state, and level 3 is the excited state. In Figure 1, this representation is given along with the significant rate constants; k's are radiationless pseudo first order rate constants; A's are radiational rate constants; B's are Einstein induced absorption or induced emission coefficients; E_ν 's are source spectral irradiances; and c is the speed of light. A further discussion of these terms is given in Appendix A. In Figure 2, the specific energy level diagrams of Ga, In, and Tl are given. In the following textual passages, the 5 basic methods for flame temperature measurements based upon laser excited fluorescence will be described (also see Appendix B).

Method 1. Linear Two Line Method (based on method in Omenetto, et al²).

In this case, the ratio of fluorescence radiance signals resulting when exciting 1→3 and measuring the fluorescence of 3→2, $B_{F \frac{3 \rightarrow 2}{1 \rightarrow 3}}$ and resulting when exciting 2→3 and measuring the fluorescence of 3→1, $B_{F \frac{3 \rightarrow 1}{2 \rightarrow 3}}$. The resulting temperature expression is

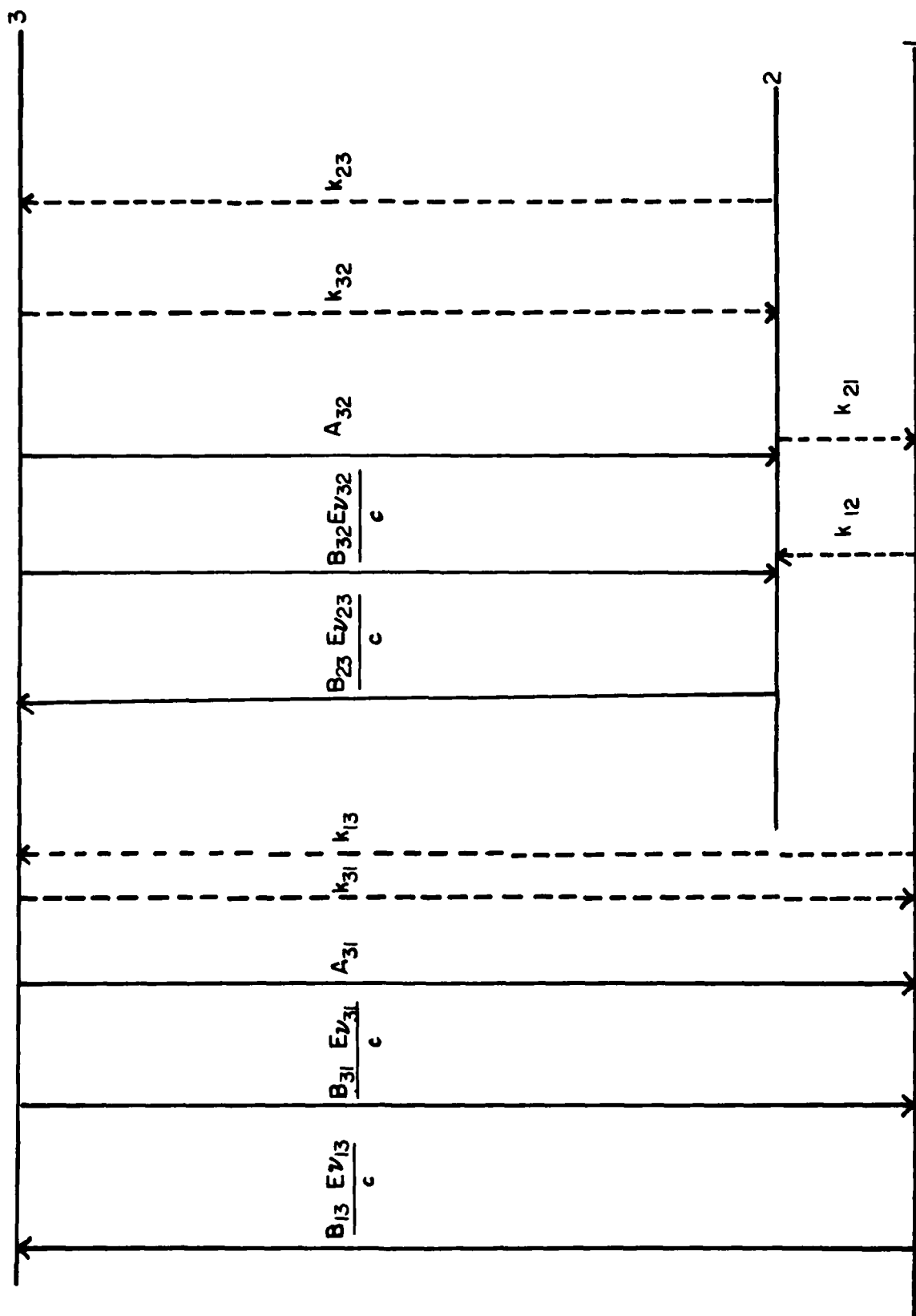


Figure 1. Energy Level Diagram and First Order Rate Constants for Activation-Deactivation of a Three Level Tl-Like Atom.

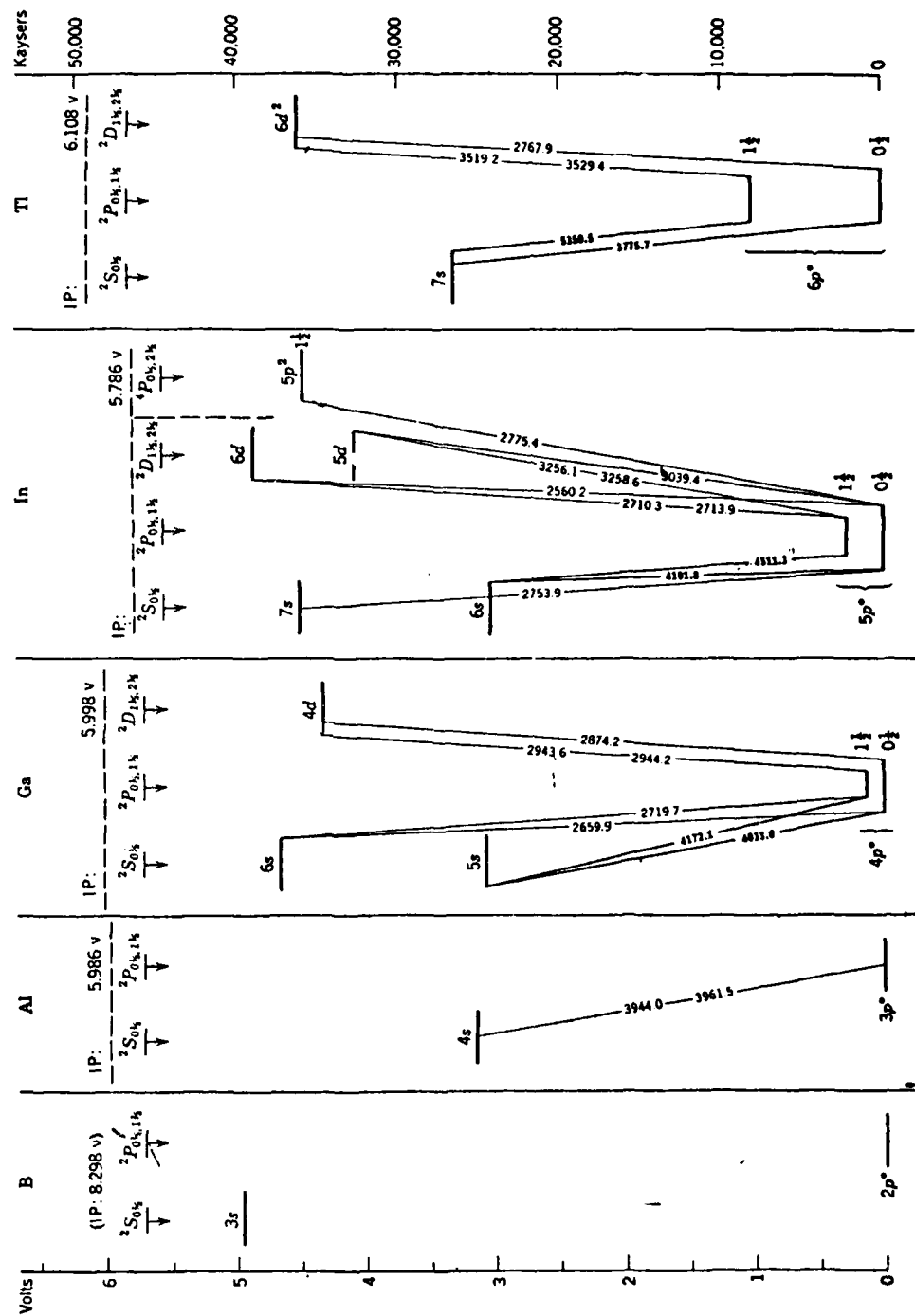


Figure 2. Atomic term diagrams for B, Al, Ga, In, and Tl.

$$T = \frac{E_{12}/k}{\ln \frac{E_{\nu 23}}{E_{\nu 13}} + 4 \ln \frac{\lambda_{23}}{\lambda_{13}} + \ln \frac{B_F^{3 \rightarrow 2}}{B_F^{3 \rightarrow 1}} \frac{1 \rightarrow 3}{2 \rightarrow 3}} \quad (1)$$

where E_{ν} is the excitation spectral irradiance at the designated transition (in $J s^{-1} m^{-2} Hz^{-1}$), λ is the wavelength (in nm) at the designated excitation lines, and E_{12} is the energy of the metastable, 2, level (in eV). This method of flame temperature measurement is independent of quenching processes but requires calibration of the spectrometric system to enable measurement of (relative) values of E_{ν} and B_F at the appropriate wavelengths. In addition to this approach, several other disadvantages are present: (a) changes in the quantum efficiency due to quenchers in the flames leads to a change in B_F values and this can deteriorate the S/N ratio; (b) the source spectral irradiance must remain on the linear part of the B_F vs E_{ν} curve; (c) at low E_{ν} values and/or in highly quenching flames, B_F will also be low causing S/N problems; (d) the post filter effect leads to deterioration of the fluorescence signal especially for the 3 \rightarrow 1 transition. Because of these serious difficulties and our aim to develop methods useful for combustors, we spent most of the contractual period involved in the development of methods with fewer difficulties and greater chances of success. Experimental results for flame temperatures via this method will be given.

Method 2. Saturation Two Line Method With Sequential Pumping

In this case, atomic fluorescence of an atomic probe is produced at 3 \rightarrow 1 or at 3 \rightarrow 2 after excitation at 1 \rightarrow 3 and at 2 \rightarrow 3, respectively. The

general expression for the flame temperature, T, is

$$T = \frac{E_{12}/k}{\ln \left\{ \left(2 + \frac{A_{32} + k_{32}}{k_{21}} \right) \left(\frac{\nu_{3j} A_{3j}}{\nu_{3i} A_{3i}} \right) \left(\frac{B_{F_{3 \rightarrow i}}}{B_{F_{3 \rightarrow j}}} \right) - \left(\frac{g_3 + g_2}{g_3} \right) \left(\frac{1}{\frac{g_1}{g_3} + \frac{g_1}{g_2} \left(\frac{A_{31} + k_{31}}{k_{21}} \right)} \right) \right\}}$$

(2)

assuming $e^{-E_{12}/kT} \ll 1$, and letting i and j be either levels 1 or 2.

The terms are defined as follows: B_F is the same as before; k's are pseudo first order rate constants; A's are Einstein coefficients of spontaneous emission (first order radiational rate constants), ν 's are frequencies of transitions, and g's are statistical weights (degeneracies). If $k_{21} \gg (A_{31} + k_{31}) \approx (A_{32} + k_{32})$ and substituting for the statistical weights, then

$$T \approx \frac{E_{12}/k}{\ln \left\{ 2 \left(\frac{\nu_{3j} A_{3j}}{\nu_{3i} A_{3i}} \right) \left(\frac{B_{F_{3 \rightarrow i}}}{B_{F_{3 \rightarrow j}}} \right) - 3 \right\}}$$

(3)

Finally, if $n_2 \ll 30 n_1$ (n_2 = population density of state 2 and n_T = total population density of all levels), then

$$T = \frac{E_{12}/k}{\ln \left\{ 2 \left(\frac{\nu_{3j} A_{3j}}{\nu_{3i} A_{3i}} \right) \left(\frac{B_{F_{3 \rightarrow i}}}{B_{F_{3 \rightarrow j}}} \right) \right\}}$$

(4)

The advantages of this approach are: (a) the signal strengths and S/N ratios for each transition are high; (b) the signals strengths are independent of source irradiance at either excitation line. The dis-

advantages of this approach are: (a) scatter of excitation radiation is potentially severe but by measuring non-resonance fluorescence this difficulty can be minimized; (b) the post filter effect can be severe but it can be minimized by measuring same fluorescence wavelength; however, in the latter case, scatter can become a problem; (c) the laser beams must have the same cross-sectional area; (d) the spectrometer system must be calibrated at $3 \rightarrow i$ and $3 \rightarrow j$. Experimental results for flame temperatures will be given via this method.

Method 3. Saturation Two Line Method With Simultaneous Pumping

In this method, both excitation transitions are pumped simultaneously in one case and in another case only one excitation transition ($1 \rightarrow 3$ or $2 \rightarrow 3$) is used. In this case, the ratios of fluorescence radiances is given by

$$\frac{B_{F_{3 \rightarrow 1}}^{<1 \rightarrow 3>}}{B_{F_{3 \rightarrow 1}}^{2 \rightarrow 3}} = \frac{\frac{g_3 + g_2}{g_3} + \frac{g_1}{g_3} e^{E_{12}/kT} + \frac{A_{31} + k_{31}}{k_{12}}}{\frac{g_1 + g_2 + g_3}{g_3}} \quad (5)$$

where all terms have been defined above. Since $k_{12} = k_{21} \frac{g_2}{g_1} e^{-E_{12}/kT}$

and substituting for the g 's ($g_1 = g_3 = 1$; $g_2 = 2$) and solving for T gives for the case of simultaneous pumping in one case and excitation at $2 \rightarrow 3$ in the other case

$$T = \frac{E_{12}/k}{\ln \left\{ 4 \left(\frac{B_{F_{3 \rightarrow 1}}^{<1 \rightarrow 3>}}{B_{F_{3 \rightarrow 1}}^{2 \rightarrow 3}} - \frac{3}{4} \frac{1}{1 + \frac{1}{2} \left(\frac{A_{31} + k_{31}}{k_{21}} \right)} \right) \right\}} \quad (6)$$

8

Finally, if $k_{21} \gg (A_{31} + k_{31})$ then,

$$T = \frac{E_{12}/k}{\ln \left\{ 4 \frac{B_{F_{3 \rightarrow 1}}^{1 \rightarrow 3}}{B_{F_{3 \rightarrow 1}}^{2 \rightarrow 3}} - 3 \right\}} \approx \frac{E_{12}/k}{\ln \left\{ 4 \frac{B_{F_{2 \rightarrow 3}}^{1 \rightarrow 3}}{B_{F_{3 \rightarrow 1}}^{2 \rightarrow 3}} \right\}}, \quad (7)$$

if $n_2 \gg 30 n_1$

The same advantages as in Method 2 applies here except Method 3 is also fairly insensitive to both scatter (weak for non-resonance line) and post filter effects (fluorescence is at same wavelengths) and there is no need for spectrometer calibration. In addition, by simultaneous excitation, n_T can be evaluated as well as the ratio $(A_{31} + k_{31})/k_{21}$. The major disadvantage of this method is the need for 2 laser beams optically aligned and matched with respect to cross-sectional area (just as for Method 2), and of course the assumptions made above must be valid. Experimental flame temperature measurements by this method will be given in this report.

Method 4. Saturation Two Line Method With Peak Detection

In this method developed by Omenetto and Winefordner,^{2,3} it is necessary to excite fluorescence $3 \rightarrow 1$ at $1 \rightarrow 3$ and a short time later or earlier $3 \rightarrow 1$ at $2 \rightarrow 3$. In this case, the atomic system acts as a 2-level atom since excitation and measurement of fluorescence is done at the peak of the excitation profile prior to relaxation of the system to a 3-level steady process. The temperature, T , in this case is given by the simplistic expression

$$T = \frac{E_{12}/k}{\ln \left\{ \frac{4}{3} \frac{B_{F_{3 \rightarrow 1}}}{B_{F_{3 \rightarrow 1} \atop 2 \rightarrow 3}} \right\}} \quad (8)$$

The advantages of this method are: (a) the k's and A's are not needed; (b) the temperature obtained is independent of source intensity since saturation must occur. The disadvantages of this method are: (a) the spectrometer system must be calibrated; (b) the laser beams must be optically-aligned and spatially matched; (c) fast electronic detection and impulse rise time of the laser pulses must be achieved to allow application of 2-level steady state saturation theory; and (d) of course saturation has to be achieved. This method is the best since it is independent of the approximations needed in the previous methods, except that saturation is necessary and the "2-level peak" must be measured.

Method 5. Laser Excitation of Probe-Thermal Excitation-Emission Method (also see Appendix C).

In this novel method, a pulsed laser is used to excite an upper level (say 3) of a probe, such as Tl, and then the ratio of a thermally excited line to a fluorescence line or of two thermally excited lines are measured. In the first case, Method 5a, the ratio of the fluorescence at 3→1 following excitation at 2→3 to the thermally excited emission at i→1 (where i = 4,5,...) is taken, and so

$$T = \frac{E_{i3}/k}{\ln \left\{ \left(\frac{g_i A_{i1} \nu_{i1}}{g_3 A_{31} \nu_{31}} \right) \left(\frac{B_{F_{3 \rightarrow 1}}}{B_{F_{i \rightarrow 1}}} \right) \right\}} \quad (9)$$

In the second case, Method 5b, the ratio of 2 thermally excited lines $j \rightarrow 1$ and $i \rightarrow 1$ (j and $i > 3$), and so

$$T = \frac{(E_{i3} - E_{j3})/k}{\ln \left\{ \left(\frac{g_i A_{i1} \nu_{i1}}{g_j A_{j1} \nu_{j1}} \right) \left(\frac{B_{F_{j \rightarrow 1}}}{B_{F_{i \rightarrow 1}}} \right) \right\}} \quad (10)$$

In these cases, the advantages are: (a) only one laser wavelength is needed; (b) saturation is not necessary; (c) there is obviously no need to match laser beams in orientation and in cross section area; (d) the post filter effect is minimized; no scatter interference; and (e) since only one laser excitation wavelength is needed, temporal temperatures, i.e., with only one pulse (~ 2 ns - 1 μ s, depending on the types of pulsed dye laser) are easy to obtain assuming the S/N ratios for the fluorescence and emission lines are sufficient. The major disadvantage is the need to calibrate the spectrometric system. The S/N ratio of the emission lines will be of the same order as the fluorescence, $3 \rightarrow 1$, due to $2 \rightarrow 3$ excitation. Results for flame temperatures by this method will also be given. The general experimental system used for flame temperature measurements is given in Figure 2, and is basically the same as described in the original research proposal.

SECTION III

THEORY OF ABSOLUTE NUMBER DENSITY AND QUANTUM EFFICIENCY DETERMINATION

Just as for the absolute temperature measurements, the measurement of concentrations (in species m^{-3}) requires the application of 2-level (peak) or 3-level steady state theory (see Omenetto and Winefordner^{2,3} and just as for methods, 2,3, and 4 for temperature measurement requires the use of high intensity pulsed dye lasers for saturation.

For a 2-level atom, the fluorescence radiance B_F is related [1] to the continuum source spectral irradiance, E_v , by

$$B_F = \left(\frac{\ell}{4\pi}\right) h_{12} A_{21} n_T \left\{ \frac{1}{1 + \frac{g_1}{g_2} \left(1 + \frac{E_v}{E_v^*}\right)} \right\} \quad (11)$$

where all terms have been previously defined except for: h = Planck's constant; ℓ = fluorescence path length, and E_v^* is the modified saturation spectral irradiance (in $\text{J s}^{-1} \text{m}^{-2} \text{Hz}^{-1}$) which is given by

$$E_v^* = \frac{c A_{21}}{B_{21} Y_{21}} = \frac{8\pi h \nu_{21}^3}{c^2 Y_{21}} \quad (12)$$

where B_{21} is the Einstein coefficient of induced emission (transitions $\text{s}^{-1} (\text{J m}^{-3} \text{Hz}^{-1})^{-1}$) and Y_{21} is the quantum efficiency for the fluorescence transition $2 \rightarrow 1$. The saturation spectral irradiance, E_v^S (i.e., the source spectral irradiance where the fluorescence radiance - 50% of the maximum possible fluorescence under saturation conditions) is related to E_v^*

$$E_{\nu}^S = \left(\frac{g_2}{g_1 + g_2} \right) E_{\nu}^* \quad (13)$$

By plotting B_F vs E_{ν} (measuring absolute values of B_F and E_{ν}), E_{ν}^S can be determined and thus Y_{21} can be obtained. Since Y_{21} is related to radiationless rate constants as k_{21} , such parameters can be determined if A_{21} is known, i.e.,

$$Y_{21} = \frac{A_{21}}{k_{21} + A_{21}} \quad (14)$$

Also since k 's are related to quenching cross-sections, one can obtain quenching cross-sections as long as the composition and temperature of the flame is known. If either plots B_F vs E_{ν} or $1/B_F$ vs $1/E_{\nu}$, it is possible to extrapolate to $E_{\nu} \rightarrow \infty$ (or $1/E_{\nu} \rightarrow 0$) and obtain the value of $B_{F_{\max}}$ which is given by

$$B_{F_{\max}} = \left(\frac{\ell}{4\pi} \right) h\nu_{12} A_{21} n_T \left(\frac{g_2}{g_1 + g_2} \right) \quad (15)$$

from which n_T can be determined as long as the g 's, ν_{12} , and A_{21} are known and ℓ and $B_{F_{\max}}$ can be absolutely measured. Such measurements have been used to estimate n_T and Y values of several atomic probes, including Sr, Ca, Na, In, etc. However, the values obtained have systematic errors of as much as a factor of 2 to 3 when compared with independent measurements of n_T and Y for the same flames. In recent weeks, we've shown that the plots of B_F vs E_{ν} (or $1/B_F$ vs $1/E_{\nu}$) give erroneous results for the near plateau and early plateau of B_F and E_{ν} . These conclusions became evident by systematic errors obtained for temperatures obtained via the use of saturation values B_F (Methods 2 and 3) obtained by plotting B_F vs E_{ν} and extrapolating to the saturation

plateau. The reason(s) for the systematic error is (are) not known to us but are certainly related to the complex effects of spectral/spatial/temporal aspects of pulsed dye lasers.

No attempt will be made here to give the corresponding expressions for 3 (or more) level atoms (one can refer to Omenetto and Winefordner² for a discussion of such cases). However, it is apparent that in these cases, the expressions relating B_F to n_T and Y_{21} also involve k 's and thus either the k 's must be known or else limiting cases (such as when levels 1 and 2 are very close together) must be applied where the effect of the k 's is minimal. In addition, the same systematic errors concerning the plateau values occur here also.

Fortunately, the simplest means of obtaining spatial/temporal n_T values for 3-level atoms is to do it via "single" pulse saturation. For examples, if the same conditions applying as for Method 4 for flame temperatures, then n_T can be evaluated from an absolute B_F measurement and using the 2-level B_F expression on the preceding page. An innovative means of measuring n_T for a 3-level atom under steady state conditions is to saturate level 3 via 1+3 and 2+3 simultaneously, and using the expression below (see Appendices A and B).

$$B_{F_{3 \rightarrow 1}} = \left(\frac{\hbar}{4\pi} \right) A_{31} h\nu_{31} n_T \left(\frac{g_3}{g_1 + g_2 + g_3} \right) \quad (16)$$

$\langle \begin{smallmatrix} 1 \rightarrow 3 \\ 2 \rightarrow 3 \end{smallmatrix} \rangle$

One can imagine this case as effectively as the 2-level case where levels 1 and 2 coalesce into one level of statistical weight, $g_1 + g_2$. Thus here, the same reasoning as for the 2-level case applied and the same

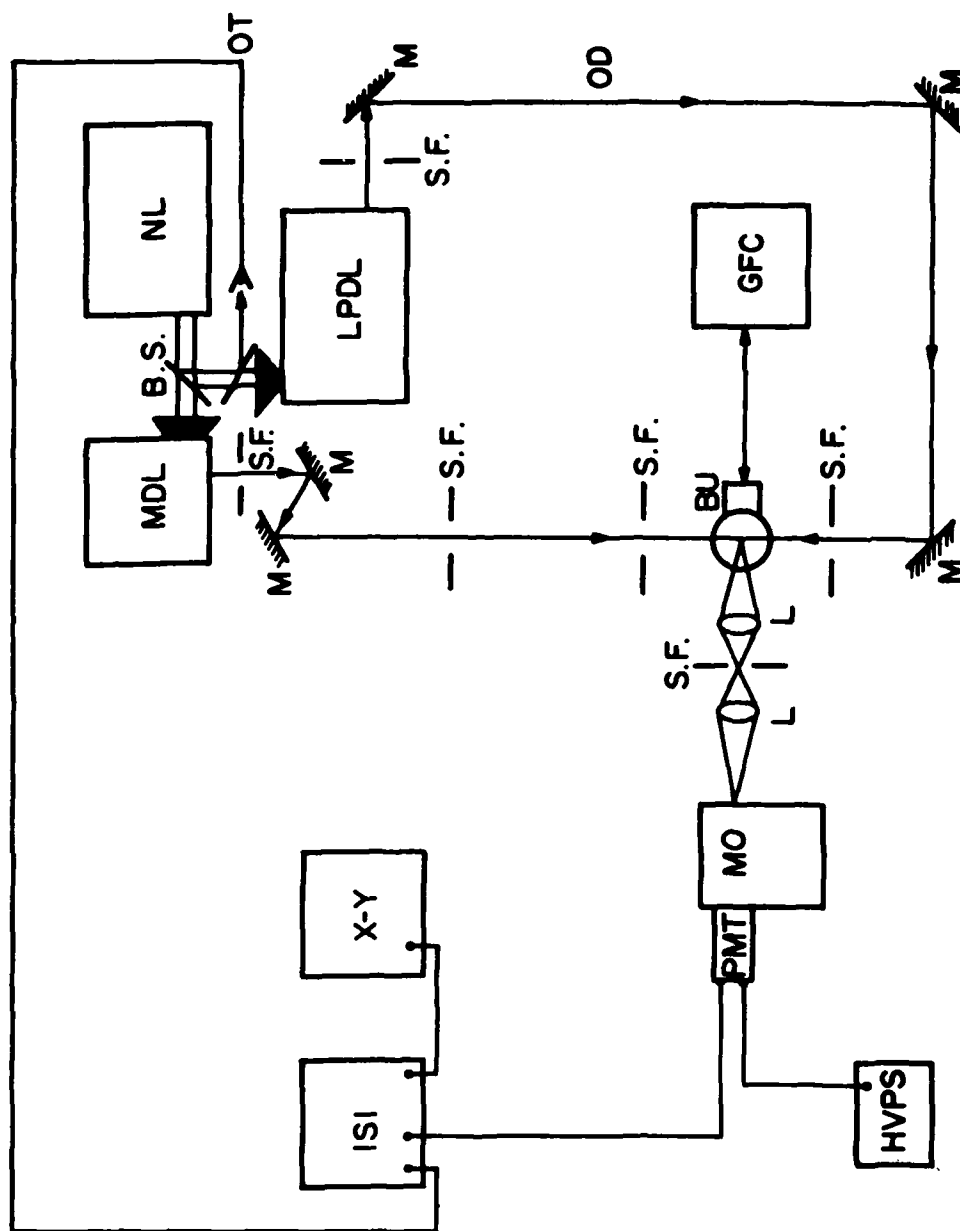
information must be available to determine n_T . Unfortunately, the measurement of Y_{31} is not possible via the approach, and, as stated above, it is still necessary to know the k 's or to be able to use certain limiting cases where the effect of the k 's are minimized.

SECTION IV

EXPERIMENTAL SYSTEM AND TECHNIQUES

All flames studies were supported on a Meker-type burner with an inner seeded flame zone surrounded by an outer flame (unseeded) of the same gas composition. The flame was surrounded by an inert gas sheath of the same composition as the major dilute gas species (i.e., Ar or N_2). The inner flame consisted of a rectangular array of 32 (4 x 8) 0.033 in. dia. holes spaced 0.045 in ϕ . The outer flame consisted of 2 rows of holes surrounding the inner flame. The total flame zone had 8 x 12 holes spaced 0.045 in ϕ . All flames were run at an unburnt total gas rise velocity of $\sim 0.4 \text{ m s}^{-1}$. The burner head was water-cooled with 25°C water and was nominally kept near ambient temperature during operation. Seed material was introduced into the inner flame in the form of an aerosol produced from the aqueous solution of the nitrate or chloride salt of Tl, In or Na. The aerosol was produced by either an ultrasonic nebulizer (operated at $\sim 20 \text{ W}$ power at 1.4 MHz) or by a Meinhart type glass concentric nebulizer. Both nebulizers functioned adequately. The ultrasonic nebulizer was somewhat less stable but provided $\sim 10 \times$ the fog density to the flame and was completely free from clogging affects at high salt concentrations. Salt concentrations used ranged from 0.1 PPM ($\sim 10^6 \text{ species cm}^{-3}$ in the flame) to as high as 10,000 PPM ($\sim 10^{11} \text{ species cm}^{-3}$ in the flame).

The instrumental arrangement is shown schematically in Figure 3. The N_2 -laser used was a Molectron Corp. model UV-14, in which the external power supply was replaced by us with an internal design power



Key: L = Lens; M = Beam Steering Mirrors; S.F. = Spatial Filters; B.S. = Beam Splitters; PMT = Photomultiplier Tube; OD = 0-100 ns Optical Delay; BU = Burner; GFC = Gas Flow Control Unit; HVPS = High Voltage Power Supply; ISI = Tektronix ISI; XY = X-Y Recorder; MDL = Molelectron Dye Laser; LPDL = Lambda Physik Dye Laser; NL = Nitrogen Laser; OT = Optical Trigger; MO = 0.1 m Grating Monochromator ($\Delta\lambda_s = 4 \text{ nm}$).

Figure 3: Instrumental Setup for Laser Excited Fluorescence Flame Temperature Measurement Methods

supply in order to reduce signal interfering radio frequency noise generated by the N_2 -laser. This N_2 -pump was used in pumping a Molelectron Corp. DL-400 dye laser and a Lambda Physik Model FL 2000 dye laser. All single laser experiments employed the Molelectron dye head. The amplifier stage of the Lambda Physik dye head was removed due to the insufficient pumping power from the N_2 -laser after beam splitting the UV-14 output. The beam expanding telescopes of both dye lasers were detuned (defocused) in order to insure that a pseudo-continuum spectral source profile would be obtained from the laser output. The laser line widths were measured by scanning the laser wavelength through the resonance transition of interest at low (linear) optical pump powers as described by Omenetto et al,¹³. Typical low power scans for $\lambda_{ex\ 1\rightarrow3}$ and $\lambda_{ex\ 2\rightarrow3}$ in T1 are shown in Figure 4. The beam was then passed through a series of circular spatial filters in order to achieve a spatially uniform intensity distribution.

The detection system consist of a wide bandwidth monochromator (Jobin Yvon Model H-10) employed as the wavelength selection device. The signal was collected by a Hamamatsu R928 photomultiplier tube with a specially-wired base for high speed transient work. Output signals were found to be linear with light intensity up to 40 mA peak current with no temporal distortion; beyond this current, the peak would become temporally distorted, and only the time integrated signal was found to be linear with light intensity. Improvements on this response could extend the linear peak current region to ≈ 1 A, and thereby extend the expected S/N ratio on single pulse measurements. The PMT was operated with an uneven dynode chain at -1400 V potential (cathode to anode).

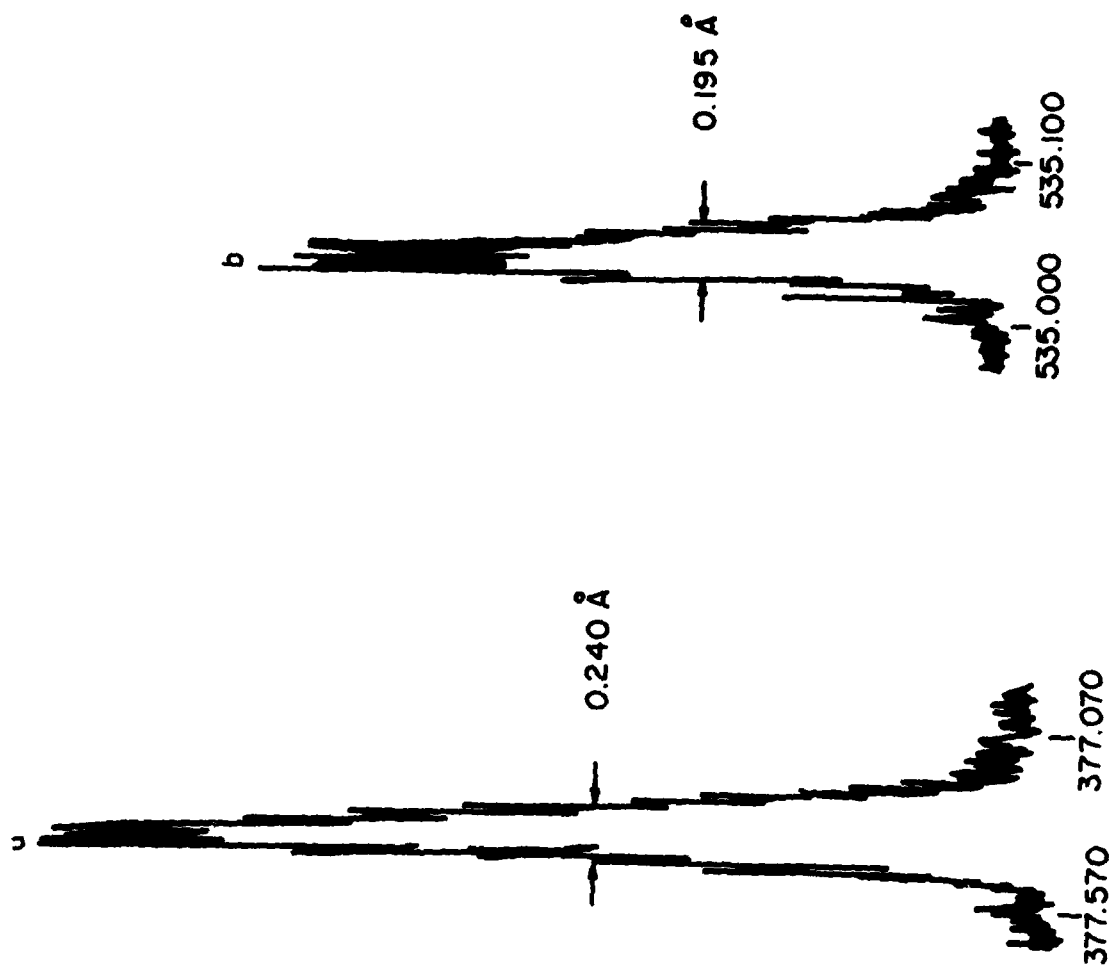


Figure 4: Fluorescence Excitation Spectra Obtained b; Scanning Laser Wavelength for Tl for Two
 Excitation Lines: Curve a. $B_{F_{3+2/1+3}}$; and curve b. $B_{F_{3+1/2+3}}$. The Laser Flux
 is 50 W cm^{-2} in both cases, (see Appendix D).

The measured rise time of a 250 ps input pulse was found to be ≈ 800 ps (for 95% signal). This signal was fed into a Tektronix Corp. Model 151 sampling oscilloscope with 350 ps rise time. Our system's overall temporal response (for 95% signal level) is ≈ 1.2 ns which was sufficient for the temporal studies and data evaluation contained in this report. In order to minimize jitter problems with the Moletron N_2 laser, an optical triggering arrangement was employed. This triggering scheme eliminated the possibility of using the PAR Boxcar detection systems in our laboratory due to their requirement of 75 ns pretrigger pulse (all attempts at signal delay of 75 ns caused distortion of the temporal waveform).

All electronic detection systems were connected to a salt-bed earth-ground in order to minimize R.F.I. problems. The noise limiting our signal detectability in this system was found to be noise in the electronic measurement system for the non-resonance cases and scatter noise in the resonance cases. The detectability limit for Tl with system was found to be ≈ 0.5 part-per-trillion in solution or $\approx 5 \times 10^3$ atoms cm^{-3} in the flame using a detection volume of $0.5 \times 1.5 \times 3$ mm³; this volume corresponds ≈ 10 -100 atoms as the absolute detectability limited for the system described. All measurements were made with an averaging time constant of 0.5 s and a repetition rate of 20 Hz. For the linear and thermally assisted temperature measurements, the species density was $\approx 5 \times 10^{10}$ cm⁻³, while $\approx 5 \times 10^9$ cm⁻³ number density was employed for the saturation measurements. (The 1.68 eV thermally-assisted measurement required $\approx 5 \times 10^{11}$ cm⁻³ densities to obtain reasonable S/N ratios).

No "single pulse" temperatures are given (we did not have available the 2 dye lasers after we had evaluated the meaning of the temporal photomultiplier scans for the saturation temperature methods). However, we did measure several "single pulse" fluorescence signals by METHOD #2 using In as a probe (this probe was later shown to give too large random temperature errors due to the small separation of levels 1 and 2) and obtained reasonably good fluorescence signals (the uncertainty in the fluorescence signals would correspond to a temperature error of <100 K with Tl as a probe). We should also point out that all flame temperatures correspond to only about 10 laser pulses for each fluorescence signal indicating the rather excellent signal-to-noise ratios with the saturation methods.

Results on Flame Temperature Measurement

The experimentally measured flame temperatures obtained by Methods 1-5 and a comparison with previously measured values by the Utrecht group and with the sodium line reversal method in one laboratory are given in TABLE I. The footnotes in Table I indicate the source of random errors. In TABLES II, III, and IV, the influence of certain experimental parameters on the flame temperatures measured by Methods #1 and #5 are given. The correlation of temperature values measured by Methods #1-5 with previously measured values is generally very good. There are obvious sources of systematic errors even between the Utrecht values as well as between the values obtained by us with the 5 methods.

The estimated random temperature errors in all of the present studies were made conservatively, i.e., using 3/5 peak-to-peak noise rather than 1/5 peak-to-peak noise as is recommended by most. It should be possible to reduce the temperature errors from ± 30 K to ± 10 K (or less) in the saturation method by using a wider gate (2 ns vs 350 ps) and extracting higher peak currents from the photomultiplier detector. In the thermally assisted temperatures (METHOD #5) and the linear method (METHOD 1), the random temperature errors due to S/N and calibration can also be reduced to nearly ± 10 K. It should be stressed that all flame temperature measurements reported here are preliminary ones and can be further refined, particularly with the present knowledge if the mechanistic aspects resulting from the present studies and the information to be obtained in future studies (refer to CONCLUSIONS).

TABLE I. PRELIMINARY FLAME TEMPERATURES VIA SEVERAL MEASUREMENT TECHNIQUES

Method	Probe	FLAME TEMPERATURES (°K) ^a	
		$H_2/O_2/Ar$	$H_2/O_2/N_2$
1 (Linear)	Tl	2345-2355 ^b ± 50	2145-2150 ^b ± 50
2 (Sat'n, Seq.)	Tl	2110 ± 30	2000 ± 30
3 (Sat'n, Sim.)	Tl	2300 ± 50	-----
4 (Peak)	Tl	2280 ± 30	2240 ± 30
5 (Thermal)	In	2220-2380 ^c ± 75	2030 ± 100
Hoomayers ¹	Na	2350	2160
Lijnse and Elsenaar ²	Na	2130	1970
Line Reversal ³	Na	2385	2320

23

Footnotes to Table I.

- Random errors in flame temperatures due to a combination of signal-to-noise ratios, spectrometer calibration errors, errors in laser spectral bandpass, etc. (also see Tables II-IV). Systematic errors are not included in ± values.
- Two temperatures are for 2 different laser irradiances on linear part of B_f vs E_v curve (see Table II and Figure 2).
- The temperature range is for a range of laser irradiances (see Table IV and Figure 3) and several thermally assisted emission transitions (see Table III).

References

- H.P. Hoomayers, Ph.D. Thesis, University of Utrecht, 1966.
- P.L. Lijnse and R.J. Elsenaar, J. Quant. Spectros. Radiat. Transfer, **12**, 1115 (1972).
- G. Zizak, University of Florida, 1980.

TABLE II. EXPERIMENTAL CONDITIONS AND INFLUENCE OF SOURCE IRRADIANCE ON LINEAR TWO-LINE (METHOD #1), FLAME TEMPERATURES. (Also refer to Figure 3).

Flame Conditions:	$H_2/O_2/Ar$:	2/1/4	:	$H_2/O_2/N_2$:	2/1/4	:	Probe-Tl
Laser Conditions:	E_1^a	= 10 W cm ⁻²					
	E_2^a	= 50 W cm ⁻²					
	$\Delta\lambda_{laser}$	1+3	=	0.23 ± 0.01	Å		
	$\Delta\lambda_{laser}$	2+3	=	0.195 ± 0.01	Å		
Fluorescence Radiances:	B_F^{max}	$(H_2/O_2/Ar)$	=	$6.2 \pm 0.2 \times 10^{-2}$	W cm ⁻² sr ⁻¹		
	B_F^{max}	$(H_2/O_2/N_2)$	=	$3.6 \pm 0.2 \times 10^{-2}$	W cm ⁻² sr ⁻¹		
	B_F^{max}	$(H_2/O_2/Ar)$	=	$1.65 \pm 0.1 \times 10^{-1}$	W cm ⁻² sr ⁻¹		
	B_F^{max}	$(H_2/O_2/N_2)$	=	$9.7 \pm 0.2 \times 10^{-2}$	W cm ⁻² sr ⁻¹		
	B_F^{max}	$(H_2/O_2/Ar)$	=	$1.6 \pm 0.1 \times 10^{-3}$	W cm ⁻² sr ⁻¹		
	B_F^{max}	$(H_2/O_2/N_2)$	=	$8.8 \pm 0.2 \times 10^{-4}$	W cm ⁻² sr ⁻¹		
Flame Temperatures:	$H_2/O_2/Ar$			2355 ± 50^b	(E ₁)		2345 ± 50^b (E ₂)
	$H_2/O_2/N_2$			2150 ± 50^b	(E ₁)		2145 ± 50^b (E ₂)

-TABLE CONTINUED-

TABLE II - CONTINUED.

Footnotes

- a. E = laser irradiance, in $W\ cm^{-2}$; $E = E_v \Delta v_L$, Δv_L = laser bandwidth, in Hz, $\Delta v_L = (\frac{c}{\lambda_0}) \Delta \lambda_L$, where c = speed of light and λ_0 = peak dye laser wavelength, (see Appendix D).
- b. The temperature errors are errors due to mainly to random errors in the laser spectral bandpass and to some extent to the signal-to-noise ratio.

TABLE III. EXPERIMENTAL CONDITIONS AND FLAME TEMPERATURES VIA THERMAL EXCITATION-EMISSION METHOD (METHOD #5).

Excitation-Luminescence Process Studied		Energy ^b of Thermally Excited Level (eV)	Flame Temperature (°K)	
<u>Luminescence</u>	<u>Excitation</u>		H ₂ /O ₂ /Ar:	H ₂ /O ₂ /N ₂ :
B _F 3→2 1→3	B _L 7→1 1→3	1.62	2230 ± 75 ^d	---
B _F 3→2 1→3	B _L 6→1 1→3	1.48	2000 ^c ± 75 ^d	---
B _F 3→2 1→3	B _L 5→1 1→3	1.45	2830 ^c ± 75 ^d	---
B _F 3→2 1→3	B _L 4→2 1→3	1.06	2230 ± 75 ^d	---
B _F 3→2 1→3	B _L 4→1 1→3	1.06	2380 ^c , 2310 ^e ± 75	2030 ± 100

TABLE CONTINUED.

TABLE III - CONTINUED

- a. Wavelengths of T1 Transitions: 3→1: 377.6 nm; 3→2: 535.0 nm; 4→1: 304 nm; 4→2: 325 nm; 5→1: 277 nm; 6→1: 275 nm; 7→1: 256 nm.
- b. Energy of Thermally Assisted Level of In Probe Above Laser Excited Level, 3. All measurements were carried out at $1.7 \times 10^5 \text{ W cm}^{-2} \text{ nm}^{-1}$.
- c. These 2 temperatures have a systematic error since both excitation transitions are within the laser spectral bandpass.
- d. Temperature errors are random errors due to calibration errors and signal-to-noise ratios.
- e. Two separate sets of measurements done at several weeks interval.

TABLE IV. INFLUENCE OF LASER IRRADIANCE UPON THERMAL EXCITATION EMISSION (METHOD 5) FLAME TEMPERATURES. (Also refer to Figure 4).

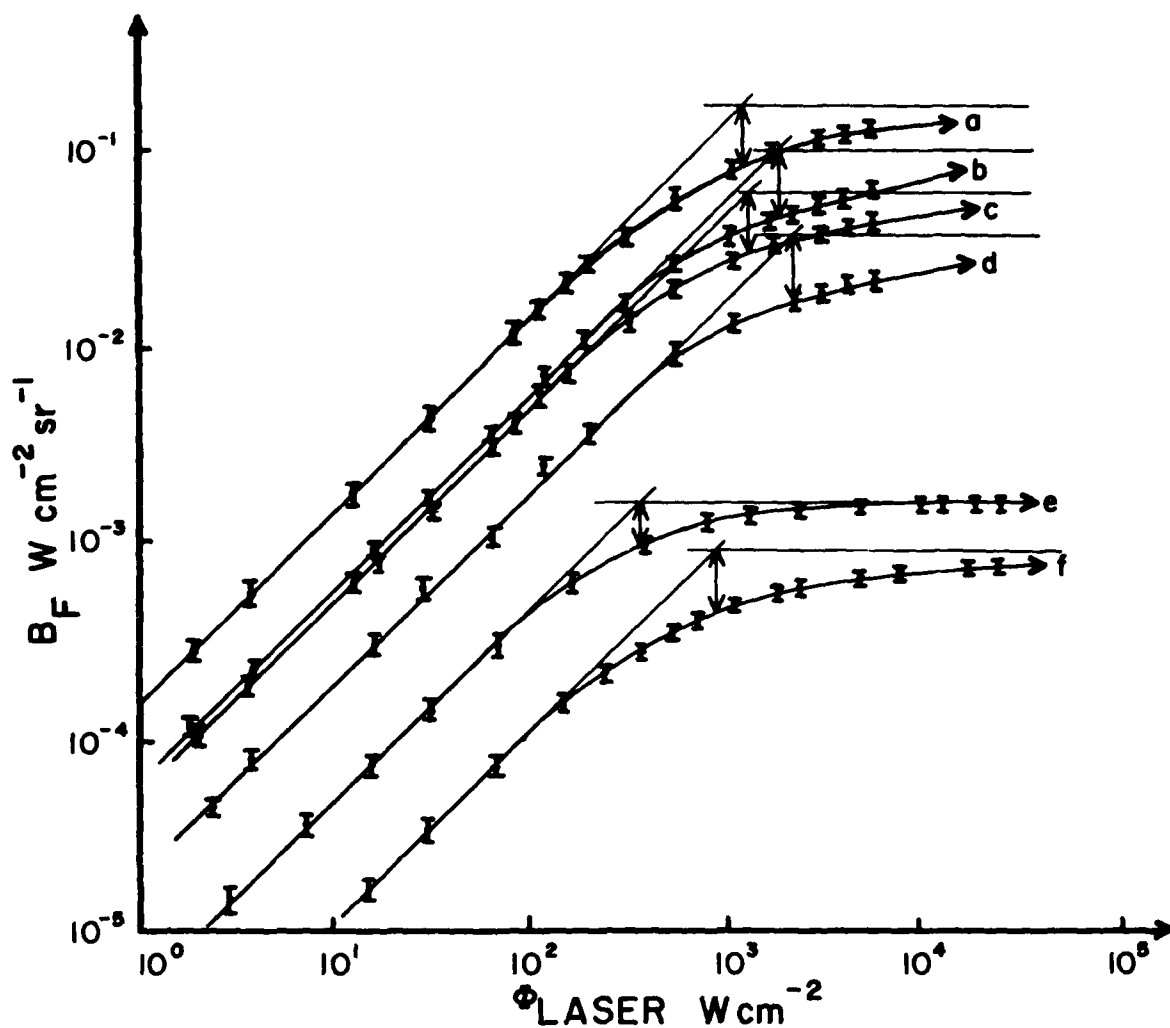
LASER IRRADIANCE (W cm^{-2}) ^a	FLAME TEMPERATURE ($^{\circ}\text{K}$): $\text{H}_2/\text{O}_2/\text{Ar}$: 2/1/4
4. $\times 10^3$	2310 \pm 75 ^b
2. $\times 10^3$	2330 \pm 75 ^b
1. $\times 10^3$	2230 \pm 100 ^b
5. $\times 10^2$	2220 \pm 100 ^b
2. $\times 10^2$	2250 \pm 100 ^b
1. $\times 10^2$	2300 \pm 100 ^b

Footnotes

- a. Laser Spectral Bandpass, $\Delta\lambda_L = 0.24 \text{ \AA}$ (see APPENDIX E for details on measuring $\Delta\lambda$).
- b. The temperature errors are random ones due mainly to error in $\Delta\lambda_L$ and calibration errors due to signal-to-noise ratio.

In Figures 5 and 6, typical B_F - E_v plots are given for several fluorescence transitions T1 in several H_2 -based flames. In Method 1, B_F values are measured for any source spectral irradiance on the linear portion of the plots. In Methods 2 and 3, B_F values must be taken on the 3-level steady state plateau region, and in Method 4 B_F values must be taken on the 2-level steady state plateau region. In Method 5, B_F values can be taken in any portion of the B_F - E_v plots.

In the linear two line fluorescence method (Method I), it is critical to have an accurate and precise calibration of source irradiances and fluorescence radiances; the former requires a careful calibration of the laser spectral bandpass for both excitation transitions. In addition, it is necessary to assure oneself that the B_F values correspond to the linear part of the B_F vs E_v curves (see TABLE II and Figure 3). The major random errors occur due to the poorer signal-to-noise ratios (as compared with Methods based on Saturation) unless higher number densities are employed (with the concomitant problems associated with scatter, post filter, etc.), calibration errors, and laser spectral bandpass errors. One must not estimate $\Delta\lambda_{\text{laser}}$ since an error of 0.004 nm can result in a flame temperature error of ≈ 200 K, and since this approach requires a pseudo-continuum, it is necessary to detune to spectrally broaden the laser output. Because of the need to match approximately laser beam geometries and the smaller S/N-ratios, this approach is less suitable for measuring temporal (<1 μ s time period) flame temperatures. In Methods 2-4, it is necessary to know whether the measurement with a suitable detector gate corresponds to either the "peak" (METHOD 4) or to the "steady state" (METHODS 2



	Fluorescence Transition	Excitation Bandwidth, Å	Flame
a.	$B_{F_{3 \rightarrow 1/1 \rightarrow 3}}$	0.23 ± 0.01	$H_2/O_2/Ar$ 2/1/4
b.	$B_{F_{3 \rightarrow 1/1 \rightarrow 3}}$	0.23 ± 0.01	$H_2/O_2/N_2$ 2/1/4
c.	$B_{F_{3 \rightarrow 2/1 \rightarrow 3}}$	0.23 ± 0.01	$H_2/O_2/Ar$ 2/1/4
d.	$B_{F_{3 \rightarrow 2/1 \rightarrow 3}}$	0.23 ± 0.01	$H_2/O_2/N_2$ 2/1/4
e.	$B_{F_{3 \rightarrow 1/2 \rightarrow 3}}$	0.20 ± 0.01	$H_2/O_2/Ar$ 2/1/4
f.	$B_{F_{3 \rightarrow 1/2 \rightarrow 3}}$	0.20 ± 0.01	$H_2/O_2/Ar$ 2/1/4

Figure 5. Fluorescence Radiance, B_F , in $W\ cm^{-2}\ sr^{-1}$, vs Laser Flux ϕ_L , $W\ cm$ for Several Flames and Several Fluorescence Transitions.

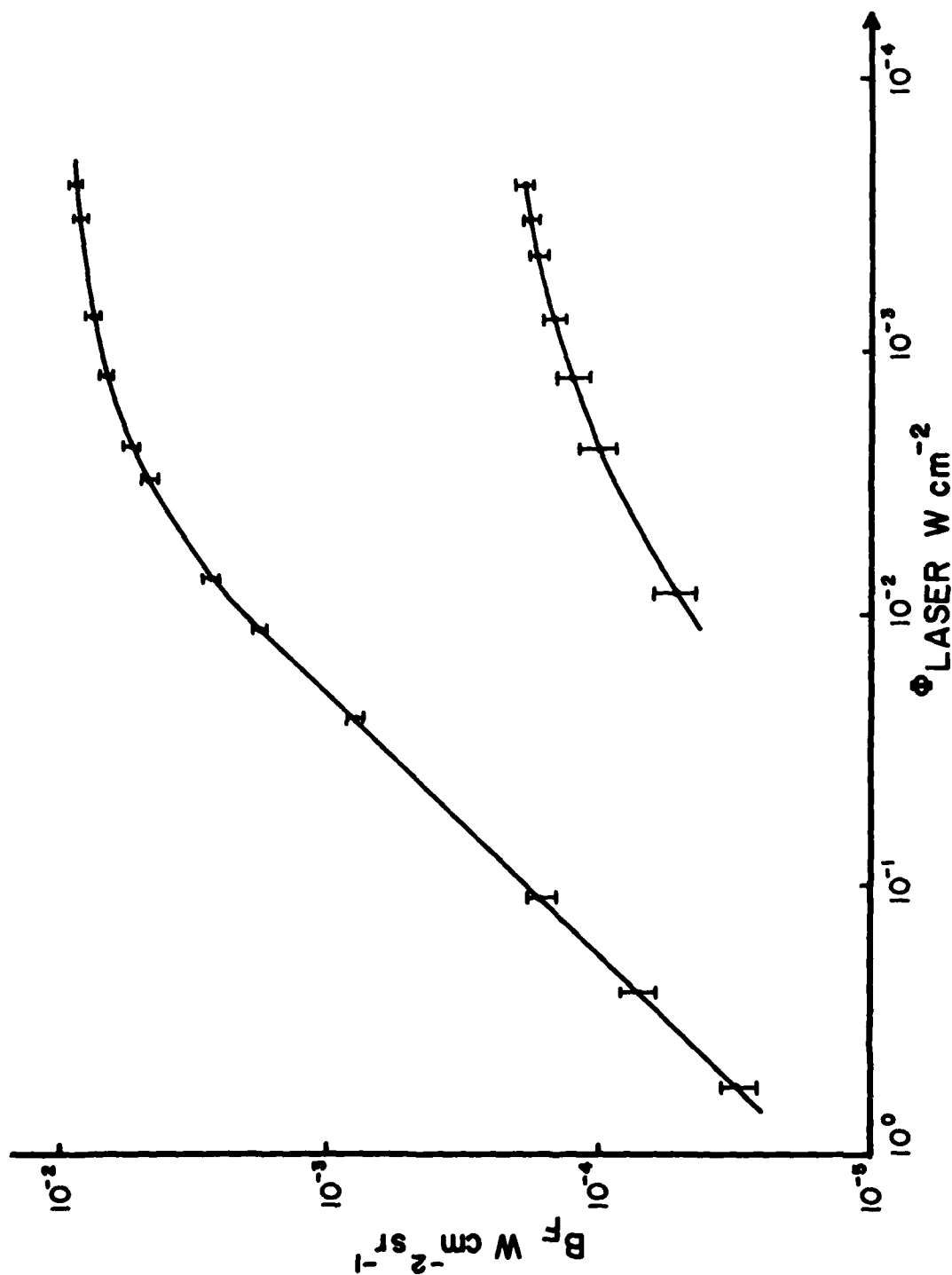


Figure 6. Fluorescence Radiance, B_F , in $W\ cm^{-2}\ sr^{-1}$, Vs Laser Flux Φ_L , in $W\ cm^{-2}$; For Laser Excited Fluorescence, $B_{F_{3+2/1+3}}$ (curve a) and For Laser Excited Thermally Assisted Emission, $B_{F_{4+1/1+3}}$ (curve b). The Laser Excitation Bandpass is $0.24 \pm 0.02\ \text{\AA}$.

and 3). In Figures 7a and 7b, the temporal scans of the fluorescence response are given for the 2 flames ($\text{H}_2/\text{O}_2/\text{Ar}$ and $\text{H}_2/\text{O}_2/\text{N}_2$). It is apparent that in the less quenching Ar-diluted flame that 2 regions corresponding to the "peak" and "steady state" cases exist, whereas in the more quenching N_2 -diluted flame only one region occurs partly due to the inadequate temporal resolution of the "peak" and "steady state" regions via our detection system. Flame temperatures obtained from the scans in Figures 7a and 7b are given in TABLE V. In METHODS 2,3, and 4, beam matching is also necessary as the necessity of a pseudo-continuum source. The exact value of $\Delta\lambda_{\text{laser}}$ is not necessary as long as the dye laser approximates a pseudo-continuum with respect to the absorption line. With commercial dye lasers, it is necessary to detune (by 0.1 or 0.2 Å) in order to approximate a pseudo-continuum, but in so doing, the laser irradiance is reduced, in some cases sufficiently to no longer saturate the excitation transition. Therefore, the excimer laser-dye laser system is needed (currently our N_2 -dye laser system is capable of peak spectral irradiances of about $1\text{-}20 \text{ MW cm}^{-2} \text{ nm}^{-1}$ in the fundamental region and about 1/10 to 1/100 of that in the doubled region; the excimer pumped dye laser will have spectral irradiances of the order of 100X greater than the present N_2 -dye laser system and should be adequate to saturate all visible and most ultraviolet resonance transitions). In addition, in METHODS 2,3, and 4, scatter and post filter errors must be of concern. The best excitation and fluorescence transitions involve $B_{F_{3 \rightarrow 1}^{2 \rightarrow 3}}$ and $B_{F_{3 \rightarrow 1}^{1 \rightarrow 3}}$ since scatter and post filter errors are minimized in the former and are small in the latter since the fluorescence signals are rather large and there is

no need to know gA-values*.

Method 5 has the greatest number of desirable characteristics for single pulse temperature measurements since there is no need to beam match or saturate. However, there is need to calibrate the spectrometric system. The greatest difficulty with this method is the need (like in Method 1) to know gA-values* which are oftentimes not accurately known. Poorly defined gA-values lead to systematic temperature errors. It is possible in this method that both peak and integrated pulse measurements will result in accurate temperatures. Studies on this will be done. Also, the most critical study to be performed involves the need to verify thermal population of the thermally-excited levels (4,5,...) in the probe, i.e., experimental measurements of collisional rate constants k_{3j} when $j = 4,5,\dots$. Such studies will be completed in the near future.

Finally, in Figure 8, indirect evidence is given indicating the possibility of thermal population of level 4. The fluorescence pulse precedes the thermal population of level 4. The fluorescence pulse precedes the thermally excited emission pulse by only ~ 1 ns which lends support to equilibration of the excited levels within a few nanoseconds.

We have also determined that plots of B_F vs E_v resulting in "saturation" plateaus give erroneous values of flame temperatures T 's,

*All gA values taken from C.H. Corliss and W.R. Bozman, NBS Monograph 53, U.S. Dept. of Commerce, 1962.

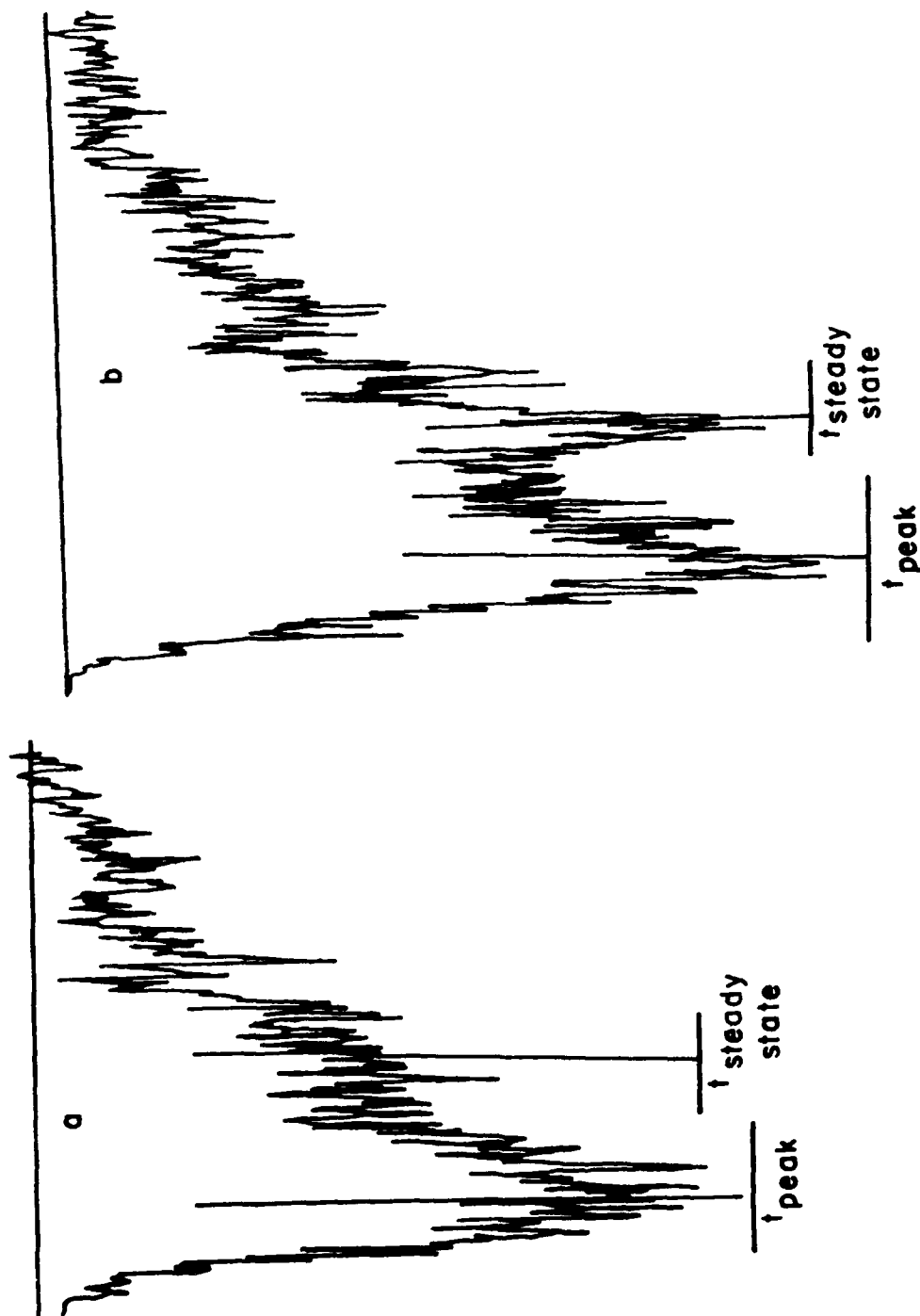


Figure 7. Temporal Scan of Tl Fluorescence Response $B_{F_{3+2}}^{1 \times 5}$ (curve a) and $B_{F_{3+2}}^{2 \times 3}$ (curve b) for $H_2/O_2/Ar$ Flame (2/1/4).

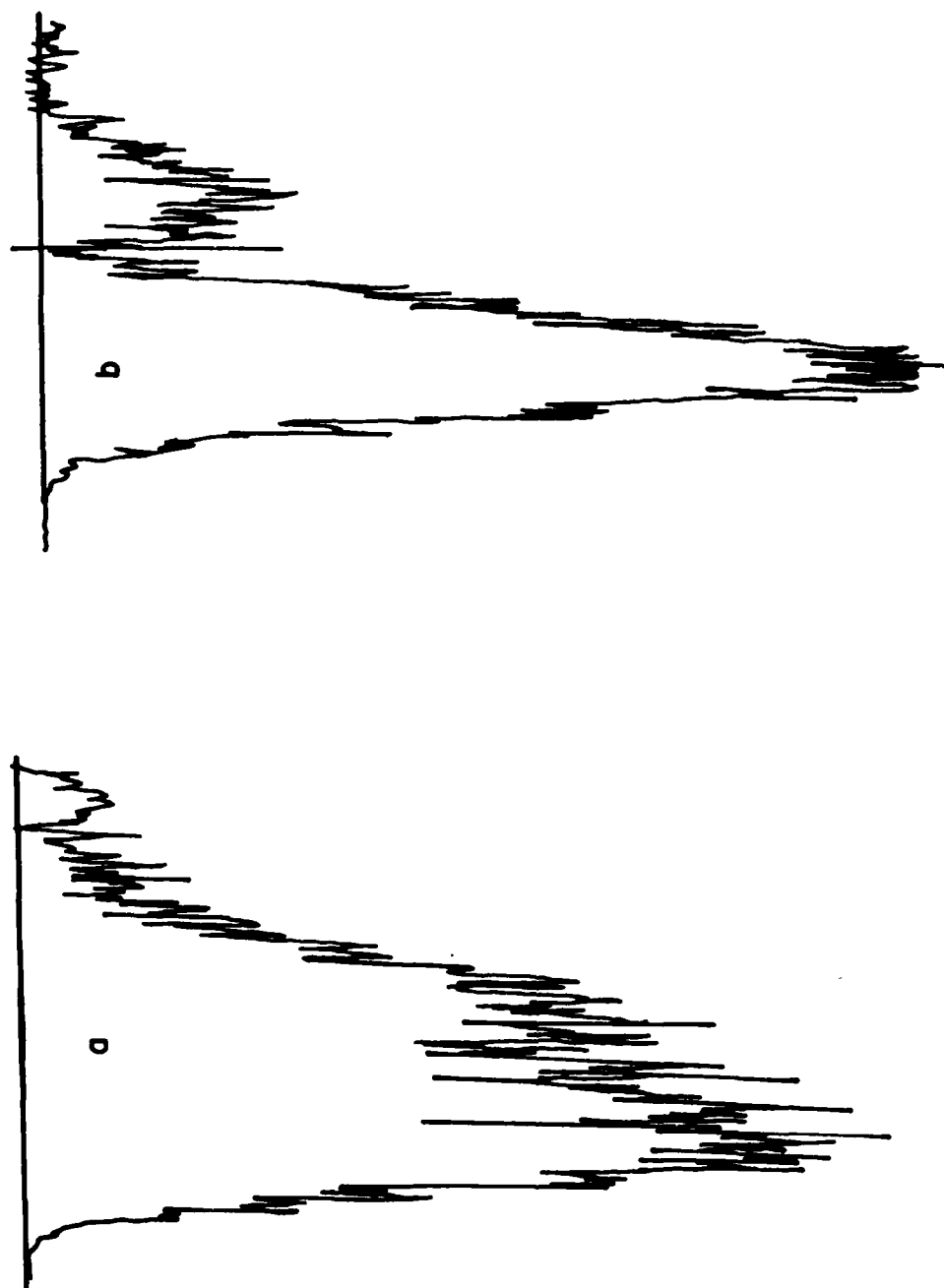


Figure 7b. Temporal Scan of Tl Fluorescence Response $B_{F_{3+2}^{1+3}}$ (curve a) and $B_{F_{3+2}^{2+3}}$ (curve b) for $H_2/O_2/N_2$ Flame (2/1/4).

TABLE V. FLAME TEMPERATURES MEASURED BY SIMULTANEOUS SATURATION METHOD (METHOD #2) BY IEC APPROACHES

Approach	Flame Temperature ($^{\circ}\text{K}$)	
	$\text{H}_2/\text{O}_2/\text{Ar}$ (see Figure 6a)	$\text{H}_2/\text{O}_2/\text{N}_2$ (see Figure 6b)
Peak ^a	2320 ± 50	$2340 \pm 50^{\text{c}}$
Steady State ^b	2370 ± 50	2160 ± 50

Footnotes

- In Figure 5a, there are definite regions corresponding to the "peak" (two level steady state) and "steady state" (3-level steady state) cases.
- In Figure 5b, quenching in the $\text{H}_2/\text{O}_2/\text{N}_2$ flame is so fast that the temporally measured photo-multiplier response convolutes the peak and steady state values. The temperatures were calculated using the ratio of BF_3 's obtained from the temporal peak values and using the T-expressions for Method #2 and #4. It is apparent that the temporal peak in a more highly quenching flame corresponds to the 3-level steady state case.
- This result is of limited value because of the reasons given in footnote b.

and concentrations, n_T 's; the saturation plateaus resulting from extrapolation techniques (i.e., $dn_3/dt \neq 0$, $dn_2/dt \neq 0$ during the N_2 -dye laser excitation pulses) and from sufficiently high laser spectral irradiances, E_v have apparent systematic errors. Therefore, previous methods based on measurement of n_T 's of OH, CN, CH, etc., from saturation plateaus easily by a factor of 2-3X in error.

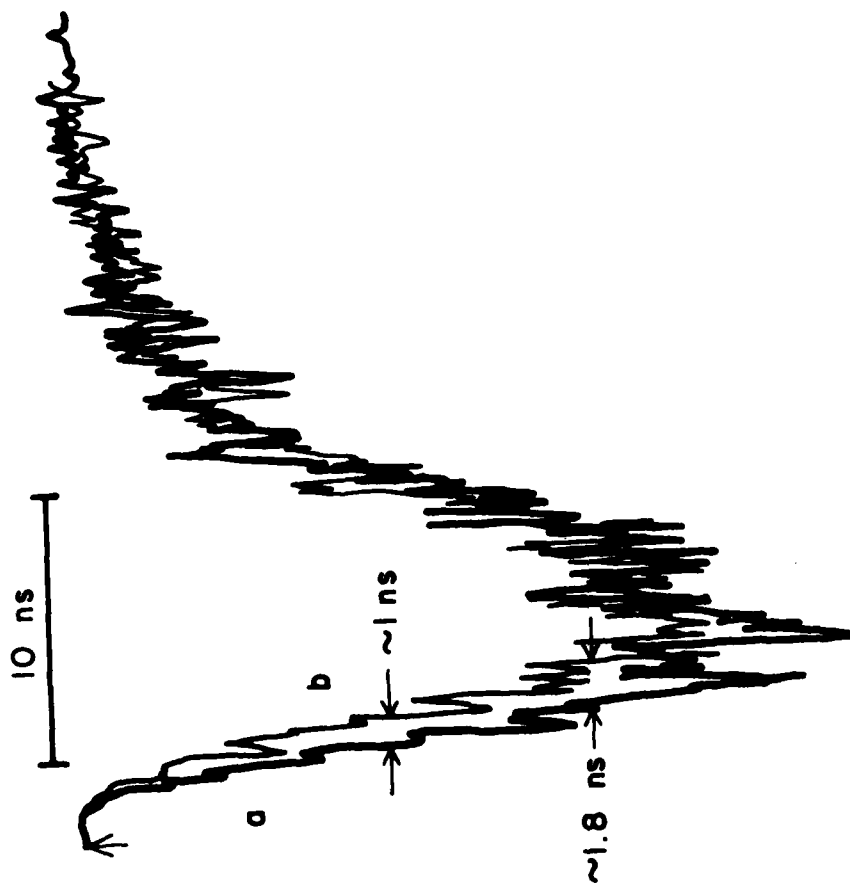


Figure 8. Temporal Scan of T1 Fluorescence $B_{F_{3 \rightarrow 2}}^{1 \rightarrow 3}$ (curve a) and Thermally Excited Emission $B_{F_{4 \rightarrow 1}}^{1 \rightarrow 5}$ for $H_2/O_2/N_2$ flame (2/1/4). Maximum photomultiplier current kept constant with neutral density filters.

SECTION V

CONCLUSIONS

Summary of Studies Completed

1. Theoretical development of 4 new methods of measuring spatial flame temperatures and comparison of these 4 methods with the linear two line fluorescence method as well as the line reversal method. The 5 fluorescence based methods are:
Method 1. Linear Two Line Method
Method 2. Saturation Two Line Method with Sequential Pumping
Method 3. Saturation Two Line Method With Simultaneous Pumping
Method 4. Saturation Two Line Method With Peak Detection
Method 5. Laser Excitation of Probe-Thermal Excitation - Emission Method.

2. Experimental verification of the above theoretical approaches to measurement of flame temperatures of H_2 -based flames. Problems, errors, and concerns associated with each method are evaluated. Extensions of the 5 methods to more quenching flames is given; basically METHOD 1 and 5 can be extended to hydrocarbon flames with mainly a problem in the reduction of fluorescence signal levels when operating on the linear portion of the B_F vs E_v curves. METHODS 2,3, and 4 require saturation to be achieved; conventional N_2 -dye laser systems are incapable of saturation of excitation transitions below ~ 500 nm. Excimer-dye laser systems possess sufficient spectral irradiance to saturation over UV excitation processes in most quenching flames.

3. Theoretical development of 2 new approaches for measuring the total number density, n_T , of species in flames. The 2 methods are based on the "peak" 2-level method and the simultaneous saturation of an upper level by 2 laser excitation processes. Problems associated with the conventional $1/B_F$ vs $1/E_v$ plot to determine n_T and Y (quantum efficiency) are indicated. The "saturation" plateau fluorescence radiances are found to give systematic errors on both the n_T and T values, and so it is recommended that saturation fluorescence signals be measured via either the "peak" or "steady state" methods (see Figures 7a and 7b).
4. Other studies completed include:
 - a. Theory and Experimental evaluation of Saturation broadening.
 - b. Experimental evaluation of n_T -values.
5. Manuscripts to be forwarded (when completed)
 - a. Theory of Fluorescence Temperature Methods
 - b. Experimental Verification of Fluorescence Temperature Methods
 - c. Theory of Fluorescence Number Density Methods
 - d. Saturation Broadening
 - e. Experimental Evaluation of n_T

Summary of Studies To Be Completed

1. Flame temperature of hydrocarbon based flames (gaseous and liquid fuel) will be completed as soon as the new excimer laser is available. Temporal ($< 1 \mu s$) based flame temperatures will also

be done when the excimer laser is available. The excimer laser will allow satisfactory pumping of 2 dye lasers for the saturation-based methods. "Temporal" temperatures were not obtained in the present work (other than proof that the fluorescence signals were sufficient to obtain accurate T's) because:

(a) 2 dye lasers were available only for 3 months of the contractual time and (b) only after return of the Lambda Physik dye laser to INRAD did we realize the basis of METHOD 5 and the meaning of the transient fluorescence signals (see Figures 6 and 7 and discussion concerning time).

2. A more thorough study of the transient fluorescence signal is still needed to: (a) prove thermal population of the thermally excited levels in METHOD 5, and (b) determine whether the "peak" and 3-level steady state portions of the fluorescence transient signals can be resolved via a faster detection system than we now possess. For example, we plan to probe level 2 of T1 by pumping 1→3 with a N_2 laser and using a Chromatix CMX-4 to monitor level 2 by pumping 2→4 (or other level).
3. Finally, we hope to transfer over methods to native molecular species in flame, e.g., OH, CH, CN, C_2 , etc.

SECTION VI
MISCELLANEOUS ITEMS

PERSONNEL ON PROJECT

The present project was performed by one post doctoral associate (Dr. Nicolo Omenetto now at CCR, European Community Center, Stabilimento di Ispra, Ispra, ITALY) for 12 months paid directly from contract funds and two full time graduate assistants (for 18 months) paid primarily via funds from other contracts (John Bradshaw and James Bower). In addition, Dr. Benjamin Smith; Dr. Georgio Zizak - Centro di Studio Per Ricerche Sulla Propulsion E Sull' Energetica, Milan, ITALY ; and Mr. John Horvath have spent 4 months and 10 months, respectively, on projects involved in this contract.

NON-EXPENDABLE EQUIPMENT PURCHASED

Equipment (non-expendable) purchased on this contract includes:

(a) Lambda Physik dye laser for \$15,000 from Inrad, Inc., 181 Legrand Ave., Northvale, NJ 07647; (b) Portable Gas (Nitrogen) Supply System for liquid nitrogen for \$1125 from Union Carbide Corp., Linde Division, 4800 West 16th Street, Indianapolis, IN 46244; (c) Kinetic Systems Gated Connector, Unibus Cable, Extender Card, Camac Crate Controller and Camac Crate with power supply from Kinetic Systems 11 Mary Knoll Drive, Lockport, IL 60441; (d) LeCroy's 12 Channel A/D Converter with 30 ns gate width to fit in the CAMAC Crate from LeCroy Research Systems, 700 South Main St., Spring Valley, NY 10977; (e) RT-11 Operating System with Fortran Extensions, Scientific and Lab Subroutine, Basic Extensions, Lab Applications and 6 Disk Cartridges;

and (e) several small items (\$220 or less) including a micro pump and a gas regulator.

The Lambda-Physik dye laser had arrived about 9 months after the start of the contract and the dye laser scan unit more than 1 year after the start of the contract. The combined system was available for the dual dye laser excitation measurements (Molelectron DL-400 was other dye laser) for less than 3 months out of the total contract period. To make matters worse, the dye laser system never met specifications concerning spectral resolution step size, wavelength accuracy and repeatability, wavelength range, and several other less serious aspects. Finally, in November 1979, the Lambda-Physik dye laser was returned to the vendor (Inrad) and the entire dye laser system was rebid (within the past 2 weeks the new dye laser - Molelectron DL-14) has arrived.

All other major items were required for temporal fluorescence measurements and computer interfacing.

REFERENCES

1. N. Omenetto, P. Benetti, and G. Rossi, Spectrochim. Acta, 27-b 453 (1972).
2. N. Omenetto, R.F. Browner, J.D. Winefordner, G. Rossi, and P. Benetti, Anal. Chem., 44, 1683 (1972).
3. P. Benetti, N. Omenetto, and G. Rossi, La Termtecnica, 29, 86 (1975).
4. H. Haraguchi, B. Smith, S. Weeks, D.J. Johnson, and J.D. Winefordner, Applied Spectroscopy, 31, 156 (1977).
5. H. Haraguchi and J.D. Winefordner, Applied Spectroscopy, 31, 195 (1977).
6. H. Haraguchi and J.D. Winefordner, Applied Spectroscopy, 31, 330 (1977).
7. J. Bradshaw, J. Bower, S. Weeks, K. Fujiwara, N. Omenetto, H. Haraguchi, and J.D. Winefordner, 10th Materials Research Symposium on Characterization of High Temperature Vapors and Gases, NBS, Gaithersburg, Maryland, 1978.
8. M. Lapp and C.M. Penney, Editors, "Laser Raman Gas Diagnostics", Plenum Press, 1974.
9. R.M. Measures, J. Appl. Phys., 39, 5232 (1968).
10. N. Omenetto and J.D. Winefordner, Chapter 4 in "Analytical Laser Spectroscopy", N. Omenetto, Editor, Wiley, 1979.
11. N. Omenetto and J.D. Winefordner, Progress in Analytical Atomic Spectroscopy, Vol. 2 (1,2), Pergamon, 1979.
12. G.D. Boutilier, M.B. Blackburn, J.M. Mermet, S.J. Weeks, H. Haraguchi, J.D. Winefordner, and N. Omenetto, Applied Optics, 17, 2291 (1978).
13. N. Omenetto, J.N. Bower, J.D. Bradshaw, C.A. Van Dijk, and J.D. Winefordner, J. Quant. Spectrosc. Radiat. Transfer, in press.

APPENDIX A
(APPL. OPTICS, 17, 2291 (1978)).

STEADY STATE ATOMIC FLUORESCENCE RADIANCE
EXPRESSIONS FOR CONTINUUM EXCITATION^a

G. D. Boutilier^b

M. B. Blackburn

J. M. Mermet^c

S. J. Weeks^d

H. Haraguchi^e

J. D. Winefordner^f

Department of Chemistry
University of Florida
Gainesville, FL 32611

and

N. Omenetto

Institute of Inorganic
and General Chemistry
University of Pavia
Viale Taramelli 12
27100 Pavia
Italy

- a. Work supported by AF-AFOSR-F44620-76-C-0005.
- b. G. D. B. wishes to acknowledge the support of a fellowship sponsored by the Procter & Gamble Co.
- c. Present address: Lab. de Physicochimie Ind., Bat. 401, INSA, 69621 Villeurbanne CEDEX, France
- d. Present address: Analytical Chemistry Division, National Bureau of Standards, Washington, D.C. 20234
- e. Present address: Department of Chemistry and Physics, National Institute for Environment, P.O. Yatabe, Ibaraki 300-21, Japan
- f. Author to whom reprint requests should be sent.

ABSTRACT

Several general expressions for the atomic fluorescence radiance excited by a laser source are presented for both 2-level and 3-level systems. The laser has been approximated to a spectral continuum since its bandwidth is assumed to be much larger than the absorption profile. Two types of 3-level systems are considered: i) systems where 2 excited states are close together, both coupled radiatively with the ground state (Na, K, Cs, etc.); and ii) systems where one level is close to the ground state, both being radiatively connected with a third excited state (Tl, In, Ga, etc). Expressions are given for both linear and saturating conditions and the use of such expressions for absolute species measurement is discussed. In our treatment, we have made the assumption that the rate equations approach is valid.

INTRODUCTION

The attractive feasibility of laser excited fluorescence spectroscopy for plasma diagnostics has been described early in 1968 by Measures¹ and recently exploited by a number of researchers for measuring spatial species concentration, temperature, and other physical parameters of interest.²⁻⁶ The laser systems which can be utilized in these studies are the N_2 -pumped dye laser, flashlamp pumped dye laser, and the cw Ar ion-pumped dye laser. Very often the laser bandwidth is much larger than the absorption profile, irrespective of the type of broadening occurring in the plasma investigated and therefore it can be approximated to a spectral continuum. For this excitation, Omenetto, et al.,⁴ have evaluated the 2-level atom fluorescence radiance expressions. Omenetto and Winefordner⁵ have discussed both the 2-level and 3-level cases and Daily^{6,7} and D'Olivares⁸ have also evaluated both the 2- and 3-level cases. Since the expressions given, apart from the different terminology, are of limited applicability, the aim of this note is to extend the derivation to other typical 3-level atomic systems and to indicate the use of such expressions for absolute species measurement. The effect of saturation with high intensity laser sources can then be consistently compared assuming the atom approximates either a 2-level or a 3-level system.

It is worth stressing that the rate equations approach is considered to be valid here. Finally, the expressions given are only applicable in the case of low optical densities ($k_{\nu}l < 0.05$).

ATOMIC FLUORESCENCE RADIANCE EXPRESSIONS

The atomic fluorescence radiance for any atom (2 or multi-level) is given⁵ by

$$B_{F_{j \rightarrow k}}^{l \rightarrow m} = \left(\frac{\ell}{4\pi} \right) Y_{P_{jk}} E_{\nu_{\ell m}} \left(\frac{h\nu_{\ell m}}{c} \right) B_{\ell m} n_{\ell} \left[1 - \frac{g_{\ell} n_m}{g_m n_{\ell}} \right] \quad (1a)$$

where:

$B_{F_{j \rightarrow k}}^{l \rightarrow m}$ = atomic fluorescence radiance for $j \rightarrow k$ radiative deactivation process and for $l \rightarrow m$ radiative excitation process, $J s^{-1} m^{-2} sr^{-1}$;

ℓ = fluorescence path length in direction of observation, m;

$Y_{P_{jk}}$ = fluorescence power efficiency, $J s^{-1}$ fluoresced/ $J s^{-1}$ absorbed (where j is upper level of fluorescence and k is lower level);

Y_{jk} = fluorescence quantum efficiency (see Appendix A), dimensionless ($Y_{P_{jk}} = Y_{jk} h\nu_{jk}/h\nu_{\ell m}$);

$E_{\nu_{\ell m}}$ = spectral irradiance of continuum source at frequency $\nu_{\ell m}$ of excitation (ℓ is lower level from which transition begins and m is upper level at which the transition ends), $J s^{-1} m^{-2} Hz^{-1}$;

$h\nu_{\ell m}$ = energy of exciting photon, J;

c = speed of light, ms^{-1} ;

$B_{\ell m}$ = Einstein coefficient of induced absorption, i.e., absorption transitions per spectral energy density per absorbing species, $m^3 J^{-1} s^{-1} Hz$;

n_{ℓ} = density (concentration) of species (absorbers) in lower level ℓ , m^{-3} ;

g_{ℓ} or g_m = statistical weights of ℓ or m levels, dimensionless; and

n_m = density (concentration) of upper level of excitation, m^{-3} .

An alternate expression for $B_{F_{j \rightarrow k}}^{l \rightarrow m}$ is

$$B_{F_{j \rightarrow k}}^{l \rightarrow m} = \left(\frac{\ell}{4\pi} \right) A_{jk} h\nu_{jk} n_j \quad (1b)$$

Two Level System

For a 2 level atom, where the levels are designated ground, 1, and, 1st excited, 2, the terms in equation 1 are: Y_{21} , $E_{v_{12}}$, $n_l = n_1$, $n_m = n_2$, $h\nu_{12}$, B_{12} , and so

$$B_{F_{21}} = \left(\frac{\ell}{4\pi} \right) Y_{21} E_{v_{12}} \left(\frac{h\nu_{12}}{c} \right) B_{12} n_1 \left[1 - \frac{g_1}{g_2} \frac{n_2}{n_1} \right] \quad (2)$$

Assuming steady state excitation/de-excitation,^{3,4} assuming negligible population in other levels ($n_T = n_1 + n_2$), and assuming negligible thermal excitation

$$n_2 = \frac{g_2}{g_1} n_1 \left(\frac{E_{v_{12}}}{E_{v_{12}} + E_{v_{12}}^*} \right),$$

$$n_1 = \frac{n_T}{1 + \frac{g_2}{g_1} \left(\frac{E_{v_{12}}}{E_{v_{12}} + E_{v_{12}}^*} \right)} \quad (3)$$

where:

$$E_{v_{12}}^* = \frac{c \Lambda_{21}}{Y_{21} B_{21}}, \text{ J s}^{-1} \text{ m}^{-2} \text{ Hz}^{-1}; \text{ and}$$

$$B_{21} = \text{Einstein coefficient of induced emission } (B_{21}g_2 \cdot B_{12}g_1),$$

$$\text{m}^3 \text{ J}^{-1} \text{ s}^{-1} \text{ Hz}.$$

The term $E_{v_{12}}^*$ is a modified saturation spectral irradiance and is related to the one given by Omenetto et al.,²⁻⁵ by D'Olivares,⁸ and by Daily⁹ by

$$E_{v_{12}}^* = E_{v_{12}}^s \left(\frac{g_2 + g_1}{g_1} \right) \quad (4)$$

The previously used saturation spectral irradiance, $E_{v_{12}}^s$, will not be used here despite its obvious physical usefulness (i.e., $E_{v_{12}}^s$ is that source spectral irradiance where the fluorescence signal is 50% of the maximum possible value) because $E_{v_{12}}^s$ is simply related to $E_{v_{12}}^*$ (evaluated from fundamental constants, c , and measureable parameters, Λ_{21} , B_{21} , Y_{21})

only for the 2-level system.

The general $B_{F_{21}}$ expression in terms of n_T for a 2-level system is

$$B_{F_{21}} = \left(\frac{\ell}{4\pi} \right) Y_{21} E_{v_{12}} \left(\frac{h\nu_{12}}{c} \right) B_{12} \left[\frac{g_1 n_T}{(g_1 + g_2) (E_{v_{12}} / E_{v_{12}}^*) + g_1} \right] \quad (5)$$

For a low intensity source ($E_{v_{12}} \ll E_{v_{12}}^*$)

$$B_{F_{21}(lo)} = \frac{\ell}{4\pi} A_{21} h\nu_{12} \left(\frac{E_{v_{12}}}{E_{v_{12}}^*} \right) \frac{g_2}{g_1} n_T \text{ or } \left(\frac{\ell}{4\pi} Y_{21} B_{12} \left(\frac{h\nu_{12}}{c} \right) E_{v_{12}} n_T \right) \quad (6)$$

For a high intensity source ($E_{v_{12}} \gg E_{v_{12}}^*$)

$$B_{F_{21}(hi)} = \frac{\ell}{4\pi} A_{21} h\nu_{12} \left(\frac{g_2}{g_1 + g_2} \right) n_T \quad (7)$$

Both expressions are consistent with those of Daily^{6,7} and Omenetto.²⁻⁵

Three Level System--General Expressions

There are two major types of 3-level atomic systems: (I) systems where the levels 2 and 3 are close together and radiative transitions between levels 2 and 3 are not allowed, e.g., Na, K, Cs, etc.; and (II) systems where levels 1 and 2 are close together and radiative transitions between 1 and 2 are not allowed, e.g., Tl, In, Ga, etc. In Appendix A, the general steady state approach for estimating the ratios, n_3/n_1 , n_3/n_2 , and n_2/n_1 is given. Below, only specific expressions for these ratios will be given. The specific excitation-deexcitation routes are given in parentheses.

Case IA(1→3). In this case, the non-radiative excitation rate constants, k_{12} and k_{13} are assumed negligible and the radiative rate constant, $A_{32} = 0$. Therefore, thermal excitation is negligible and assuming radiative excitation of level 3 from level 1, the ratios of n_3/n_1 and n_2/n_1 are

$$\frac{n_3}{n_1} = \frac{g_3}{g_1} \left(\frac{E_{\nu_{13}}}{E_{\nu_{13}} + E_{\nu_{13}}^*} \right) \quad (8)$$

$$\frac{n_2}{n_1} = \frac{g_3}{g_1} \left(\frac{E_{\nu_{13}}}{E_{\nu_{13}} + E_{\nu_{13}}^*} \right) \left(\frac{k_{32}}{A_{21} + k_{21} + k_{23}} \right) \quad (9)$$

where:

$E_{\nu_{13}}$ = excitation spectral irradiance at exciting frequency ν_{13} ,
 $J s^{-1} m^{-2}$;

$E_{\nu_{13}}^*$ = spectral irradiance needed to make the density of n_3 50% of
 n_1 assuming $g_1 = g_3$, $J s^{-1} m^{-2}$;

A_{21} = Einstein coefficient of radiation emission for radiative
deactivation process, $2 \rightarrow 1$, s^{-1} ;

k 's = non-radiative rate constants for processes shown, s^{-1} ; and

g 's = statistical weights of levels shown, dimensionless.

The term $E_{\nu_{13}}^*$ is defined by

$$E_{\nu_{13}}^* = \frac{cA_{31}}{Y_{31}B_{31}} = \frac{cg_3A_{31}}{g_1Y_{31}B_{13}}, \quad (10)$$

where:

B_{31} = Einstein coefficient of induced emission for process $3 \rightarrow 1$,
 $m^3 J^{-1} s^{-1} Hz$;

B_{13} = Einstein coefficient of induced (radiative) excitation for
process, $1 \rightarrow 3$, $m^3 J^{-1} s^{-1} Hz$;

and Y_{31} , the fluorescence quantum efficiency¹⁰ for the radiative process $3 \rightarrow 1$
is given by

$$Y_{31} = \frac{A_{31}}{A_{31} + k_{31} + k_{32} \left[1 - \frac{k_{32}k_{23}}{(A_{31} + k_{31} + k_{32})(A_{21} + k_{21} + k_{23})} \right]}, \quad (11)$$

where the term in brackets in the denominator accounts for the increase in quantum efficiency via the cyclic factor¹¹ of crossover from 3→2 and re-crossover from 2→3.

Case I Aa(1→3, 3→1). Solving for n_1 in terms of n_T ($n_T = n_1 + n_2 + n_3$) utilizing equations 8 and 9 and substituting for n_1 into equation 1a gives

$$B_{F_{3 \rightarrow 1}} = \left(\frac{\ell}{4\pi} \right) A_{31} h\nu_{13} n_T \left[\frac{1}{1 + \frac{k_{32}}{A_{21} + k_{21} + k_{23}} + \frac{g_1}{g_3} \left(1 + \frac{E_{v13}^*}{E_{v13}} \right)} \right] \quad (12)$$

Case I Ab(1→3, 3→2, 2→1). Solving for n_1 in terms of n_T utilizing equations 8 and 9 and substituting¹⁰ for $Y_{21} = X_{32} Y_{21}$ where

$$X_{32} = \frac{k_{32}}{A_{31} + k_{31} + k_{32} \left[1 - \frac{k_{23} k_{32}}{(A_{31} + k_{31} + k_{32})(A_{21} + k_{21} + k_{23})} \right]} \quad (13)$$

and

$$Y_{21} = \frac{A_{21}}{A_{21} + k_{21} + k_{23}} \quad (14)$$

gives

$$B_{F_{2 \rightarrow 1}} = \left(\frac{\ell}{4\pi} \right) A_{21} h\nu_{12} n_T \left[\frac{1}{1 + \left(\frac{A_{21} + k_{23} + k_{21}}{k_{32}} \right) \left(1 + \frac{g_1}{g_3} \left[1 + \frac{E_{v13}^*}{E_{v13}} \right] \right)} \right] \quad (15)$$

X_{32} is the crossing efficiency for populating level 2 from level 3 and Y_{21} is the radiative efficiency for 2→1 luminescence.

Case IB(1→2). With the same assumptions as previously given (k_{12} , k_{13} , $A_{32}^{(0)}$), and assuming radiative excitation of level 2 with non-radiative crossover to level 3 and then radiative deexcitation, the ratios of n_2/n_1 and n_3/n_1 are given by

$$\frac{n_2}{n_1} = \frac{g_2}{g_1} \left(\frac{E_{v12}}{E_{v12} + E_{v12}^*} \right) \quad (16)$$

$$\frac{n_3}{n_1} = \frac{g_2}{g_1} \left(\frac{E_{v12}}{E_{v12} + E_{v12}^*} \right) \left(\frac{k_{23}}{A_{31} + k_{31} + k_{32}} \right), \quad (17)$$

where all terms are defined in the manner previously given for similar or identical terms. The term E_{v12}^* is defined as

$$E_{v12}^* = \frac{cA_{21}}{Y_{21}B_{21}} = \frac{g_2 cA_{21}}{g_1 Y_{21}B_{12}}, \quad (18)$$

and Y_{21} defined as

$$Y_{21} = \frac{A_{21}}{A_{21} + k_{21} + k_{23} \left[1 - \frac{k_{23}k_{32}}{(A_{21}+k_{21}+k_{23})(A_{31}+k_{31}+k_{32})} \right]}. \quad (19)$$

Case I Ba(1→2, 2→1). Solving for n_1 in terms of n_T utilizing equations (16) and (17) and substituting for n_T gives

$$B_{F2+1} = \left(\frac{\ell}{4\pi} \right) A_{21} h\nu_{12} n_T \left[\frac{1}{1 + \frac{k_{23}}{A_{31}+k_{31}+k_{32}} + \frac{g_1}{g_2} \left(1 + \frac{E_{v12}^*}{E_{v12}} \right)} \right]. \quad (20)$$

Case I Bb(1→2, 2→3, 3→1). Solving for n_1 in terms of n_T utilizing equations (16) and (17) and substituting for $Y_{31} = \chi_{23}y_{31}$ where

$$\chi_{23} = \frac{k_{23}}{A_{21} + k_{21} + k_{23} \left[1 - \frac{k_{23}k_{32}}{(A_{21}+k_{21}+k_{23})(A_{31}+k_{31}+k_{32})} \right]}, \quad (21)$$

and

$$y_{31} = \frac{A_{31}}{A_{31} + k_{31} + k_{32}}, \quad (22)$$

gives

$$B_{F3+1} = \frac{\ell}{4\pi} A_{31} h\nu_{13} n_T \left[\frac{1}{1 + \left(\frac{A_{31}+k_{31}+k_{32}}{k_{23}} \right) \left(1 + \frac{g_1}{g_2} \left[1 + \frac{E_{v12}^*}{E_{v12}} \right] \right)} \right]. \quad (23)$$

χ_{23} and y_{31} are exactly analogous to χ_{32} and y_{21} respectively.

Case IIA(1+3). In this case non-radiative rate constants k_{13} and k_{23} can be assumed negligible and radiative rate constant $A_{21} \sim 0$. Assuming radiative excitation of level 3 via level 1, the ratios n_3/n_1 and n_3/n_2 are given by

$$\frac{n_3}{n_1} = \frac{g_3}{g_1} \left(\frac{E_{v13}}{E_{v13} + E_{v13}^*} \right), \quad (24)$$

$$\frac{n_3}{n_2} = \frac{k_{21}}{A_{32} + k_{32} + \frac{g_1}{g_3} k_{12} \left[1 + \frac{E_{v13}^*}{E_{v13}} \right]}, \quad (25)$$

where E_{v13}^* is defined by

$$E_{v13}^* = \frac{cA_{31}}{Y_{31}B_{31}} = \frac{cg_3A_{31}}{g_1Y_{31}B_{13}}, \quad (26)$$

and Y_{31} is defined by

$$Y_{31} = \frac{A_{31}}{A_{31} + A_{32} + k_{31} + k_{32}}, \quad (27)$$

and Y_{32} by

$$Y_{32} = \frac{A_{32}}{A_{31} + A_{32} + k_{31} + k_{32}}, \quad (28)$$

where the cyclic crossover¹¹ term for such a case is omitted, i.e., the upper and middle levels are not both radiatively connected to the lower level (also, k_{13} and k_{23} are negligibly small). The terms k_{21} and k_{12} are the non-radiational rate constants for collisional de-excitation and excitation and are related by

$$k_{21} = k_{12} \frac{g_1}{g_2} \exp(E_{12}/kT) \quad (29)$$

where E_{12} is the energy separation between levels 1 and 2, T is the flame temperature, and k is the Boltzmann constant.

Case II Aa(1→3, 3→1). For this case, solving for n_3 in terms of n_T , utilizing equations 24 and 25 and substituting for Y_{31} from equation 26 gives

$$B_{F_{3 \rightarrow 1}} = \left(\frac{\ell}{4\pi} \right) A_{31} h\nu_{13} n_T \left[\frac{1}{1 + \frac{g_1}{g_3} \left(1 + \frac{E_{v13}^*}{E_{v13}} \right) \left(1 + \frac{g_2}{g_1} \exp(-E_{12}/kT) \right) + \left(\frac{A_{32} + k_{32}}{k_{21}} \right)} \right] \quad (30)$$

Case II Ab(1→3, 3→2). For this case, solving for n_3 in terms of n_T utilizing equations 24 and 25 and substituting for Y_{32} gives

$$B_{F_{3 \rightarrow 2}} = \left(\frac{\ell}{4\pi} \right) A_{32} h\nu_{23} n_T \left[\frac{1}{1 + \frac{g_1}{g_3} \left(1 + \frac{E_{v13}^*}{E_{v13}} \right) \left(1 + \frac{g_2}{g_1} \exp(-E_{12}/kT) \right) + \left(\frac{A_{32} + k_{32}}{k_{21}} \right)} \right] \quad (31)$$

Case II B (2→3). For this case, non-radiative rate constants, k_{13} and k_{23} are negligible and the radiative constant $A_{21} \approx 0$. Assuming radiative excitation of level 3 via level 2, the ratios n_3/n_1 and n_3/n_2 are

$$\frac{n_3}{n_1} = \frac{g_2}{g_1} \frac{k_{21} \exp(-E_{12}/kT)}{\frac{g_2}{g_3} k_{21} \left[1 + \frac{E_{v23}^*}{E_{v23}} \right] + A_{31} + k_{31}} \quad (32)$$

$$\frac{n_3}{n_2} = \frac{g_3}{g_2} \left(\frac{E_{v23}}{E_{v23} + E_{v23}^*} \right) \quad (33)$$

Case II Ba(2→3, 3→2). Solving for n_3 in terms of n_T utilizing equations 32 and 33 and substituting for Y_{32} utilizing equation 28 gives

$$B_{F_{3 \rightarrow 2}} = \left(\frac{\ell}{4\pi} \right) A_{32} h\nu_{23} n_T \left[\frac{1}{1 + \frac{g_2}{g_3} \left(1 + \frac{E_{v23}^*}{E_{v23}} \right) \left(1 + \frac{g_1}{g_2} \exp(E_{12}/kT) \right) + \left(\frac{A_{31} + k_{31}}{k_{12}} \right)} \right] \quad (34)$$

Case II Bb(2→3, 3→1). Solving for n_3 in terms of n_T utilizing equations 32 and 33 and substituting for Y_{31} utilizing equation 27 gives

$$B_{F_{3 \rightarrow 1}}^{2 \rightarrow 3} = \left(\frac{\ell}{4\pi} \right) A_{31} h\nu_{13} n_T \left[\frac{1}{1 + \frac{g_2}{g_3} \left(1 + \frac{E_{v23}^*}{E_{v23}} \right) \left(1 + \frac{g_1}{g_2} \exp(E_{12}/kT) \right) + \left(\frac{A_{31} + k_{31}}{k_{12}} \right)} \right] \quad (35)$$

Three Level System--Limiting Expressions

In this section of the manuscript, the limiting expressions for the 8 cases above will be given. The limiting expressions correspond to the low intensity case (conventional sources, i.e., $E_v^* \gg E_v$) and the high intensity case (laser sources, i.e., $E_v \gg E_v^*$).

Case I Aa(1→3, 3→1). Low Intensity.

$$B_{F_{3 \rightarrow 1}}^{1 \rightarrow 3} (Lo) = \left(\frac{\ell}{4\pi} \right) A_{31} h\nu_{13} n_T \left(\frac{g_3}{g_1} \right) \left(\frac{E_{v13}}{E_{v13}^*} \right) \quad (12a)$$

Case I Aa(1→3, 3→1). High Intensity.

$$B_{F_{3 \rightarrow 1}}^{1 \rightarrow 3} (Hi) = \left(\frac{\ell}{4\pi} \right) A_{31} h\nu_{13} n_T \left[\frac{1}{1 + \frac{g_1}{g_3} + \frac{k_{32}}{A_{21} + k_{23} + k_{21}}} \right] \quad (12b)$$

Case I Ab(1→3, 3→2, 2→1). Low Intensity.

$$B_{F_{2 \rightarrow 1}}^{1 \rightarrow 3} (Lo) = \left(\frac{\ell}{4\pi} \right) A_{21} h\nu_{12} n_T \left[\frac{g_3 k_{32} E_{v13}}{g_1 (A_{21} + k_{23} + k_{21}) E_{v13}^*} \right] \quad (15a)$$

Case I Ab(1→3, 3→2, 2→1). High Intensity.

$$B_{F_{2 \rightarrow 1}}^{1 \rightarrow 3} (Hi) = \left(\frac{\ell}{4\pi} \right) A_{21} h\nu_{12} n_T \left[\frac{1}{1 + \left(\frac{A_{21} + k_{23} + k_{21}}{k_{32}} \right) \left(1 + \frac{g_1}{g_3} \right)} \right] \quad (15b)$$

Case I Ba(1→2, 2→1). Low Intensity.

$$B_{F_{2 \rightarrow 1}}^{1 \rightarrow 2} (Lo) = \left(\frac{\ell}{4\pi} \right) A_{21} h\nu_{12} n_T \left[\frac{g_2 E_{v12}}{g_1 E_{v12}^*} \right] \quad (20a)$$

Case I Ba(1→2, 2→1). High Intensity.

$$B_{F_{2 \rightarrow 1}}^{(Hi)} = \left(\frac{\ell}{4\pi} \right) A_{21} h\nu_{12} n_T \left[\frac{1}{1 + \frac{g_1}{g_2} + \frac{k_{23}}{A_{31} + k_{31} + k_{32}}} \right] \quad (20b)$$

Case I Bb(1→2, 2→3, 3→1). Low Intensity.

$$B_{F_{3 \rightarrow 1}}^{(Lo)} = \left(\frac{\ell}{4\pi} \right) A_{31} h\nu_{13} n_T \left[\frac{g_2 k_{23} E_{v_{12}}}{g_1 (A_{31} + k_{31} + k_{32}) E_{v_{12}}^*} \right] \quad (23a)$$

Case I Bb(1→2, 2→3, 3→1). High Intensity.

$$B_{F_{3 \rightarrow 1}}^{(Hi)} = \left(\frac{\ell}{4\pi} \right) A_{31} h\nu_{13} n_T \left[\frac{1}{1 + \left(\frac{A_{31} + k_{31} + k_{32}}{k_{23}} \right) \left(1 + \frac{g_1}{g_2} \right)} \right] \quad (23b)$$

Case II Aa(1→3, 3→1). Low Intensity.

$$B_{F_{3 \rightarrow 1}}^{(Lo)} = \left(\frac{\ell}{4\pi} \right) A_{31} h\nu_{13} n_T \left[\frac{g_3 E_{v_{13}}}{g_1 E_{v_{13}}^* \left[1 + \frac{g_2}{g_1} \exp(-E_{12}/kT) \right]} \right] \quad (30a)$$

Case II Aa(1→3, 3→1). High Intensity.

$$B_{F_{3 \rightarrow 1}}^{(Hi)} = \left(\frac{\ell}{4\pi} \right) A_{31} h\nu_{13} n_T \left[\frac{1}{1 + \frac{g_1}{g_3} + \frac{g_2}{g_3} \exp(-E_{12}/kT) + \left(\frac{A_{32} + k_{32}}{k_{21}} \right)} \right] \quad (30b)$$

Case II Ab(1→3, 3→2). Low Intensity.

$$B_{F_{3 \rightarrow 2}}^{(Lo)} = \left(\frac{\ell}{4\pi} \right) A_{32} h\nu_{23} n_T \left[\frac{g_3 E_{v_{13}}}{g_1 E_{v_{13}}^* \left[1 + \frac{g_2}{g_1} \exp(-E_{12}/kT) \right]} \right] \quad (31a)$$

Case II Ab(1→3, 3→2). High Intensity.

$$B_{F_{3 \rightarrow 2}}^{(Hi)} = \left(\frac{\ell}{4\pi} \right) A_{32} h\nu_{23} n_T \left[\frac{1}{1 + \frac{g_1}{g_3} + \frac{g_2}{g_3} \exp(-E_{12}/kT) + \left(\frac{A_{32} + k_{32}}{k_{21}} \right)} \right] \quad (31b)$$

3. In saturation fluorescence measurements of n_T , B_F under steady state conditions must be measured, i.e., the radiative lifetime of the excited state must be much less than the temporal pulse width of the exciting source. Also, the source intensity must be such that the fluorescence radiance will increase by less than a few percent if the source intensity increases by orders of magnitude. Pulsed resonance spectroscopy where saturation is achieved and the transient decay is observed to determine n_T is difficult to perform experimentally.

4. For 3-level Case I atoms and for 1 \rightarrow 3 excitation, Y_F contains a cyclic term involving levels 2 and 3, i.e., crossover and crossback. This term is identical to the intersystem crossing-recrossing term in phosphorescence of organic molecules.

5. Spatial atom profiles (determination of absolute n_T values) via saturation fluorescence spectrometry (laser excitation with observation of fluorescence from a small volume excited by the laser) can be obtained if the atom (or molecule) is excited and de-excited as a 2-level system, or if the atom (or molecule) is a 3-level Case I (levels 2 and 3 close together). In the former case, one only has to measure B_F and if A_{21} , ν_{12} , g_1 and g_2 are known, then n_T can be calculated. In the latter case, one has to measure (absolute radiance) 3 \rightarrow 1 fluorescence $B_{F_{3\rightarrow 1}}^{1\rightarrow 3}$ and the ratio n_3/n_2 by measuring the ratio $\frac{B_{F_{2\rightarrow 1}}^{1\rightarrow 3}}{B_{F_{3\rightarrow 1}}^{1\rightarrow 3}} [= n_2/n_3 = k_{32}/(A_{21}+k_{21}+k_{23})]$. By use of equation 12b, assuming saturation (high intensity source) has been achieved, n_T can be estimated by substituting of values for A_{31} , $h\nu_{13}$, g_1 , g_3 and the ratio n_2/n_3 . For atoms of type Case II, it is not possible to determine n_T unless

$$\frac{g_1 + g_3}{g_3} > \left(\frac{A_{32} + k_{32}}{k_{21}} + \frac{g_2}{g_3} \exp(-E_{12}/kT) \right)$$

resulting in the simplification of equation 30b to

$$B_{F, \frac{3 \rightarrow 1}{1 \rightarrow 3}}(III) \approx \left(\frac{c}{4\pi} \right) A_{31} h\nu_{13} n_T \left(\frac{g_3}{g_1 + g_3} \right)$$

or simply the 2 level approximation for a 3-level case.

6. The definition of a saturation spectral irradiance is possible, i.e., the source spectral irradiance where the fluorescence radiance becomes 50% of the maximum possible value but no meaningful information results for the 3-level system since E_V^S depends upon not only measureable or known radiative transition probabilities, A's, but also upon difficult to measure and/or unknown radiationless rate constants, k's. Therefore, in this note, no attempt was made to give such values despite the simplicity of the resulting E_F expressions. (Refer to Appendix B for a general approach to evaluation of E_V^S).

7. The relative error resulting in the evaluation of n_T if the atom is assumed to be a 2-level case¹ and it is in fact, a 3-level Case I (Na) is -45% (excitation of level 2) or -22% (excitation of level 3) and if the atom is assumed to be a 3 level Case I but the crossover terms involving $3 \leftrightarrow 2$ are neglected⁷ is $\approx +44\%$ (excitation of level 2) and $+11\%$ (excitation of level 3). These values are calculated for an air-acetylene flame.²

8. Apparently anomalous saturation spectral irradiance values will be obtained if the source irradiance is not constant across the focal volume. Daily¹⁵ has discussed the effect of a Gaussian laser beam irradiance distribution on atomic fluorescence signals for several excitation geometries.

REFERENCES

1. R. M. Measures, J. Appl. Phys., 39, 5232 (1968).
2. B. W. Smith, J. D. Winefordner, and N. Omenetto, J. Appl. Phys., 48, 2676 (1977).
3. S. J. Weeks, N. Omenetto, and J. D. Winefordner, University of Florida, unpublished results.
4. N. Omenetto, P. Benetti, L. P. Hart, J. D. Winefordner, and C. Th. J. Alkemade, Spectrochim. Acta, 28B, 289 (1973).
5. N. Omenetto and J. D. Winefordner, Chapter on "Atomic Fluorescence Spectroscopy with Laser Excitation," in ANALYTICAL LASER SPECTROMETRY, N. Omenetto, editor, John Wiley, New York, in press.
6. J. W. Daily, Appl. Opt., 15, 955 (1976).
7. J. W. Daily, Appl. Opt., 16, 568 (1977).
8. D. R. D'Olivares, Ph.D. Thesis, Indiana University, Bloomington, Ind., 1976.
9. J. W. Daily, University of California at Berkeley, private communication.
10. F. R. Lipsett, "The Quantum Efficiency of Luminescence," Chapter in PROGRESS IN DIELECTRICS, Vol. 7, Iliffe Books Ltd., London.
11. A. Maitland and M. H. Dunn, J. Phys., 6D, 1266 (1973).
12. C. Th. J. Alkemade and P. T. J. Zeegers, Chapter on "Excitation and De-excitation Processes in Flames," in SPECTROCHEMICAL METHODS OF ANALYSIS, J. D. Winefordner, editor, John Wiley, New York, 1971.
13. J. D. Winefordner, S. G. Schulman, and T. C. O'Haver, LUMINESCENCE SPECTROMETRY IN ANALYTICAL CHEMISTRY, John Wiley, New York, 1973.
14. S. P. McGlynn, T. Azumi, and M. Kinoshita, MOLECULAR SPECTROSCOPY OF THE TRIPLET STATE, Prentice-Hall, Inc., Englewood Cliffs, New Jersey, 1969.

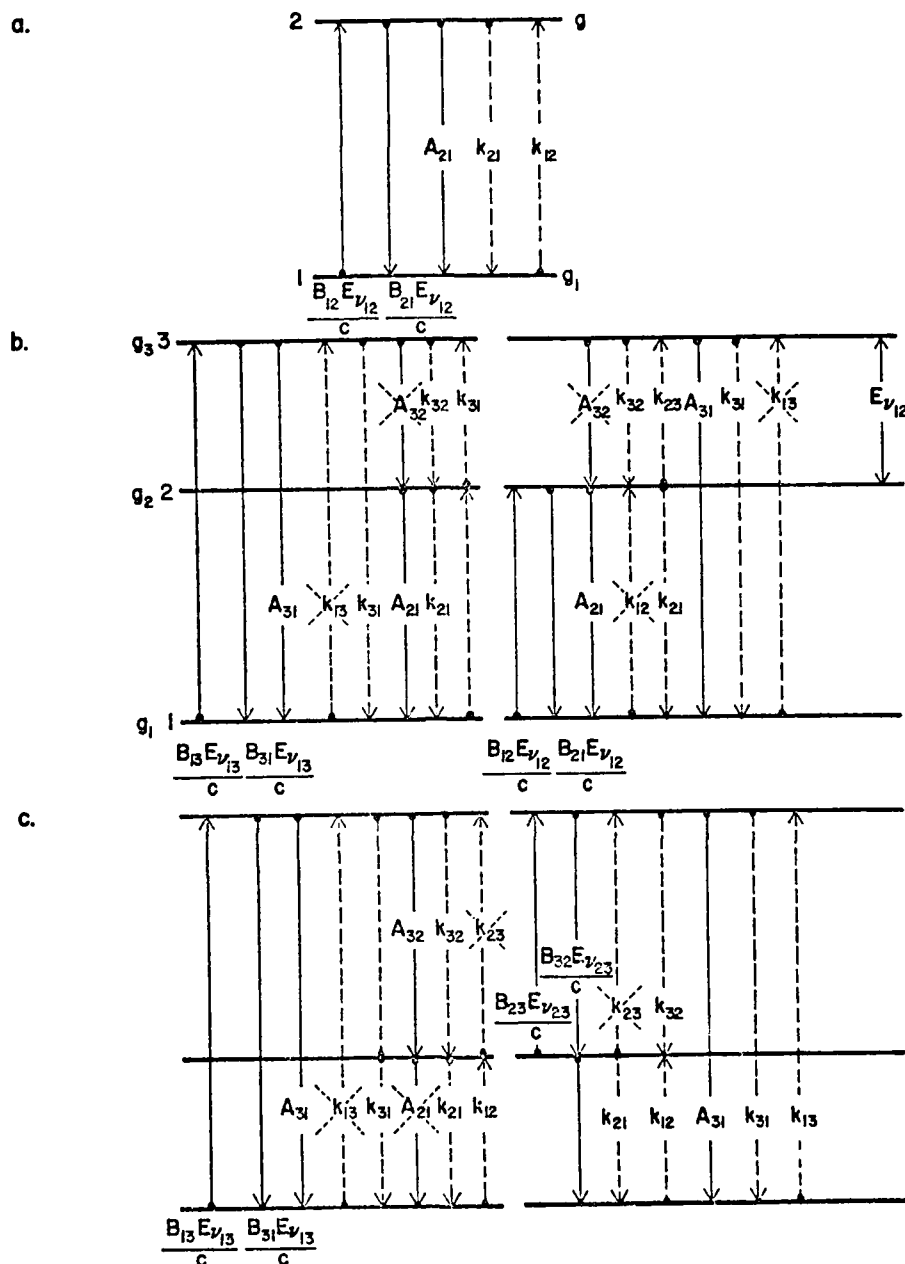


Figure 1A. a. Two Level Atomic System with Radiational, A, and Radiationless, k, Rate Constants.
 b. Three Level CASE I (e.g., Na) Atomic System With Radiational, A, and Radiationless, k, Rate Constants (k_{13} , k_{12} , $A_{32} \approx 0$). Left hand diagram is for $1 \rightarrow 3$ excitation. Right hand diagram is for $1 \rightarrow 2$ excitation.
 c. Three Level CASE II (e.g., Tl) Atomic System With Radiational, A, and Radiationless, k, Rate Constants (k_{13} , k_{23} , $A_{21} \approx 0$). Left hand diagram is for $1 \rightarrow 3$ excitation. Right hand diagram is for $2 \rightarrow 3$ excitation.

APPENDIX A1

STEADY STATE APPROACH TO CONCENTRATION EXPRESSIONS

Assuming that the rate equations approach can be safely applied and that the 3 levels can all be coupled radiatively, the general expressions for the rate of change of concentrations in states 1, 2, and 3 are given by

$$0 = \frac{dn_3}{dt} = - \left[\frac{B_{31}E_{v13}}{c} + \frac{B_{32}E_{v23}}{c} + A_{31} + A_{32} + k_{31} + k_{32} \right] n_3 + \left[\frac{B_{13}E_{v13}}{c} + k_{13} \right] n_1 + \left[\frac{B_{23}E_{v23}}{c} + k_{23} \right] n_2$$

Eqn. (A1)

$$0 = \frac{dn_2}{dt} = - \left[\frac{B_{23}E_{v23}}{c} + \frac{B_{21}E_{v12}}{c} + A_{21} + k_{21} + k_{23} \right] n_2 + \left[\frac{B_{32}E_{v23}}{c} + A_{32} + k_{32} \right] n_3 + \left[\frac{B_{12}E_{v12}}{c} + k_{12} \right] n_1$$

Eqn. (A2)

$$n_T = n_1 + n_2 + n_3 \quad (A3)$$

By setting the above equations equal to zero for steady state conditions, we can solve for the ratios n_2/n_1 , n_3/n_2 , and n_3/n_1 obtaining the following expressions

$$\frac{n_2}{n_1} = \frac{\left[\frac{B_{12}E_{v12}}{c} + k_{12} \right] + \frac{\left[\frac{B_{32}E_{v23}}{c} + A_{32} + k_{32} \right] \left[\frac{B_{13}E_{v13}}{c} + k_{13} \right]}{\left[\frac{B_{31}E_{v13}}{c} + \frac{B_{32}E_{v23}}{c} + A_{31} + A_{32} + k_{31} + k_{32} \right]} - \frac{\left[\frac{B_{23}E_{v23}}{c} + \frac{B_{21}E_{v12}}{c} + A_{21} + k_{21} + k_{23} \right] - \frac{\left[\frac{B_{32}E_{v23}}{c} + A_{32} + k_{32} \right] \left[\frac{B_{23}E_{v23}}{c} + k_{23} \right]}{\frac{B_{31}E_{v13}}{c} + \frac{B_{32}E_{v23}}{c} + A_{31} + A_{32} + k_{31} + k_{32}}}{\left[\frac{B_{23}E_{v23}}{c} + \frac{B_{21}E_{v12}}{c} + A_{21} + k_{21} + k_{23} \right] - \frac{\left[\frac{B_{32}E_{v23}}{c} + A_{32} + k_{32} \right] \left[\frac{B_{23}E_{v23}}{c} + k_{23} \right]}{\frac{B_{31}E_{v13}}{c} + \frac{B_{32}E_{v23}}{c} + A_{31} + A_{32} + k_{31} + k_{32}}} \quad (A4)$$

$$\frac{n_3}{n_2} = \frac{\frac{B_{23}E_{v23}}{c} + \frac{B_{21}E_{v12}}{c} + A_{21} + k_{23} + k_{21} - \frac{\left(\frac{B_{12}E_{v12}}{c} + k_{12}\right)\left(\frac{B_{21}E_{v12}}{c} + A_{21} + k_{21}\right)}{\frac{B_{13}E_{v13}}{c} + \frac{B_{12}E_{v12}}{c} + k_{12} + k_{13}}}{\left(\frac{B_{32}E_{v23}}{c} + A_{32} + k_{32}\right) + \frac{\left(\frac{B_{12}E_{v12}}{c} + k_{12}\right)\left(\frac{B_{31}E_{v13}}{c} + A_{31} + k_{31}\right)}{\left(\frac{B_{13}E_{v13}}{c} + \frac{B_{12}E_{v12}}{c} + k_{12} + k_{13}\right)}} \quad (A5)$$

$$\frac{n_3}{n_1} = \frac{\frac{B_{13}E_{v13}}{c} + k_{13} + \frac{\left(\frac{B_{23}E_{v23}}{c} + k_{23}\right)\left(\frac{B_{12}E_{v12}}{c} + k_{12}\right)}{\left(\frac{B_{23}E_{v23}}{c} + \frac{B_{21}E_{v12}}{c} + A_{21} + k_{23} + k_{21}\right)}}{\left(\frac{B_{31}E_{v13}}{c} + \frac{B_{32}E_{v23}}{c} + A_{31} + A_{32} + k_{31} + k_{32}\right) - \frac{\left(\frac{B_{23}E_{v23}}{c} + k_{23}\right)\left(\frac{B_{32}E_{v23}}{c} + A_{32} + k_{32}\right)}{\left(\frac{B_{23}E_{v23}}{c} + \frac{B_{21}E_{v12}}{c} + A_{21} + k_{23} + k_{21}\right)}}$$

Obviously (see specific cases in the manuscript) these expressions simplify when one particular 3-level case is considered and/or when excitation is performed at a selected transition.

For an atom with a complex set of energy levels and potential transitions, e.g., the transition elements, the actinide elements, and the rare earths, even more complex expressions result because more than 3 levels will be involved. In such a case, summations over activation and deactivation routes from or to a specific level must be made. Because of the limited use of such structurally-spectrally complex atoms in flame diagnostics via atomic fluorescence, no specialized expressions will be given here.

APPENDIX A2

SATURATION SPECTRAL IRRADIANCE, E_v^s

Omenetto et al.,²⁻⁵ D'Olivares,⁸ and Daily⁹ have utilized a parameter called the saturation spectral irradiance, E_v^s , which is useful experimentally because it is the value of source spectral irradiance when the fluorescence radiance is 50% of the maximum possible value (i.e., $B_{F_{\max}}$ is plateau value when $E_v \rightarrow \infty$).

For a 2-level atom, $E_{v_{12}}^s$ is given by

$$E_{v_{12}}^s = \left(\frac{c}{B_{21}} \right) \left(\frac{g_2}{g_1 + g_2} \right) (k_{21} + A_{21}) = \left(\frac{g_2}{g_1 + g_2} \right) E_{v_{12}}^* \quad (B1)$$

For a 3 level atom of the Na type, $E_{v_{lu}}^s$, is given by

$$E_{v_{lu}}^s = \left(\frac{c}{B_{ul}} \right) \left[\frac{k_{ul} + k_{uu'} + A_{ul} - k_{uu'} \left(\frac{k_{u'u}}{k_{u'l} + k_{u'u} + A_{u'l}} \right)}{1 + \frac{g_l}{g_u} + \frac{k_{uu'}}{k_{u'l} + k_{u'u} + A_{u'l}}} \right] \quad (B2a)$$

or

$$E_{v_{lu}}^s = E_{v_{lu}}^* \frac{g_l}{g_u} \left[\frac{1}{1 + \frac{g_l}{g_u} + \frac{k_{uu'}}{k_{u'l} + k_{u'u} + A_{u'l}}} \right] \quad (B2b)$$

where the terms are as defined previously (l is the ground state, u is the radiationally excited upper state, and u' is the other excited upper state). Experimentally one can plot B_F vs E_V and determine E_V^S by simply estimating E_V^S at $B_{F_{\max}}/2$. Theoretically, it is difficult (in many cases, impossible) to estimate E_V^S because of the lack of information on the radiationless rate constants, k_s . The expression for $E_{V_{lu}}^S$ converts to the $E_{V_{12}}^S$ expression for the 2 level atom if one assumes all k and A terms with u' are zero.

For a three-level atom of the T_l^2 type, a different expression results namely

$$E_{V_{lu}}^S = \left(\frac{c}{B_{lu}} \right) \frac{(A_{ul} + A_{ul'} + k_{ul} + k_{ul'})}{\frac{g_l}{g_u} + \frac{k_{ll'} + A_{ul'} + k_{ul'}}{k_{ll'} + k_{l'l}}} \quad (B3a)$$

or

$$E_{V_{lu}}^S = \frac{\frac{g_l}{g_u} E_{V_{lu}}^*}{\frac{g_l}{g_u} + \frac{k_{ll'} + A_{ul'} + k_{ul'}}{k_{ll'} + k_{l'l}}} \quad (B3b)$$

where u is the upper level, l is the lower level from which radiational excitation occurs, and l' is the other low level (for T_l^2 , $u = 3$, $l = 1$ or 2 , and $l' = 2$ or 1 , respectively). The above expression (B3) converts to the two-level case with appropriate substitutions.

APPENDIX B
(manuscript submitted to APPL. OPTICS)

FIVE LASER EXCITED FLUORESCENCE
METHODS TO MEASURE SPATIAL FLAME TEMPERATURES
PART I. THEORETICAL BASIS

J.D. Bradshaw^b
N. Omenetto^c
G. Zizak^d
J.N. Bower^e
J.D. Winefordner^f

Department of Chemistry
University of Florida
Gainesville, FL 32611

- a. Research supported by AF-AFOSR-F49620-80-C-0005 and by AF-33615-78C-2036.
- b. Present Address: Department of Chemistry, University of Florida, Gainesville, FL 32611
- c. Present Address: CCR, European Community Center, Stabilimento di Ispra, Anal. Chem. Div., Bat. 29, 21020 ISPRA (Varese) ITALY
- d. On leave from: CNPM-Politecnico, Viale F. Baracca 69, 20068 Peschiera Borromeo, Milano, ITALY
- e. Present Address: E.R. Squibb & Sons, Georges Road, New Brunswick, N.J. 08903
- f. Author to whom all reprint requests should be sent.

ABSTRACT

Five methods for measurement of flame temperatures based upon laser excited fluorescence are discussed with respect to the derived expressions, the assumptions necessary, the advantages, and the disadvantages. The use of each of the five methods for measuring spatial (flame volumes of $\leq 1 \text{ mm}^3$) and temporal (flame temperatures corresponding to $\leq 1 \text{ } \mu\text{s}$ time period) is given. The five methods consist of one based upon linearity between the fluorescence signal and the laser spectral irradiance, of three based upon saturation, and of a fifth which is not critically dependent upon the laser spectral irradiance.

Introduction.

Atomic fluorescence excited with a spectrally quasi-continuum source has been shown to be a reliable method of measuring flame temperatures.¹⁻⁷ In fact, it combines the advantages of optical methods, namely not disturbing the combustion process, with the capability of providing spatially resolved measurements: the latter feature is common to all "scattering" methods, including those based on Raman methods.⁸

The use of a laser as an excitation source for atomic fluorescence has the obvious advantage that the spatial resolution can be improved because of the low divergence of the collimated beam coupled with its high spectral radiance. The use of a pulsed laser has the additional characteristic when used with a gated detection system of measuring temporal (short time period) temperatures.

Both Measures⁹ and Omenetto and Winefordner^{10,11} have discussed the use of laser saturation of probe transitions and the measurement of appropriate fluorescence transitions for estimation of flame temperatures. These reports indicated that neither calibration of the electro-optical detection system was needed nor was measurement of the laser power.

In this paper, we give the theoretical expressions of 5 fluorescence-based methods for flame temperature measurement including predicted advantages and disadvantages of each method. Two of the methods have been previously described.¹⁻¹¹ All five methods are described with consistent terminology using the well-known steady state approach; the general expressions and symbolism are according to the manuscript of Boutilier, et al.¹²

Theoretical Basis

Boundary Conditions and General Expressions. In all five methods, a 3-level probe, such as Tl, In, Ga, Pb, etc., is assumed to be in the flame. This can be experimentally accomplished by nebulization of a salt solution containing the inorganic probe to produce an aerosol which is partially and reproducibly transferred to the flame system under study. Such methods are described by Herrmann and Alkemade.¹³ It can also be accomplished by metal vapor generation or vaporization of volatile metal complexes.

An energy level diagram with appropriate symbols for activation and deactivation rates is given in Figure 1. For an atomic probe, such as Tl, excited at either 1→3 or at 2→3 (see Figure 1) the following assumptions can be made: $k_{13} \approx 0$; $k_{23} \approx 0$; $A_{21} = 0$. Solving for the ratio of n_3/n_1 and n_2/n_1 for steady state conditions¹² ($dn_3/dt = 0$ and $dn_2/dt = 0$) under continuum or pseudo continuum excitation gives

$$\frac{n_3}{n_1} = \frac{\frac{B_{13}E_{v13}}{c} + \frac{\left(\frac{B_{23}E_{v23}}{c}\right)k_{12}}{\frac{B_{23}E_{v23}}{c} + k_{23} + k_{21}}}{\left[\frac{B_{31}E_{v13}}{c} + \frac{B_{32}E_{v23}}{c} + A_{31} + A_{32} + k_{31} + k_{32}\right] - \left[\frac{\frac{B_{23}E_{v23}}{c} + k_{23} \frac{B_{32}E_{v32}}{c} + A_{32} + k_{31}}{\frac{B_{23}E_{v23}}{c} + k_{21}}\right]}$$

$$\frac{n_2}{n_1} = \frac{k_{12} + \left[\frac{\left(\frac{B_{32}E_{v13}}{c} + A_{32} + k_{32}\right) \frac{B_{13}E_{v13}}{c}}{\frac{B_{31}E_{v13}}{c} + \frac{B_{32}E_{v23}}{c} + A_{31} + A_{32} + k_{31} + k_{32}}\right]}{\left(\frac{B_{23}E_{v23}}{c} + k_{21}\right) - \left[\frac{\left(\frac{B_{32}E_{v23}}{c} + A_{32} + k_{32}\right) \left(\frac{B_{23}E_{v23}}{c}\right)}{\frac{B_{31}E_{v13}}{c} + \frac{B_{32}E_{v23}}{c} + A_{31} + A_{32} + k_{31} + k_{32}}\right]} \quad (2)$$

The fluorescence radiance, B_F , in $J\ m^{-2}s^{-1}sr^{-1}$, is given by

$$B_F = \left(\frac{\ell}{4\pi}\right) A_{em} h\nu_{em} n_u \quad (3)$$

where ℓ is the emission (fluorescence) path length, in m, A_{em} is the spontaneous emission probability for the fluorescence process in s^{-1} , $h\nu_{em}$ is the energy of the emission photon, in J, and n_u is the population density of the upper level involved in the fluorescence transition, in m^{-3} . For the two fluorescence transitions involved in the case of Tl-like probes, $B_{F_{3\rightarrow1}}$ and $B_{F_{3\rightarrow2}}$ are

$$B_{F_{3\rightarrow1}} = \left(\frac{\ell}{4\pi}\right) A_{31} h\nu_{31} n_3 \quad (4)$$

$$B_{F_{3\rightarrow2}} = \left(\frac{\ell}{4\pi}\right) A_{32} h\nu_{32} n_3 \quad (5)$$

Using equations (1) and (2) with the necessary condition

$$n_T = n_1 + n_2 + n_3 \quad (6)$$

and with either Equation (4) or (5) allows evaluation of $B_{F_{3\rightarrow1}}$ and $B_{F_{3\rightarrow2}}$ in terms of n_T and appropriate excitation conditions i.e., E_v .

Method I. Two Line Linear Method¹⁻⁷ In this method, the fluorescence at $3\rightarrow1$ excited via $2\rightarrow3$, $B_{F_{3\rightarrow1, 2\rightarrow3}}$, and the fluorescence at $3\rightarrow2$ excited via

$1\rightarrow3$, $B_{F_{3\rightarrow2, 1\rightarrow3}}$ are measured under linear B_F vs E_v conditions. Evaluating

Equations 4 and 5 for these conditions gives¹²

$$B_{F_{\substack{3 \rightarrow 1 \\ 2 \rightarrow 3}}} = \left(\frac{\ell}{4\pi}\right) A_{31} h\nu_{31} n_T \frac{g_3 E_{\nu_{23}}}{g_2 E_{\nu_{23}} \left[1 + \frac{g_1}{g_2} \exp(E_{12}/kT) \right]} \quad (7)$$

$$B_{F_{\substack{3 \rightarrow 2 \\ 1 \rightarrow 3}}} = \left(\frac{\ell}{4\pi}\right) A_{32} h\nu_{32} n_T \frac{g_3 E_{\nu_{13}}}{g_1 E_{\nu_{13}} \left[1 + \frac{g_2}{g_1} \exp(E_{12}/kT) \right]} \quad (8)$$

where all terms are defined in the caption of Figure 1 except

$E_{\nu_{23}}^*$ = modified saturation spectral irradiance with excitation at ν_2 :

$$E_{\nu_{23}}^* = \frac{c A_{32}}{B_{32} Y_{32}} = \frac{8\pi h \nu_{23}^3}{c^2 Y_{32}} \quad \text{and} \quad Y_{32} = \frac{A_{32}}{A_{31} + A_{32} + k_{32} + k_{31}} \quad (9)$$

$E_{\nu_{13}}^*$ = modified saturation spectral irradiance with excitation at ν_1 :

$$E_{\nu_{13}}^* = \frac{c A_{31}}{B_{31} Y_{31}} = \frac{8\pi h \nu_{31}^3}{c^2 Y_{31}} \quad \text{and} \quad Y_{31} = \frac{A_{31}}{A_{31} + A_{32} + k_{31} + k_{32}} \quad (10)$$

where ν is the frequency, in Hz, of the appropriate excitation transition and Y is the quantum efficiency of the designated fluorescence process of the probe in the specific environment of concern. Dividing Equation (8) by (7) and using the more common units $\text{J s}^{-1} \text{m}^{-2} \text{nm}^{-1}$ for the source spectral irradiances, we obtain the following expression for the temperature, T

$$T_1 = \frac{E_{12}/k}{\ln\left(\frac{E_{\lambda_{23}}}{E_{\lambda_{13}}}\right) + 6 \ln\left(\frac{\lambda_{23}}{\lambda_{13}}\right) + \ln\left(\frac{B_{F_{3+2}}}{B_{F_{3+1}}}\right)} \quad (11)$$

Method II. Saturation Two Level Peak Method (Pseudo-Two Level Steady State)

In this method, the ratio of the fluorescence radiance resulting from pumping both 1-3 and 2-3 sequentially is measured. However, in this method, it is assumed that at a sufficiently high source spectral irradiance (and fast rise time), the pumping time, $t_p^\#$, is sufficiently short to assure that $t_p^{-1} \gg k_{31} + k_{32} + A_{31} + A_{32}$. In this case, the system reduces to a pseudo-two level system consisting of only the states being pumped. In other words, $\frac{B_{12}E_{12}}{c}$ and $\frac{B_{21}E_{12}}{c}$ dominate over all other rates in a period of time which is much shorter than the upper level's lifetime, τ . In this case not only must $t_p^\#$ be sufficiently small, but the measurement system for the resultant fluorescence radiance must also be sufficiently fast to resolve temporally the fluorescence temporal waveform in order to obtain accurate measure of the steady state levels for the fluorescence radiance, which first rises to a pseudo-two level steady-state value (peak) with a response time controlled by t_p and then relaxes to its three level steady state value controlled by k_{31} , k_{32} , k_{12} , k_{21} , A_{31} , A_{32} (see Figure 2). This process has been described by Measures⁹, and by Omenetto and Winefordner.^{10,11}

[#] The pumping time, t_p , is given by¹⁰; $t_p \equiv \tau \left(\frac{E_{v0}^S}{E_{v0} + E_{v0}^S} \right)$, where τ is the effective lifetime ($\tau = 1/\sum k_{sp} Y$) and $E_{v0}^S \propto \frac{1}{Y}$. For $E_{v0} \gg E_{v0}^S$, then $t_p \neq \tau_h(Y)$.

The 3→1 fluorescence radiance for 1→3 excitation and for 2→3 excitation under saturation 2-level conditions are given^{10,11} by

$$B_{F_{3 \rightarrow 1}}^{1 \rightarrow 3} = \left(\frac{g}{4\pi}\right) A_{31} h\nu_{31} n_3 = \left(\frac{g}{4\pi}\right) A_{31} h\nu_{31} n_T \left(\frac{g_3}{g_1 + g_3}\right) \quad (12)$$

$$B_{F_{3 \rightarrow 1}}^{2 \rightarrow 3} = \left(\frac{g}{4\pi}\right) A_{31} h\nu_{31} n'_3 = \left(\frac{g}{4\pi}\right) A_{31} h\nu_{31} n_T \left(\frac{g_2}{g_1}\right) \exp(-E_{12}/kT) \left(\frac{g_3}{g_2 + g_3}\right) \quad (13)$$

where n_T is essentially the population of the ground level prior to laser excitation

Dividing Equation (12) by (13) gives

$$\frac{B_{F_{3 \rightarrow 1}}^{1 \rightarrow 3}}{B_{F_{3 \rightarrow 1}}^{2 \rightarrow 3}} = \left(\frac{g_2 + g_3}{g_1 + g_3}\right) \left(\frac{g_1}{g_2}\right) \exp(E_{12}/kT) \quad (14)$$

Solving for T and introducing the g values for T1 gives

$$T_{II} \equiv \frac{E_{12}/k}{\ln \left[\frac{4}{3} \left(\frac{B_{F_{3 \rightarrow 1}}^{1 \rightarrow 3}}{B_{F_{3 \rightarrow 1}}^{2 \rightarrow 3}} \right) \right]} \quad (15)$$

Method III. Saturation Two Line Method With Sequential Pumping.

In this method, the ratio of fluorescence signals are measured after sequential excitation of fluorescence under saturation conditions assuming the system has relaxed to its three level state (see Method II). Because several ratios can be used, four fluorescence radiance expressions will be

given by evaluating Equations 4 and 5 assuming saturation conditions apply, i.e.,

$$B_{F_{3 \rightarrow 1}^{1 \rightarrow 3}} = \left(\frac{g}{4\pi} \right) A_{31} h \nu_{31} n_T \left[\frac{1}{\frac{g_1 + g_3}{g_3} + \left(\frac{g_2}{g_3} \right) \exp(-E_{12}/kT) + \frac{A_{32} + k_{32}}{k_{21}}} \right] \quad (16)$$

$$B_{F_{3 \rightarrow 2}^{1 \rightarrow 3}} = \left(\frac{\nu_{32} A_{32}}{\nu_{31} A_{31}} \right) B_{F_{3 \rightarrow 1}^{1 \rightarrow 3}} \quad (17)$$

$$B_{F_{3 \rightarrow 1}^{2 \rightarrow 3}} = \left(\frac{g}{4\pi} \right) A_{31} h \nu_{31} n_T \left[\frac{1}{\frac{g_2 + g_3}{g_3} + \left(\frac{g_1}{g_3} \right) \exp(E_{12}/kT) + \frac{A_{31} + k_{31}}{k_{12}}} \right] \quad (18)$$

$$B_{F_{3 \rightarrow 2}^{2 \rightarrow 3}} = \left(\frac{\nu_{32} A_{32}}{\nu_{31} A_{31}} \right) B_{F_{3 \rightarrow 1}^{2 \rightarrow 3}} \quad (19)$$

In general, the ratio of $B_{F_{3 \rightarrow 1}^{i \rightarrow 3}} / B_{F_{3 \rightarrow j}^{i \rightarrow 3}}$, where i and j correspond to levels

1 or 2, is given by

$$\frac{B_{F_{3 \rightarrow i}^{1 \rightarrow 3}}}{B_{F_{3 \rightarrow j}^{2 \rightarrow 3}}} = \left(\frac{\nu_{3i} A_{3i}}{\nu_{3j} A_{3j}} \right) \left[\frac{\frac{g_2 + g_3}{g_3} + \left[\frac{g_1}{g_3} + \frac{g_1}{g_2} \left(\frac{A_{31} k_{31}}{k_{21}} \right) \right] \exp(E_{12}/kT)}{\frac{g_1 + g_3}{g_3} + \frac{A_{32} + k_{32}}{k_{21}}} \right] \quad (20)$$

as long as a probe is chosen where $\exp(-E_{12}/kT) \ll 1$ (or $E_{12}/T \ll 10^{-3} \text{ eV K}^{-1}$) this corresponds Ti or Pb for flame temperatures below $\sim 4000 \text{ K}$ but does

not apply to Ga or In for flame temperatures between 2000 and 4000 K.

Solving for T (and introducing $g_1 = g_3 = 1$; $g_2 = 2$) gives

$$T_{III} = \frac{E_{12}/k}{\ln \left\{ \frac{2 + \frac{A_{32} + k_{32}}{k_{21}}}{\frac{1}{2} \left(2 + \frac{A_{31} + k_{31}}{k_{21}} \right)} \right\} \left\{ \frac{\nu_{3j} A_{3j}}{\nu_{3i} A_{3i}} \right\} \left\{ \frac{B_{F_{3 \rightarrow i}}}{B_{F_{3 \rightarrow j}}} \right\} - 3 \left[\frac{2}{2 + \left(\frac{A_{31} + k_{31}}{k_{21}} \right)} \right]} \quad (21)$$

If in addition, the following assumption is valid, $k_{21} \gg (A_{31} + k_{31}) \approx (A_{32} + k_{32})$, then Equation (21) reduces to

$$T_{III}' \approx \frac{E_{12}/k}{\ln \left[2 \left(\frac{\nu_{3j} A_{3j}}{\nu_{3i} A_{3i}} \right) \left(\frac{B_{F_{3 \rightarrow i}}}{B_{F_{3 \rightarrow j}}} \right) - 3 \right]} \quad (21')$$

Finally if $n_2 \ll 30 n_T$ and since $\nu_{3j} A_{3j} / \nu_{3i} A_{3i} \approx 1$, then Equation (18) reduces further to

$$T_{III}'' \approx \frac{E_{12}/k}{\ln \left[2 \left(\frac{B_{F_{3 \rightarrow i}}}{B_{F_{3 \rightarrow j}}} \right) \right]} \quad (21'')$$

Method IV. Saturation Two Line Method With Simultaneous Pumping.

In this method, which is similar to Method III, the ratio of the fluorescence radiance resulting from pumping both 1 \rightarrow 3 and 2 \rightarrow 3 simultaneously to the fluorescence resulting from pumping one of the fluorescence transitions

given in Method II (under saturation conditions) is measured. From Equations (1), (2), (4), (5), and (6), the fluorescence radiance for simultaneous pumping is given by

$$B_{F_{3 \rightarrow 1}} = \left(\frac{g}{4\pi} \right) h\nu_{31} A_{31} n_T \left[\frac{g_3}{g_1 + g_2 + g_3} \right] \quad (22)$$

$\begin{matrix} 1 \rightarrow 3 \\ \langle 2 \rightarrow 3 \rangle \end{matrix}$

if the fluorescence at 3→1 is measured and by

$$B_{F_{3 \rightarrow 2}} = \left(\frac{\nu_{32} A_{32}}{\nu_{31} A_{31}} \right) B_{F_{3 \rightarrow 1}} \quad (23)$$

$\begin{matrix} 1 \rightarrow 3 \\ \langle 2 \rightarrow 3 \rangle \end{matrix}$ $\begin{matrix} 1 \rightarrow 3 \\ \langle 2 \rightarrow 3 \rangle \end{matrix}$

if the fluorescence at 3→2 is measured. For the case, where the ratio of

$B_{F_{3 \rightarrow 1}}$ to $B_{F_{3 \rightarrow 2}}$ is measured

$\begin{matrix} 1 \rightarrow 3 \\ \langle 2 \rightarrow 3 \rangle \end{matrix}$ $\begin{matrix} 2 \rightarrow 3 \end{matrix}$

$$\frac{B_{F_{3 \rightarrow 1}}}{B_{F_{3 \rightarrow 2}}} = \frac{\frac{g_2 + g_3}{g_3} + \left[\frac{g_1}{g_3} + \frac{g_1}{g_2} \left(\frac{A_{31} + k_{31}}{k_{21}} \right) \right] \exp(E_{12}/kT)}{\frac{g_1 + g_2 + g_3}{g_3}} \quad (24)$$

$\begin{matrix} 1 \rightarrow 3 \\ \langle 2 \rightarrow 3 \rangle \end{matrix}$ $\begin{matrix} 2 \rightarrow 3 \end{matrix}$

Solving for T from Equation (24) and evaluating the g's gives

$$T_{IV} = \frac{E_{12}/k}{\ln \left[4 \left(\frac{B_{F_{3 \rightarrow 1}}}{B_{F_{3 \rightarrow 1} + \frac{A_{31} + k_{31}}{k_{21}}}} \right) - 3 \right]} \quad (25)$$

and, as previously in Method III, if $k_{21} \gg (A_{31} + k_{31})$, then

$$T_{IV}' \approx \frac{E_{12}/k}{\ln \left[4 \left(\frac{B_{F_{3 \rightarrow 1}}}{B_{F_{3 \rightarrow 1} + \frac{A_{31} + k_{31}}{k_{21}}}} \right) - 3 \right]} \quad (25')$$

and finally as in Method III, if $n_2 \ll 30_{n_T}$, then

$$T_{IV}'' \approx \frac{E_{12}/k}{\ln \left[4 \left(\frac{B_{F_{3 \rightarrow 1}}}{B_{F_{3 \rightarrow 1} + \frac{A_{31} + k_{31}}{k_{21}}}} \right) - 3 \right]} \quad (25'')$$

The case where the ratio of $B_{F_{3 \rightarrow 1}}$ to $B_{F_{3 \rightarrow 1}}$ is measured is not considered
 $\frac{B_{F_{3 \rightarrow 1}}}{B_{F_{3 \rightarrow 1} + \frac{A_{31} + k_{31}}{k_{21}}}}$ $\frac{B_{F_{3 \rightarrow 1}}}{B_{F_{3 \rightarrow 1}}}$

here because this case is limited by the precision in the measurement
 (i.e., the ratio varies from $\frac{1}{2}$ at $T \rightarrow 0$ to a maximum of $\frac{1}{2}$ at $T \rightarrow \infty$).

In the above cases in this method, it is assumed that measurement of the fluorescence radiance occurs in the three level temporal regime (see

Method II). If instead we take the case where the 2 3 excitation occurs just prior to the simultaneous pumping of 1 3 and 2 3 (see Figure 3) and if $t_{p_{2\ 3}}$ is fast enough to achieve a pseudo-two level system, then the observed fluorescence radiance ration $B_{F_{3 \rightarrow 1}^{peak} / B_{F_{3 \rightarrow 1}^{2 \rightarrow 3} < \frac{1 \rightarrow 3}{2 \rightarrow 3} >}}$ is given by,

$$\frac{B_{F_{3 \rightarrow 1}^{peak}}}{B_{F_{3 \rightarrow 1}^{2 \rightarrow 3} < \frac{1 \rightarrow 3}{2 \rightarrow 3} >}} = \left(\frac{g_1(g_2 + g_3)}{g_2(g_1 + g_2 + g_3)} \right) \exp(-E_{12}/kT) \quad (26)$$

Substituting for the g's yields

$$T_{IV_{peak}} \equiv \frac{E_{12}/k}{\ln \left[\left(\frac{8}{3} \right) \left(\frac{B_{F_{3 \rightarrow 1}^{2 \rightarrow 3} < \frac{1 \rightarrow 3}{2 \rightarrow 3} >}}{B_{F_{3 \rightarrow 1}^{peak}}} \right) \right]} \quad (27)$$

It should be noted that $T_{IV_{peak}}$ is completely independent of k_{12} , k_{21} , k_{31} , k_{32} , A_{31} , A_{32} .

Method V. Fluorescence-thermally Assisted Fluorescence Method.

In this method, only one laser excitation wavelength is needed and achievement of saturation is not necessary (see Figure 4). Here, the upper level of the probe, 3 in our case, is excited via a laser and then either the ratio of the fluorescence 3 \rightarrow 1 to the thermally assisted fluorescence from a close lying upper level, say 4 \rightarrow 1, is measured or the ratio of

the thermally assisted fluorescence from two close lying upper levels, say 5+1 to 4+1 is measured.

Solving the steady state equations¹⁰ (in a system similar to that shown in Figure 4) for, n_3/n_4 , gives

$$\frac{n_3}{n_4} = \frac{k_{43}}{k_{34}} + \frac{k_{41} + A_{41}}{k_{34}} \quad (28)$$

where it is assumed that $A_{43} = 0$ and that the color temperature of the sources of excitation are large compared to the thermal temperature under consideration; this assumption is valid under most cases employing laser excitation (i.e., $\frac{B_{13}E_{13}}{c} \gg k_{13}, k_{14}, \text{ or } k_{34}$). The ratio of fluorescence radiances $B_{F_{3 \rightarrow 1}}/B_{TF_{4 \rightarrow 1}}$ is proportional to n_3/n_4 . In addition if we assume that the energy difference between levels 4 and 3, E_{34} , compared to E_{13} , is significantly small (i.e., $\exp(-E_{34}/kT) \gg \exp(-E_{13}/kT)$) to allow us to assume that $k_{34} \gg k_{41} + A_{41}$, then equation (26) reduces to,

$$\frac{n_3}{n_4} = \frac{k_{43}}{k_{34}} \quad (29)$$

which is simply the Boltzmann distribution where,

$$\frac{n_4}{n_3} = \frac{g_4}{g_3} e^{-E_{34}/kT} \quad (30)$$

Including other levels such as in the Tl-type atomic system will

further complicate analysis of n_i/n_j for various levels, but under the same set of limiting conditins, where it is assumed that the Boltzmann distribution applies (i.e., E_{ij} not too large for the given T), then we will employ

$$\frac{n_i}{n_j} = \frac{g_i}{g_j} e^{-E_{ji}/kT} \quad (31)$$

for all levels with i and j the upper level being pumped.

In the case of Tl-like atomic probes we can obtain the thermally assisted fluorescence radiance expression given by:

$$B_{TF_{i \rightarrow 1}}^{1 \rightarrow 3} = \left(\frac{\ell}{4\pi}\right) A_{i1} h_{i1} \left(\frac{g_i}{g_3}\right) \exp(-E_{i3}/kT) n_T \left[\frac{1}{\frac{g_1 + g_3}{g_3} + \frac{g_1}{g_3} \exp(-E_{12}/kT) + \frac{A_{32} + k_{32}}{k_{21}}} \right] \quad (32)$$

$$B_{TF_{i \rightarrow 1}}^{2 \rightarrow 3} = \left(\frac{\ell}{4\pi}\right) A_{i1} h_{i1} \left(\frac{g_i}{g_3}\right) \exp(E_{i3}/kT) n_T \left[\frac{1}{\frac{g_2 + g_3}{g_3} + \frac{g_1}{g_3} \exp(-E_{12}/kT) + \frac{A_{31} + k_{31}}{k_{12}}} \right] \quad (33)$$

Taking the ratio of $B_{F_{3 \rightarrow h}}^{g \rightarrow 3}$ to $B_{TF_{i \rightarrow 1}}^{g \rightarrow 3}$, where h is the lower level of the

fluorescence transition, g is the lower level (1 or 2) of the excitation transition, and i is the upper level produced by thermal excitation of the laser excited level, 3, gives

$$\frac{B_{F_{3 \rightarrow h}}}{B_{TF_{i \rightarrow 1}}}_{g \rightarrow 3} = \left(\frac{A_{3h} \nu_{3h} g_3}{A_{i1} \nu_{i1} g_i} \right) \exp(E_{i3}/kT) \quad (34)$$

and solving for T gives

$$T = \frac{E_{i3}/k}{\ln \left[\left(\frac{g_i A_{i1} \nu_{i1}}{g_3 A_{3h} \nu_{3h}} \right) \left(\frac{B_{F_{3 \rightarrow h}}}{B_{TF_{i \rightarrow 1}}}_{g \rightarrow 3} \right) \right]} \quad (35)$$

Taking the ratio of 2 thermally excited emission lines gives

$$\frac{B_{TF_{i \rightarrow 1}}}{B_{TF_{j \rightarrow 1}}}_{g \rightarrow 3} = \left(\frac{A_{i1} \nu_{i1} g_i}{A_{j1} \nu_{j1} g_j} \right) \exp\left(\frac{E_j - E_i}{kT}\right) \quad (36)$$

and solving for T gives

$$T_V = \frac{(E_j - E_i)/k}{\ln \left[\left(\frac{A_{j1} \nu_{j1} g_j}{A_{i1} \nu_{i1} g_i} \right) \left(\frac{B_{TF_{i \rightarrow 1}}}{B_{TF_{j \rightarrow 1}}}_{g \rightarrow 3} \right) \right]} \quad (37)$$

Theoretical Comparison of Methods.

Method I. The advantages of this method are:

- (i) saturation is not necessary and in fact must not be approached; thus relatively low laser irradiances can and must be used;
- (ii) it is independent of non-radiative activation and deactivation rate constants and radiative deactivation rate constants, i.e., no assumptions are needed to obtain the expression for T_I ; and
- (iii) temporal flame temperatures can be obtained by passing both beams through the flame of interest but delaying one beam (pulse) and measuring the ratio of B_F values for the individual pulses. The time integrated as well as the time dependent fluorescence radiance may be measured in this method, since it is assumed that $\frac{B_{lu}E_{lu}}{c} \gg k_{lu}$ and $E_{v0} \ll E_{v0}^S$ (i.e., $k_{ul}'s + A_{ul}'s \gg \frac{B_{lu}E_{lu}}{c}$). Therefore, the fluorescence temporal waveform will follow the source temporal waveform linearly at all points in time where these conditions hold. Both the fluorescence radiance and the source spectral irradiance require the same integration time, τ_{meas} , and the same time delay, τ_{delay}

The disadvantages of this method are:

- (i) because the fluorescence radiance values, B_F , depend linearly upon the source spectral irradiance, E_v , and the flame quantum efficiency, Y , the fluorescence signal strengths are lower than in saturation based methods for equal n_T 's;
- (ii) for the 3→1 fluorescence process, the post filter effect causes a reduction in the fluorescence signal;

- (iii) B_F vs E_v must be linear, i.e., measurements must be taken on the linear portion of the B_F vs E_v plot;
- (iv) the source spectral irradiances at 1+3 and at 2+3 must be calibrated in relative irradiance units and the fluorescence radiances at 3+2 and at 3+1 must be calibrated in relative radiance units assuming equal τ_{meas} and τ_{delay} ;
- (v) the two laser beams resulting in excitation at 1+3 and at 2+3 must be matched in terms of optical alignment and must not cause saturation even in the central portion of the beams;
- (vi) single pulse temperature measurements require an accurate repeatable measure of $\Delta\lambda_{\text{laser}}$ from pulse to pulse since the source spectral irradiance must be accurately known; and
- (vii) the paired measurement of 1+3 and 2+3 excitation must occur on a time scale such that $\Delta Y/\Delta t = 0$.

Methods II and IV_{peak}. The advantages of these methods are:

- (i) the non-radiational and radiational rate constants do not enter the T_{II} relationship, i.e., no approximations are required;
- (ii) temporal temperatures are more easily obtained since only the fluorescence radiances need to be measured; and
- (iii) high speed "real-time" temperature computation is more accessible due to the simplistic relationship for T_{II} , and $T_{IV\text{peak}}$.

The disadvantages of these methods are:

- (i) the laser pulses must be spatially homogeneous which usually requires spatial filtering of the dye lasers output limiting this technique to high power Nd-YAG and excimer pumped dye laser systems for low quantum efficiency combustors (atmospheric

hydrocarbon flames);

- (ii) the laser pulse rise time(s) must be sufficiently "fast" enough to allow t_p^{-1} to be much larger than all the other collisional rates, which may further limit the technique to cavity-dumped systems when Y is very small;
- (iii) the detection system must be "fast" enough not to significantly distort the temporal information content, i.e., the pseudo-two level peak region, and have sufficient sensitivity to assure a single pulse $S/N > 10$ (i.e., greater than 10^2 photons measured per τ_{meas});

- (iv) scatter errors (Mie scatter primarily) may be appreciable for resonance processes; non-resonance fluorescence minimizes this problem, it is recommended that $B_{F_{3 \rightarrow 1, 1 \rightarrow 3}}$ and $B_{F_{3 \rightarrow 1, 2 \rightarrow 3}}$ be

used in Method II (and III) because the weaker signal, $B_{F_{3 \rightarrow 1, 2 \rightarrow 3}}$

is immune to scatter and $B_{F_{3 \rightarrow 1, 1 \rightarrow 3}}$ (as well as $B_{F_{3 \rightarrow 1, 1 \rightarrow 3, 2 \rightarrow 3}}$ in Method IV)

is (are) large compared to the scatter signals;

- (v) the post filter factor^{10,11} will cause errors for any fluorescence process involving the ground state, e.g., $B_{F_{3 \rightarrow 1, 1 \rightarrow 3}}$ or $B_{F_{3 \rightarrow 1, 2 \rightarrow 3}}$

(or $B_{F_{3 \rightarrow 1, 1 \rightarrow 3, 2 \rightarrow 3}}$); however, by measuring the fluorescence at the same

wavelength for both fluorescence processes in the ratios

(in Methods II, III, or IV), the post filter effect cancels;

- (vi) the laser beams must not only be homogeneous as in item (i) above but also must have the same cross-sectional areas and must be optically aligned to interact with the same region of the flame gases, and in fact, the same species when making temporal temperature measurements; and
- (vii) full saturation, i.e., $E_{v_0} > 10E_{v_0}^s$, must be achieved, i.e., it is not desirable to plot B_F vs E_v and to extrapolate to the plateau.

Methods III and IV. The advantages of these two similar methods are

- (i) since "saturation" must occur, only fluorescence radiances need to be measured;
- (ii) "real-time" temperature computations are easily accessible assuming the validity of the T_{III} and T_{IV} equations;
- (iii) single pulse temperature measurements are easily achieved in both methods; however, Method IV is more easily adapted since the first laser can be set at $E_{v_{23}}$ and $B_{F_{3 \rightarrow 1, 2 \rightarrow 3}}$ measured and while

the $E_{v_{23}}$ pulse is still on, the second laser at $E_{v_{13}}$ can be pulsed yielding $B_{F_{3 \rightarrow 1, 1 \rightarrow 3, 2 \rightarrow 3}}$, i.e., there is no need for delaying

one pulse relative to the other pulse long enough to be certain that, the system under study has regained thermodynamic equilibrium, that the fluorescence temporal waveforms do not overlap and that all electronic echos and/or reflections from the first pulse have been damped out as is necessary for Methods I, II, and III.

The disadvantages of these methods are:

- (i) the same ones as (i), (iv), (v), (vi) of Method II;
- (ii) the laser pulse must be temporally long enough to assure the pseudo-three level steady state condition;
- (iii) while extrapolation to the maximum fluorescence radiance may be employed in Method III, it can not be used in Method IV; in addition, it can only be employed in those cases of Method III where steady state is achieved (i.e., $\Delta t_{\text{laser}} \gg \frac{1}{\Sigma(k_{ul} + A_{ul})}$) or else extrapolation will yield an erroneous result;
- (iv) if the laser pulse and measurement times become too long, the excited state reactions must also be taken into account, and the rate equations will require subsequent modifications (it should be noted that unless photoionization occurs, Methods II and IV_{peak} do not have this problem);
- (v) the disadvantage listed in item (iv) indicates limited use of high power C.W. or long pulse flashlamp pumped dye lasers while the disadvantages in items (ii) and (iii) indicate the limited use of shorter pulse N₂, Nd-YAG, and excimer pumped dye lasers;
- (vi) the measurement system need not be as "fast" as is required in Method II but it still must be able to measure the three level fluorescence without temporal distortion and;
- (vii) unless the assumptions made to obtain T_{III}" or T_{III}" and T_{IV} or T_{IV}" are valid or alternately verified then, the non-radiational and radiational rate constants (i.e. k's and A's) must be known to obtain an accurate temperature (the assumpt

AD-A089 375

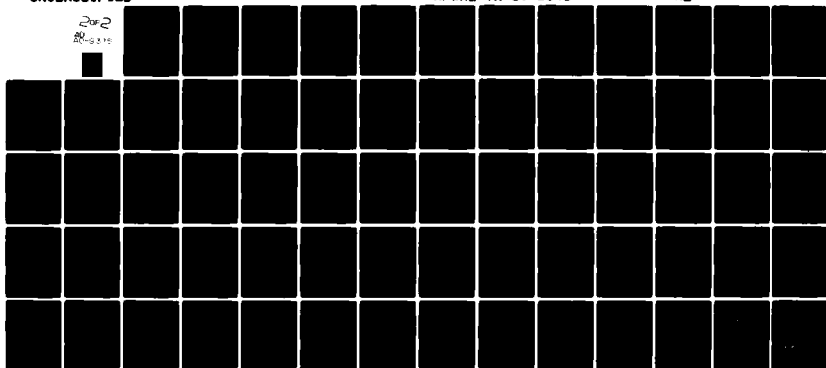
FLORIDA UNIV GAINESVILLE DEPT OF CHEMISTRY F/G 21/2
TEMPORAL AND SPATIAL TEMPERATURE MEASUREMENTS OF COMBUSTION FLA--ETC(U)
MAY 80 J D WINEFORDNER F33615-78-C-2038

UNCLASSIFIED

AFWAL-TR-80-2045

NL

202
20-0 2 10



END
DATE
FILMED
-10-80
DTIC

made to obtain T_{II} , and T_{III} , appear to be reasonable based upon measured values of k 's and A 's.¹⁴

Method V. The advantages of this method are:

- (i) saturation is not necessary but can occur;
- (ii) there is only one laser beam (wavelength) and so there are no matching of beam problems and homogeneity of the beam is not critical;
- (iii) scatter and post filter problems are minimal because the $B_{3+2, 1+3}$ value is large and immune to the post filter effect and scatter errors, whereas $B_{TF_{i+1}}$ is immune to scatter and $B_{TF_{i+2}}$ is also fairly insensitive to the post filter effect;
- (iv) temporal temperatures are most ideally done with one laser pulse since no timing problems are necessary, but rather simply the simultaneous measurement of the fluorescence and emission or of two emission signals;
- (v) this method also adapts itself readily to real time since only the fluorescence radiances need to be measured and T_V allows easy temperature computation from single pulse measurements; and
- (vi) as in Method I (for $E_{v_0} \lesssim E_{v_0}^S$), either integrated or time dependent measurements are applicable.

The disadvantages of this method are:

- (i) the collisional rate constants k_{3i} and k_{3j} must be sufficiently large to assure that levels i and j are thermally populated on a time scale of that of the laser pulse; temporal analysis of the fluorescence, thermally assisted fluorescence, and the excitation pulse allow evaluation of this effect, but this must be

- verified for significant changes in flame conditions; and
- (ii) if the ratio of fluorescence (directly pumped by laser source) to thermally-assisted fluorescence radiances is employed with a time integrated technique, then further assumptions must be made in order to determine whether $E_{\nu_0} >> E_{\nu_0}^S$; in which case, the thermally assisted fluorescence population rate cannot possibly follow the laser pulse and the two signals are not correlated in a single way. As pointed out in item (i), thorough studies are needed to investigate the effect of the technique (integrated or temporally resolved peak)^{how} is affected by the temporal shape of the signals.

FINAL COMMENT

All five methods can be used to obtain spatial flame temperatures, i.e., temperatures corresponding to $\approx 1 \text{ mm}^3$ of flame gases. Methods I, II, III, and IV can be used for temporal flame temperatures as long as the two laser beams are properly matched and aligned and the timing between the 2 laser pulses is properly monitored; temporal temperatures corresponding to $\approx 1 \text{ } \mu\text{s}$ should be obtainable by this approach. Method V is experimentally implemented most easily since only one laser pulse is needed which simplifies greatly the measurement process. Methods II, III, and IV strictly require saturation resulting in problems with use of many commercial dye laser systems especially in the UV when doubling of the dye laser output is needed with the concomitant loss in spectral irradiance (also, unfortunately, the saturation spectral irradiance αE_{ν}^* depends upon ν_{exc}^3 and so much more source spectral irradiance is needed in the UV than in the visible region for excitation). Method I strictly requires linearity, between B_{ν} and E_{ν} , whereas in Method V, in some cases E_{ν} is limited to near or below saturation. In Methods III and IV, certain critical assumptions regarding

the rate constants must be valid to obtain accurate flame temperatures, and fluorescence measurements must be made in the portion of the fluorescence pulses where the 3-level steady state saturation limitation applies. In Method II and IV_{peak}, no assumptions concerning rate constants are needed, but the experimental system must allow measurement on the peak (2 level steady state) of the fluorescence pulse. Methods I, II, III, and IV all require careful beam matching, alignment, and homogeneity, whereas, Method V is independent of these factors. Methods II, III, and IV do not require spectrometer calibration as long as the same fluorescence line is measured for the ratio, whereas, Methods I and V require calibration of the fluorescence spectrometer system and Method I requires an additional calibration of the source excitation spectral irradiance. All of the methods should have comparable S/N ratios for equivalent metastable energies; whereas Method I will have the lowest average signals, the increase in measurement time should produce similar S/N ratios to methods II, III, IV, and I (S/N estimations for various conditions have been previously estimated⁷). All of these methods are based on pseudo-continuum excitation conditions, and in many commercial dye lasers detuning or other line broadening techniques must be initiated to assure this (when $E_{v_0} \ll E_{v_0}^S$, $\Delta\lambda_{\text{laser}}$ should be $\geq 0.2 \text{ \AA}$). In many cases, even though the total laser energy output may remain about the same after line broadening, the laser spectral irradiance may be severely reduced.

Experimental flame temperatures obtained by these methods for hydrogen based flames will be given in a later manuscript.

REFERENCES

1. N. Omenetto, P. Benetti, and G. Rossi, Spectrochim. Acta, 27B, 453(1972).
2. N. Omenetto, R.F. Browner, J.D. Winefordner, G. Rossi, and P. Benetti, Anal. Chem., 44, 1683(1972).
3. P. Benetti, N. Omenetto, and G. Rossi, La Termotecnica, 29, 86(1975).
4. H. Haraguchi, B. Smith, S. Weeks, D.J. Johnson, and J.D. Winefordner, Applied Spectroscopy, 31, 156(1977).
5. H. Haraguchi and J.D. Winefordner, Applied Spectroscopy, 31, 195(1977).
6. H. Haraguchi and J.D. Winefordner, Applied Spectroscopy, 31, 330(1977).
7. J. Bradshaw, J. Bower, S. Weeks, K. Fujiwara, N. Omenetto, H. Haraguchi, and J.D. Winefordner, 10th Materials Research Symposium on Characterization of High Temperature Vapors and Gases, NBS, Gaithersburg, Maryland, 1978.
8. M. Lapp and C.M. Penney, Editors, "Laser Raman Gas Diagnostics", Plenum Press, 1974.
9. R.M. Measures, J. Appl. Phys., 39, 5232(1968).
10. N. Omenetto and J.D. Winefordner, Chapter 4 in "Analytical Laser Spectroscopy", N. Omenetto, Editor, Wiley, 1977.
11. N. Omenetto and J.D. Winefordner, Progress In Analytical Atomic Spectroscopy, Vol. 2(1,2), Pergamon, 1979.
12. G.D. Boutilier, M.B. Blackburn, J.M. Mermet, S.J. Weeks, H. Haraguchi, J.D. Winefordner, and N. Omenetto, Applied Optics, 17, 2291(1978).
13. R. Herrmann and C.Th.J. Alkemade, "Flame Photometry", P.T. Gilbert, translator; John Wiley, New York, 1963.

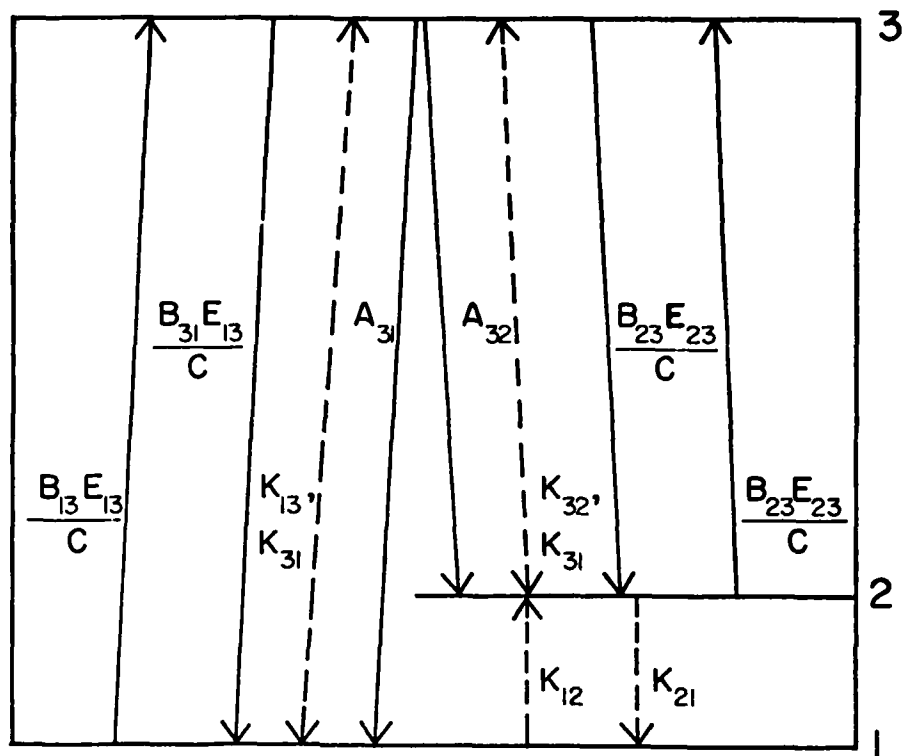


Figure 1B. Energy Level Diagram of 3-Level Tl-Like Atom With Activation (Solid Lines) and Deactivation (Dashed Lines) Rate Constants Shown (see text for definition).

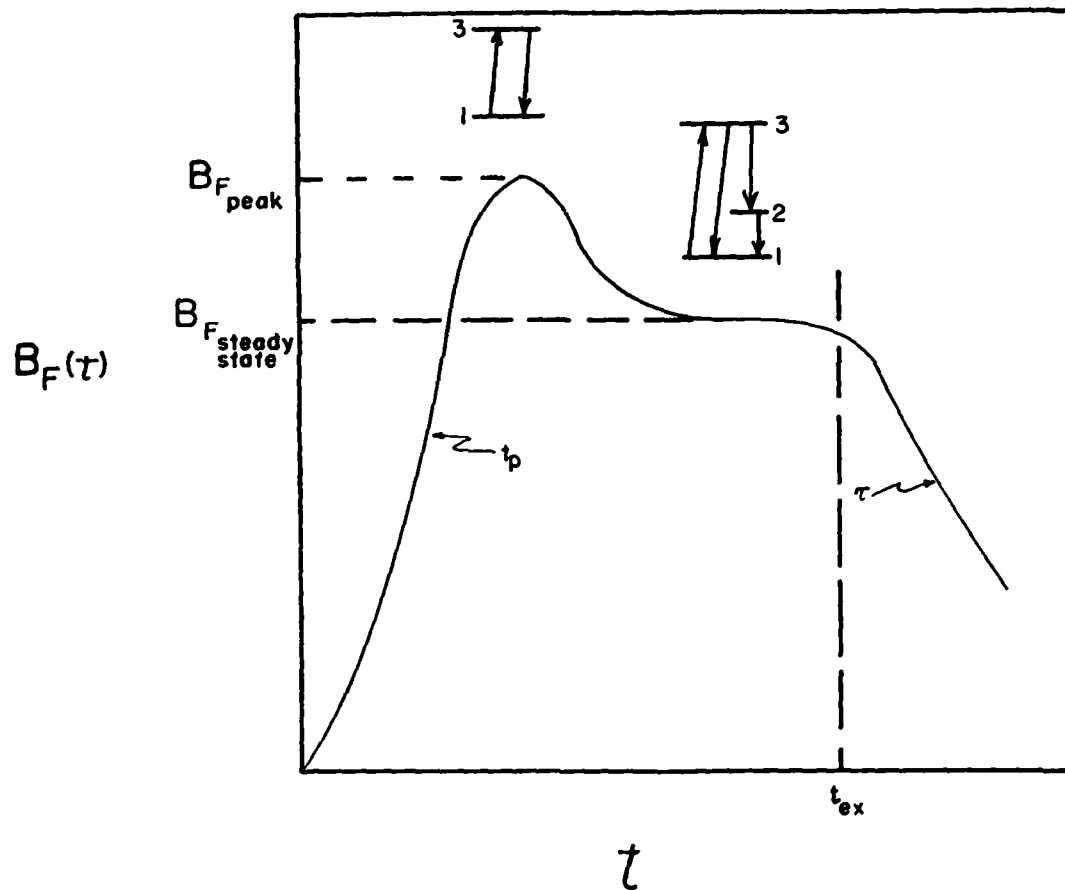


Figure 2B. Hypothetical Fluorescence Temporal Waveform Produced With a Rectangular Excitation Pulse (t_{ex} long). Demonstrating the 2-Level Peak and the 3-Level Steady State Plateau.

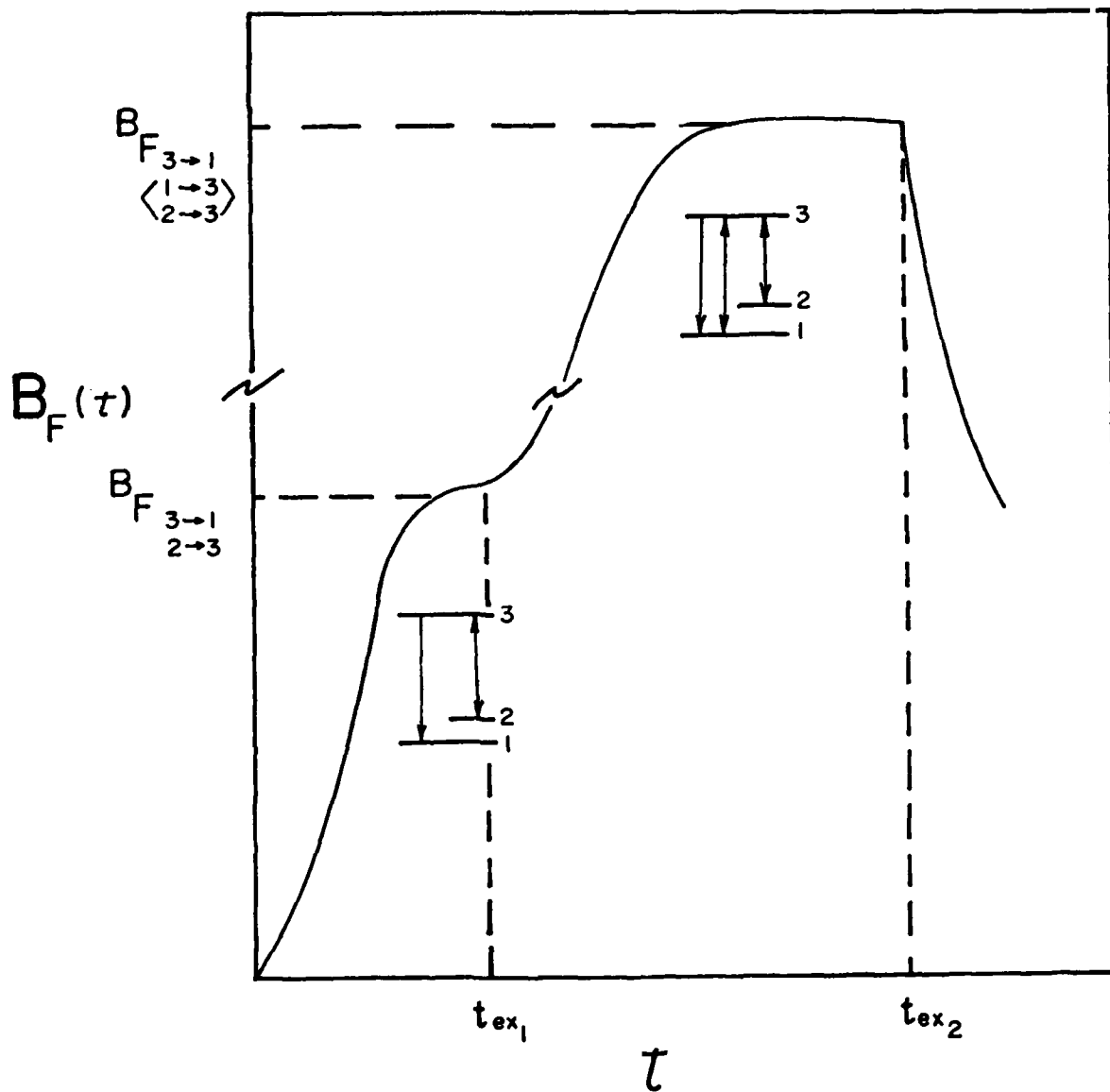


Figure 3B. Hypothetical Fluorescence Temporal Waveform Produced By Excitation First With $2 \rightarrow 3$ to Saturate the $3 \rightarrow 1$ Fluorescence and Then While $2 \rightarrow 3$ Excitation Occurs, Excitation Occurs Simultaneously at $2 \rightarrow 3$ and $1 \rightarrow 3$ to Saturate the $3 \rightarrow 1$ Fluorescence. During the Excitation Time, t_{ex} , only the $2 \rightarrow 3$ Excitation Pulse is "On". During the Excitation Time Between t_{ex_1} and t_{ex_2} Both $2 \rightarrow 3$ and $1 \rightarrow 3$ Excitation Pulses are "On".

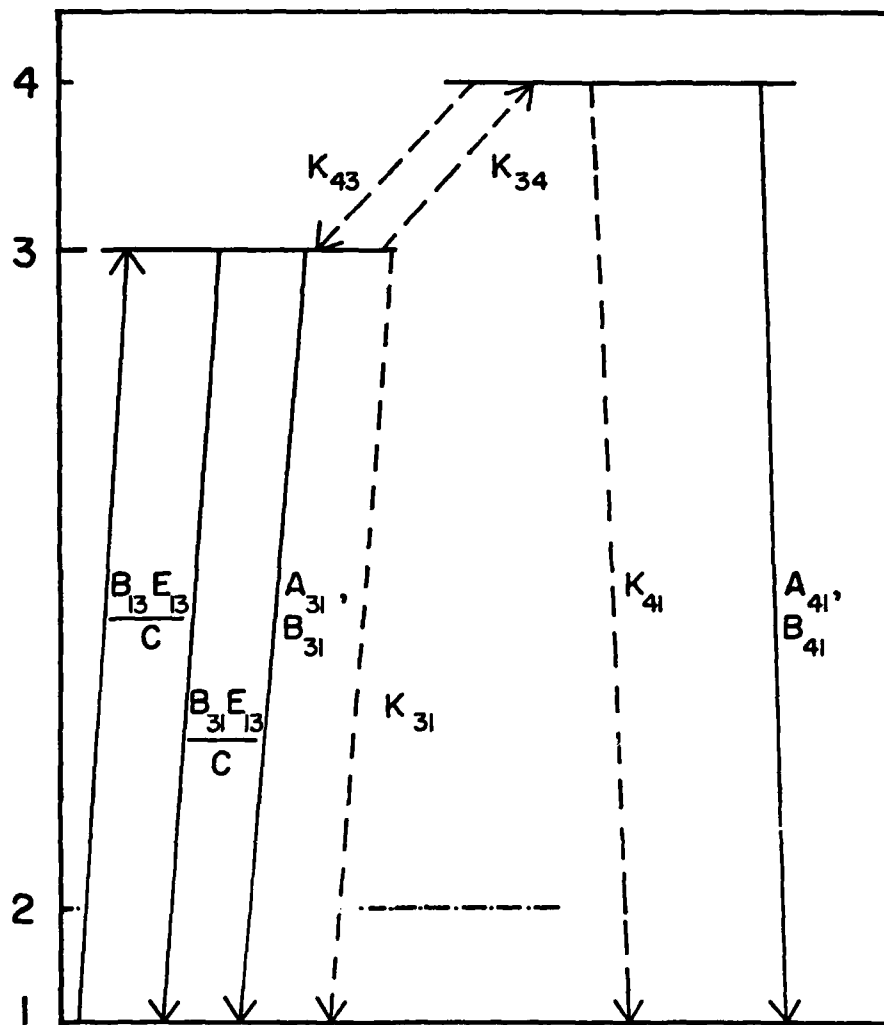


Figure 4B. Energy Level Diagram of Multi-Level Atom, e.g., Tl, with Activation (Solid Lines) and Deactivation (Dashed Lines) Rate Constants Shown (see text for definitions). Level 2 is Shown but is Not Important to the Processes Shown.

APPENDIX C
(manuscript submitted to APPL. SPECTROSC.)

THERMALLY ASSISTED FLUORESCENCE: A NEW TECHNIQUE
FOR LOCAL FLAME TEMPERATURE MEASUREMENT^a

G. Zizak^b

J.D. Bradshaw^c

J.D. Winefordner^e

Department of Chemistry
University of Florida
Gainesville, FL 32611

- a. Work supported by AFSOR-AF-F49620-80-C-0005 and by Wright Patterson Air Force Base AF-F33615-78-C-2038.
- b. On leave: CNPM-Politecnico Viale F. Baracca 69-20068 Peschiera Borromeo-Milano-Italy.
- c. Present address: Chemistry Department, University of Florida, Gainesville, FL 32611.
- d. Author to whom reprint requests should be sent.

ABSTRACT

The theoretical basis of a new technique called thermally assisted atomic fluorescence for measurement of local spatial-temporal flame temperatures is given. In this method, the ratio of fluorescence signals from a radiatively excited level and a higher collisionally excited level or from two higher collisionally excited levels of an inorganic probe, such as In or Tl, is related to the flame temperature. The conditions necessary for the measured flame temperature to be identical to the translational (Boltzmann) flame temperature are given. The experimental system and conditions for making flame temperature measurements, which consists basically of a single pulsed dye laser and a gated detector, are described. The assumption of steady state conditions is discussed as well as several anomalies in terms of fluorescence from certain energy levels of Tl. The accuracy and precision of the measured flame temperatures for several methane-air flames are discussed.

INTRODUCTION

Laser induced fluorescence (LIF) is one of the most promising techniques for combustion diagnostics, as it is spatially (and temporally) precise, very sensitive and capable of detecting trace species. Although LIF is mainly employed for species concentration determination [1,2], it seems that temperature measurements can also be performed.

A great deal of work has been done to assess the applicability of the two-line atomic fluorescence method [3,4,5] to flame diagnosis, while other possible techniques, employing LIF, have been theoretically developed [6,7].

A different approach consists of measuring the fluorescence from collisionally excited states following radiative excitation. If the collisional rates are fast enough to allow a new Boltzmann distribution during the laser pulse, from the thermally assisted fluorescence, the local temperature can be measured.

A partial Boltzmann equilibrium, corresponding to the flame temperature, has been found, for Na atoms, in a H_2-O_2 -Ar flame as a result of two-photon laser excitation [8]. Assuming a modified two-level model, a relatively low deviation from the Boltzmann distribution was calculated for the rotational levels of the OH molecule [9], and rotational and vibrational temperatures, of the OH molecule, as a result of collisional energy transfer, have been recently measured in methane-air flames, using laser induced fluorescence [10,11]. However, the lack of knowledge of the magnitude

of quenching rates, the non-Boltzmannian rotational population distribution for the OH molecules, and the dependence of vibrational transfer upon the rotational level [11] indicate more studies have to be carried out, especially for molecules. These difficulties can be partially overcome by seeding the flames with inorganic atoms and measuring well-characterized thermally assisted fluorescence lines. In this way, spatially resolved temperature measurements can be performed, and a better understanding of the collisional energy redistribution can be determined.

THEORETICAL CONSIDERATIONS

Two Level System

It is generally assumed that thermodynamic equilibrium exists in atmospheric combustion flames; however, this is not "rigorously true", because of radiative losses always present in flames. By solving the rate equations for the steady state case for a two level system (as indicated in Fig. 1) in the absence of an external radiation source, the ratio $(n_2/n_1)_{II}$

[CONTINUE WITH PAGE 4]

is given by:

$$\left(\frac{n_2}{n_1}\right) = \left(\frac{1}{1 + \frac{A_{21}}{k_{21}}}\right) \left(\frac{n_2}{n_1}\right)_B \quad (1)$$

where $(n_2/n_1)_B$ is the population ratio as given by the Boltzmann relationship and A_{21} and k_{21} are the radiative and quenching rates from level 2 to level 1.

Hence, from the ratio (n_2/n_1) , an "optical" temperature, T_{op} , different from the "true" translational temperature, is given by:

$$\frac{1}{T_{op}} = \frac{1}{T_{tr}} - \frac{k}{\Delta E_{21}} \ln\left(\frac{k_{21}}{k_{21} + A_{21}}\right) \quad (2)$$

where ΔE_{21} is the energy difference between the levels 1 and 2, and k is the Boltzmann constant. This well-known deviation is normally negligible because $A_{21} \ll k_{21}$, but it is useful to remember that whatever optical diagnostic technique is used to measure the ratio n_2/n_1 , the resulting temperature will be the "optical" temperature, corresponding to the actual population distribution which may be different (frequently very little different) from the Boltzmann distribution obtained by the translational temperature.

Three-level system

The above considerations are further complicated by the fact that for most atomic or molecular systems, the two-level model is inadequate. A three-level system, which is a more realistic model (see Fig. 2) can also be solved assuming steady state conditions. In addition, if there is no

radiative excitation by an external source, the ratio $(n_2/n_1)_{III}$ is then given by:

$$\left(\frac{n_2}{n_1}\right)_{III} = \frac{k_{12}(k_{32} + k_{31} + A_{31}) + k_{13} k_{32}}{(k_{21} + A_{21})(k_{32} + k_{31} + A_{31}) + k_{23}(k_{31} + A_{31})} \quad (3)$$

From this expression, it can be seen the $(n_2/n_1)_{III}$ ratio is quite different from the Boltzmann ratio. However, if it has been previously accepted that the n_2/n_1 ratio is Boltzmannian, then one is forced to accept:

$$\left(\frac{n_2}{n_1}\right)_{III} \approx \left(\frac{n_2}{n_1}\right)_{II} \approx \left(\frac{n_2}{n_1}\right)_B = \frac{k_{12}}{k_{21}} = \frac{g_2}{g_1} \exp\left(-\frac{\Delta E_{21}}{kT_{tr}}\right); \quad (4)$$

Therefore, the validity of the Boltzmannian equation (4) forces the assumption that $k_{13} = k_{23} = 0$ and $A_{21} \ll k_{21}$, or that the radiative losses are negligible ($A_{21} \ll k_{21}$, $A_{31} \ll k_{31}$, $A_{32} \ll k_{32}$).

Considering now the case in which an external source of spectral irradiance $E_{\nu_{12}}$ irradiates a three level system, the ratio n_3/n_2 is given (refer to Boutilier, et al [12]) by

$$\frac{n_3}{n_2} = \frac{k_{23}(k_{13} + B_{12} \frac{E_{12}}{c} + k_{12}) + k_{13}(B_{21} \frac{E_{12}}{c} + k_{21} + A_{21})}{(k_{32} + A_{32})(k_{13} + B_{12} \frac{E_{12}}{c} + k_{12}) + (k_{31} + A_{31})(B_{12} \frac{E_{12}}{c} + k_{12})} \quad (5)$$

Expression (5) can be rearranged as:

$$\frac{n_3}{n_2} = \frac{k_{23}}{(k_{32} + A_{32})} \frac{1 + \frac{k_{13}(B_{21} E_{12}/c + A_{21})}{k_{13} k_{21} + k_{23}(k_{13} + B_{12} E_{12}/c + k_{12})}}{1 + \frac{A_{31} k_{12} + k_{31} B_{12} E_{12}/c + A_{31} B_{12} E_{12}/c}{(k_{13} + B_{12} E_{12}/c + k_{12})(k_{32} + A_{32}) + k_{31} k_{12}}} \times \quad (6)$$

$$\times \frac{(k_{13} + B_{12} E_{12}/c + k_{12}) + (k_{13} k_{21})/k_{23}}{(k_{13} + B_{12} E_{12}/c + k_{12}) + (k_{31} \cdot k_{12})/(k_{32} + A_{32})}$$

Also, since $A_{32} \ll k_{32}$ is valid in most three level cases and

$$\frac{k_{13} k_{21}}{k_{23}} = \frac{k_{31} \cdot k_{12}}{k_{32}} \quad (7)$$

Then it can be readily shown that:

$$\frac{n_3}{n_2} = \left(\frac{k_{23}}{k_{32}}\right) \frac{1 + \frac{B_{12} E_{12}}{k_{12} c} \exp(-\frac{E_{21}}{KT}) + \frac{A_{21}}{k_{21}}}{1 + \frac{B_{12} E_{12}}{k_{12} c} (1 + \frac{A_{31}}{k_{31}}) + \frac{A_{31}}{k_{31}}} \quad (8)$$

where:

$$C = 1 + \frac{k_{23}}{k_{13} k_{21}} (k_{13} + k_{12} + B_{12} \frac{E_{12}}{c}) = 1 + \frac{k_{32}}{k_{31} k_{12}} (k_{13} + k_{12} + B_{12} \frac{E_{12}}{c}) \quad (9)$$

Several limiting cases of expression 8 are now possible. If no external source is present, the ratio n_3/n_2 is:

$$\frac{n_3}{n_2} = \left(\frac{k_{23}}{k_{32}}\right) \cdot \frac{1 + \frac{A_{21}/k_{21}}{C}}{1 + \frac{A_{31}/k_{31}}{C}} \quad (9)$$

Once again the two levels (3 and 2) are in a Boltzmann equilibrium only if $A_{21} \ll k_{21}$ and $A_{31} \ll k_{31}$, i.e., the radiative losses must be negligible. However if radiative losses are negligible (A 's \ll k 's) and an external source of spectral irradiance $E_{\nu_{12}}$ is present, then the ratio n_3/n_2 becomes:

$$\frac{n_3}{n_2} = \left(\frac{k_{23}}{k_{32}}\right) \frac{1 + \frac{B_{12} E_{12}}{C \cdot k_{12}} \exp(-E_{12}/kT)}{1 + \frac{B_{12} E_{12}}{C \cdot k_{12}}} \quad (10)$$

and upon rearrangement and substitution for C

$$\frac{n_3}{n_2} = \left(\frac{k_{23}}{k_{32}}\right) \frac{\frac{B_{12} E_{12}}{k_{12}} \exp(-E_{12}/kT) + \frac{k_{32}}{k_{31}} + (1 + \frac{k_{32}}{k_{31}} + \frac{k_{32}}{k_{31}} \cdot \frac{k_{13}}{k_{12}})}{\frac{B_{12} E_{12}}{k_{12}} [1 + \frac{k_{32}}{k_{31}}] + (1 + \frac{k_{32}}{k_{31}} + \frac{k_{32}}{k_{31}} \cdot \frac{k_{13}}{k_{12}})} \quad (11)$$

Assuming $B_{12} E_{12}/c \gg k_{12}$ (a condition generally achieved with laser irradiances), the ratio is given by:

$$\frac{n_3}{n_2} = \left(\frac{k_{23}}{k_{32}}\right) \left(\frac{\exp\left(-\frac{E_{12}}{kT}\right) + \frac{k_{32}}{k_{31}}}{1 + \frac{k_{32}}{k_{31}}} \right) \quad (12)$$

and assuming common flame temperatures (~ 2000 K) and atomic energy levels (~ 1 eV)

$$\frac{n_3}{n_2} \approx \left(\frac{k_{23}}{k_{32}}\right) \left(\frac{k_{32}}{k_{31} + k_{32}} \right) \quad (13)$$

Now if radiative losses are not negligible, i.e., A_{21} and A_{31} cannot be disregarded then the ratio n_3/n_2 is

$$\frac{n_3}{n_2} = \left(\frac{k_{23}}{k_{32}}\right) \frac{\frac{B_{12} E_{12}/c}{k_{12}} \left[\exp\left(-\frac{E_{12}}{kT}\right) + \frac{k_{32}}{k_{31}} \right] + \left(1 + \frac{k_{32}}{k_{31}} + \frac{k_{32} k_{13}}{k_{31} k_{12}} + \frac{A_{21}}{k_{21}}\right)}{\frac{B_{12} E_{12}/c}{k_{12}} \left[1 + \frac{A_{31}}{k_{31}} + \frac{k_{32}}{k_{31}} \right] + \left(1 + \frac{k_{32}}{k_{31}} + \frac{k_{32} k_{13}}{k_{31} k_{12}} + \frac{A_{31}}{k_{31}}\right)} \quad (14)$$

Assuming an intense external source, i.e., $B_{12} E_{12}/c \gg k_{12}$, then:

$$\frac{n_3}{n_2} = \frac{k_{23}}{k_{32}} \frac{\exp\left(-\frac{E_{21}}{kT}\right) + \frac{k_{32}}{k_{31}}}{\frac{A_{31} + k_{31} + k_{32}}{k_{31}}} \quad (15)$$

and assuming common flame and atom conditions:

$$\frac{n_3}{n_2} \approx \left(\frac{k_{23}}{k_{32}}\right) \left(\frac{k_{32}}{k_{31} + A_{31} + k_{32}}\right) \quad (16)$$

Therefore in all the above cases, the ratio n_3/n_2 is not given by the simple Boltzmann relationship of k_{23}/k_{32} and only approaches it in a limiting situation. The general behavior of the ratio n_3/n_2 is qualitatively shown in Fig. 3.

The same result as given in equation (16) can be more easily found from equation (5) considering $k_{13} = 0$, i.e., the population of level 3 is obtained only by collisional coupling with level 2. However, the assumption $k_{13} = 0$ can lead to some misunderstanding. Equation (16) is independent of the $E_{v_{12}}$ value; however, for low irradiances, the assumption $k_{13} = 0$ means that $n_2 k_{23} \gg n_1 k_{13}$ and $k_{32} \gg k_{31}$. In effect, for low external source irradiances, equation (16) must reduce to the Boltzmann distribution.

It is therefore possible to determine the temperature of a system by measuring the ratio of two fluorescence lines, one coming from the radiatively excited level (resonant or non-resonant, $B_{F_{21/12}}$), and the other one coming from an upper thermally excited level (such as $B_{F_{31/12}}$), that is:

$$\frac{B_{F_{31/12}}}{B_{F_{21/12}}} = \left(\frac{v_{31}}{v_{21}}\right) \left(\frac{A_{31}}{A_{21}}\right) \left(\frac{g_3}{g_2}\right) \left(\frac{k_{32}}{k_{31} + A_{31} + k_{32}}\right) \exp\left(-\frac{\Delta E_{32}}{kT}\right) \quad (17)$$

and so

$$T = \frac{\Delta E_{32}/k}{\ln\left(\frac{A_{31} g_3}{A_{21} g_2}\right) + \ln\left(\frac{k_{32}}{k_{31} + A_{31} + k_{32}}\right) + \ln\left(\frac{\lambda_{21}}{\lambda_{31}}\right) + \ln\left(\frac{B_{F_{21/12}}}{B_{F_{31/12}}}\right)} \quad (18)$$

This technique is similar to the classical emission two-line ratio technique for temperature measurement, except that it is a local technique. Of course, using only one laser excitation line and observing the two fluorescence lines with two optical detectors, it is possible to measure spatially and temporally resolved temperatures.

The disadvantages of this technique are the need to have accurate A -values (at least accurate ratios) and to have an accurate calibration to account for the spectral response of the optical set-up. However, this problem is minimized by using a calibrated lamp. The value of the ratio $k_{32}/(k_{32} + A_{31} + k_{31})$ is needed; however, for common flame conditions and with seeding atoms like Tl, where $\Delta E_{12} \sim 3$ eV and $\Delta E_{23} \sim 1$ eV, the correction factor in equation (16) is negligible, i.e., is essentially unity.

Four-level system

Now consider a four level system, where the 4th level is any one of the levels shown as a manifold of levels in Figure 4. Also, let

$$\begin{aligned}
 A_{21}^* &= A_{21} + k_{21} + B_{21} E_{\nu_{12}}/c \\
 A_{32}^* &= A_{32} + k_{32} \\
 A_{42}^* &= A_{42} + k_{42} \\
 A_{34}^* &= A_{34} + k_{34} \\
 A_{43}^* &= A_{43} + k_{43} \\
 A_{31}^* &= A_{31} + k_{31} \\
 A_{41}^* &= A_{41} + k_{41}
 \end{aligned}
 \tag{19}$$

The rate equations can then be written as:

$$\begin{aligned}\frac{d n_2}{d t} &= n_1 [B_{12} \frac{E_{\nu_{12}}(t)}{c} + k_{12}] + n_3 A_{32}^* + n_4 A_{42}^* - n_2 [A_{21}^* + k_{23} + k_{24}] \cdot \\ \frac{d n_3}{d t} &= n_2 k_{23} + n_1 k_{13} + n_4 A_{43}^* - n_3 [A_{32}^* + A_{31}^* + A_{34}^*] \cdot \\ \frac{d n_4}{d t} &= n_3 A_{34}^* + n_2 k_{24} + n_1 k_{14} - n_4 [A_{41}^* + A_{42}^* + A_{43}^*] \\ n_1 + n_2 + n_3 + n_4 &= n_T\end{aligned}\tag{20}$$

With the assumption $k_{13} = k_{14} = 0$, the steady state solutions, for the ratios n_3/n_2 and n_3/n_4 are given by:

$$\frac{n_3}{n_2} = \left(\frac{k_{23}}{A_{32}^*} \right) \left(\frac{1 + \left(\frac{k_{24}}{k_{23}} \right) \frac{A_{43}^*}{A_{41}^* + A_{42}^* + A_{43}^*}}{1 + \frac{A_{31}^*}{A_{32}^*} + \frac{A_{34}^*}{A_{32}^*} \left(1 - \frac{A_{43}^*}{A_{41}^* + A_{42}^* + A_{43}^*} \right)} \right)\tag{21}$$

$$\frac{n_3}{n_4} = \left(\frac{A_{43}^*}{A_{34}^*} \right) \left(\frac{1 + \frac{k_{23}}{A_{43}^*} \left(\frac{A_{41}^* + A_{42}^*}{k_{23} + k_{24}} \right)}{1 + \frac{k_{24}}{A_{34}^*} \left(\frac{A_{32}^* + A_{31}^*}{k_{23} + k_{24}} \right)} \right)\tag{22}$$

With the assumption that radiative losses are negligible, i.e., $A \ll k$, then

$$\frac{n_3}{n_4} = \left(\frac{k_{43}}{k_{34}}\right) \left(\frac{1 + \frac{k_{41}}{k_{43}(1 + \frac{k_{24}}{k_{23}}) + k_{42}}}{1 + \frac{k_{31}}{k_{34}(1 + \frac{k_{23}}{k_{24}}) + k_{32}}} \right) \quad (23)$$

Therefore the ratio of n_3/n_4 is not Boltzmannian but rather include k_{31} and k_{41} rate constants that are not balanced by the upwards collisional rate constants of k_{13} and k_{14} , because of our previous assumption ($k_{13} = k_{14} = 0$). However, if $k_{41} \ll (k_{42} + k_{43})$ and $k_{31} \ll (k_{32} + k_{34})$ the ratio n_3/n_4 is once again Boltzmannian even under excitation by an external source.

Moreover with the same assumption given above ($A \ll k$), $k_{41} \ll (k_{43} + k_{42})$ and $k_{31} \ll (k_{32} + k_{34})$, and since

$$\frac{k_{24} \cdot k_{43}}{k_{23}} \equiv \frac{k_{42} \cdot k_{34}}{k_{32}} \quad (24)$$

the ratio n_3/n_4 becomes:

$$\frac{n_3}{n_2} = \left(\frac{k_{23}}{k_{32}}\right) \left(\frac{k_{32} + k_{34} \left(\frac{k_{42}}{k_{42} + k_{43}} \right)}{k_{32} + k_{31} + k_{34} \left(\frac{k_{42}}{k_{42} + k_{43}} \right)} \right) \quad (25)$$

Now, if the following condition is valid $k_{31} \ll k_{32} + k_{34}[k_{42}/(k_{42} + k_{43})]$, than a Boltzmann distribution occurs between levels 3 and 2.

Remembering that level 4 can be of any level in a manifold of levels (see Fig. 4), it seems that the general conclusion would be that, apart from the radiative losses under external source excitation, in a steady state case, all levels above the excitation level are always in Boltzmann equilibrium. However if in the absence of external source excitation, levels 3 and 4 are mainly populated via the coupling $k_{12} + k_{23}$ and $k_{12} + k_{24}$ (assumption $k_{13} = k_{14} = 0$), then a Boltzmann equilibrium will be also between these levels and the excited level 2. In the other case in which the main thermal population of levels 3 and 4 comes from level 1, through k_{13} and k_{14} , laser excitation perturbs the distribution and the ratios between the highly excited levels and the radiatively excited level is not Boltzmannian. However, in most situations, any correction made will be small.

In a multi-level system, the temperature can also be evaluated using the expression (18), with or without the correction factor that can be derived from Equation (25), but now there is the possibility of measuring two thermally assisted fluorescence lines ($B_{F_{j/12}}, B_{F_{i/12}}$), coming from different energy levels (E_j, E_i), then the temperature can be obtained by the expression:

$$T = \frac{\Delta E_{ij}/k}{\ln\left(\frac{\lambda_i g_i}{\lambda_j g_j}\right) + \ln\left(\frac{\lambda_j}{\lambda_i}\right) + \ln\left(\frac{B_{F_{j/12}}}{B_{F_{i/12}}}\right)} \quad (26)$$

Another possibility is to consider many thermally assisted lines, coming

from different energy levels. If it is assumed that during the time of the laser pulse, the system reaches a new thermodynamic equilibrium, from a set of different thermally assisted lines, the temperature can be evaluated from the slope of a plot of $\ln(B_{F_j/12} / \nu_j A_j g_j)$ versus $\Delta E_j/k$.

EXPERIMENTAL

The apparatus used to test the possibilities of the thermally assisted fluorescence (THAF) technique is reported in Fig. 5. A Nitrogen laser (Molelectron UV-14) pumped dye laser (Molelectron DL-400) is used for this study. The optical triggering is achieved by a quartz plate and a photodiode (EGG-FND 100). The fluorescence fluxes are collected by a JY H10 monochromator with the aid of a quartz lens and neutral density filters to produce approximately the same fluorescence signals for different lines. A Tektronix 1S1 (sampling unit) is used with the scan facility of the PAR-160 to scan a fast gate (0.35 ns) along the fluorescence pulse. The signals are visualized by a Hewlett-Packard 1220 A oscilloscope and a MFE plotmatic x-y 715 recorder.

For this study, there was the necessity of a detector with a response time fast enough to follow the fluorescence pulses. This was achieved using a Hamamatsu R928 squirrel-cage photomultiplier, supplied with high voltage (-1400 V) and a laboratory constructed voltage divider following the suggestion found in the literature for nanosecond studies [13,14,15,16].

With the apparatus used, for transient pulse measurements, rise times less than 1 ns are achieved, but unfortunately ringing appeared. However, we were concerned with reaching steady state conditions and therefore with mainly the "rising portion" and not with the decay portion of the fluorescent

transient, and the presence of a ringing could be ignored when measuring signals at the peak of the curve where steady state conditions could be assessed.

One of the aims of this work is to investigate the possibility of measuring the fluorescence from highly excited levels even for quenching flames, and so a methane-air flame is chosen for the experiments. The gases are regulated by precision rotameters (Matheson) and the metal solutions are seeded into the flame by pneumatic nebulization with a concentric glass nebulizer (T-230-A3 J.E. Meinhard). 1000 ppm solution of In and Tl are used to investigate four flames with composition given in Table I.

RESULTS AND DISCUSSION

For these investigations, steady state conditions must be reached during the laser pulse. A preliminary investigation on Tl in a methane-air flame indicated that all thermally assisted fluorescence lines with upper levels within 1.5 eV above the radiatively excited level have their fluorescence peak at the same time, roughly 1 ns after the fluorescence peak from the radiatively excited level^(Fig. 6). The redistribution of the population among the upper levels seems to happen approximately at the same time, and steady state conditions seem to be reached just before the end of the laser pulse. Moreover, the good agreement found in the temperature measurements confirmed that the laser pulses used are sufficiently long to reach steady state conditions at least in the methane-air flame.

The first element used as a thermometric species was In; in Fig. 7 a simplified energy scheme with the transitions investigated is given. The transition between the 6s level and the ground state is pumped by the dye laser and the fluorescence of the resonant line (4101.76 \AA), the

3258-3256 Å doublet from the 5d levels and the 3039 Å line are measured. The other possible lines of In happened to interfere with each other and are not measured. In Fig. 8 a typical fluorescence pulse from the 5d level is given as recorded with our apparatus.

The temporal shape of the signal is well-characterized with a distinct rise time and a well-defined decay curve. The temperature found in the middle of two slightly different flames are reported in Table II. The good agreement between the temperature measured suggests that the precision of the technique is good and the errors can be less than a few percent.

More measurements were performed using Tl as the seeding element. The energy levels and the fluorescence lines observed for the first set of experiments with Tl are reported in Fig. 9. The 7s level from the ground state is excited and fluorescence at the strong resonant (3776 Å) and Stokes line (5350 Å), and the 3519-3529 Å doublet, from the 6d thermally excited levels are all observed.

The results and the temperatures are in Table II. One consideration is evident at this point. The temperatures calculated using the intensities of the 3776 Å line are about 100 K less than those using the 5350 Å line. Comments on this will be given later in the paper. One of the attributes of this technique is that it is possible to pump highly excited levels where several energy levels within ≈ 1.5 eV are present.

In a second set of measurements on Tl the 6d levels are pumped by frequency doubling the dye laser output; fluorescence lines coming from the 6d, 8s and 7d levels, could all be observed (see Fig. 10). The results are summarized in Table II. Considerable discrepancies are found for temperature calculations when considering the 2767 Å or the 3525 Å

fluorescence lines from the same 6d level.

Because the 3776, 5350, 2767 and 3525 Å fluorescence lines give the same results (temperatures) with either the boxcar averager with a 15 ns gate width or with the Tektronix 1S1 sampling unit, appreciable ionization is not present when using a 5 ns laser pulse [17].

With integrated measurement, i.e., the boxcar averager approach, exciting the 7s level with the 3776 Å line fluorescence lines coming from the 7s, 6d, 8s and 7d levels are observed. The latter is 1.9 eV above the excitation level. Plots of $\ln\left(\frac{B_F \cdot \lambda}{gA}\right)$ versus level energy are reported in Fig. 10 for both the temporally resolved (1S1 plug-in) and integrated (boxcar averager) techniques. It is apparent that the fluorescence lines at 5350, 3525 and 3229 Å result in a straight line, corresponding to a 1626 K temperature and showing a Boltzmannian distribution for the population. On the other hand, the fluorescence lines at 3776, 2767, and 2920 Å deviate from the straight line portion. The optical system was recalibrated, but no particular differences were found. The only explanation at this point is that the A-values reported in the literature [18] are not correct.

CONCLUSIONS

We have performed a theoretical analysis of the population ratio for thermally excited levels in a multilevel scheme and steady state conditions and we have shown the possibility of using thermally assisted lines to measure the temperature of the flames. We have also performed an experimental study on the applicability of this technique on a methane-air flame and we have shown that using particular lines accurate temperature measurement can be performed. However, more studies are needed to define the correct A-values for the atomic transitions and to show the applicability

of this technique in different experimental conditions.

REFERENCES

1. A.C. ECKBRETH, P.A. BONCZYK, J.F. VERDIECK, Investigations of CARS and Laser Induced Saturated Fluorescence for Practical Combustion Diagnosis. UTRC R79-954403-13 (1979).
2. D. STEPOWSKI and M.J. COTTEREAU, Appl. Opt. **18**, 354(1979).
3. N. OMENETTO, R.F. BROWNER, J.D. WINEFORDNER, G. ROSSI, and P. BENETTI, Anal. Chem., **44**, 1683(1972).
4. H. HARAGUCHI, B. SMITH, S. WEEKS, D.J. JOHNSON, and J.D. WINEFORDNER, Appl. Spectrosc., **31**, 156(1977).
5. J. BRADSHAW, J. BOWER, S. WEEKS, K. FUJIWARA, N. OMENETTO, H. HARAGUCHI, and J.D. WINEFORDNER, 10th Material Research Symposium on Characterization of High Temperature Vapors and Gases, NBS, Gaithersburg, Maryland, 1978.
6. N. OMENETTO and J.D. WINEFORDNER, Progress in Analytical Atomic Spectroscopy, Vol. 2 (1,2) (Pergamon, 1979).
7. J.D. BRADSHAW, N. OMENETTO, G. ZIZAK, J.N. BOWER, and J.D. WINEFORDNER, "Five Laser Excited Fluorescence Methods to Measure Spatial Flame Temperatures. Part I Theoretical Basis, Appl. Opt. submitted.
8. C.A. VAN DIJK, P.J.TH. ZEEGERS, and C.TH.J. ALKEMADE, J. Quant. Spectrosc. Radiat. Transfer, **21**, 115(1979).
9. R.P. LUCHT and N.M. LAURENDEAU, Appl. Opt., **18**, 856(1979).
10. J.H. BECHTEL, Appl. Opt., **18**, 2100(1979).
11. D.R. CROSLLEY and G.P. SMITH, Appl. Opt., **19**, 517(1980).
12. G.D. BOUTILIER, M.B. BLACKBURN, J.M. MERMET, S.J. WEEKS, H. HARAGUCHI, J.D. Winefordner, and N. OMENETTO, Appl. Opt., **17**, 2291(1978).
13. F.E. LYTLE, Anal. Chem., **46**, 545A(1974).
14. F.E. LYTLE, Anal. Chem., **46**, 817A(1974).
15. G. BECK, Rev. Sci. Instrum., **47**, 537(1976).
16. J.M. HARRIS, F.E. LYTLE and T.C. MCCAIN, Anal. Chem., **48**, 2095(1976).
17. R.A. VAN CALCAR, M.J.M. VAN DE VEN, B.K. VAN UITERT, K.J. BIEWENGA, T.J. HOLLANDER, and C.TH.J. ALKEMADE, J. Quant. Spectrosc. Radiat. Transfer, **21**, 11(1979).
18. C.H. CORLISS and W.R. BOZMAN, Experimental Transition Probabilities for Spectral Lines of Seventy Elements, NBS, Monograph 53 (1962).

TABLE I. Gas Composition For the Four Flame Investigated

Flame	Methane (ℓ/m)	Air (ℓ/m)
1	.50	6.1
2	.51	6.1
3	.50	7.1
4	.50	6.6

TABLE II. Summary of the Temperatures Measured
in Three Different Flames

Flame	Line Observed (Å)	Level Energy (cm ⁻¹)	Temperature (k)
1 ^a	4102.	24373	1725-1699
	3257.	32900	
2 ^a	4102	24373	1785
	3257	32900	
	4102	24373	1769
	3039	32892	
3 ^b	3776	26478	1465-1426
	3525	36159	
	5350	26478	1565-1539
	3525	36159	
3 ^c	2768	36118	743
	3229	38746	
	3525	36159	1442
	3229	38746	
	3229	38746	2408
	2920	42030	
	3525	36159	1843
	2920	42030	
	2768	36118	1199
	2920	42030	

- a: In as thermometric species. Excitation line at 4101.76 Å
b: Tl as thermometric species. Excitation line at 3775.7 Å
c: Tl as thermometric species. Excitation line at 2767.8 Å

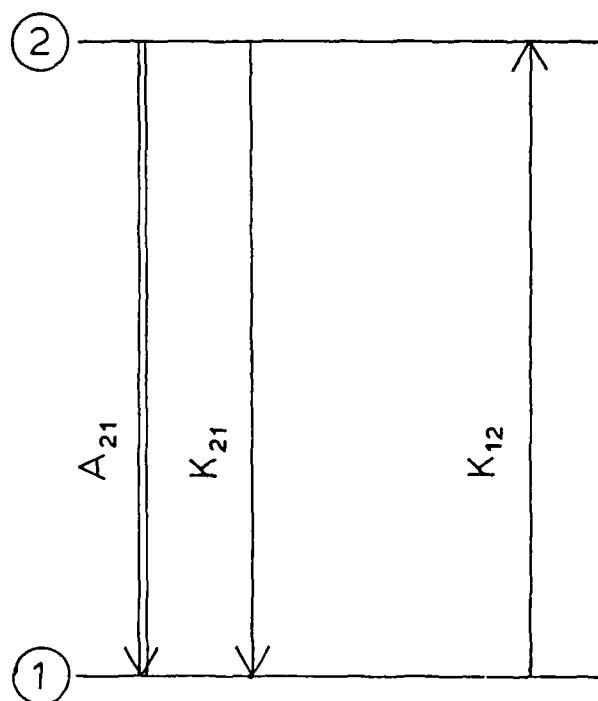


Figure 1C. Two-Level System, Showing Deviation from the Boltzmann Distribution.

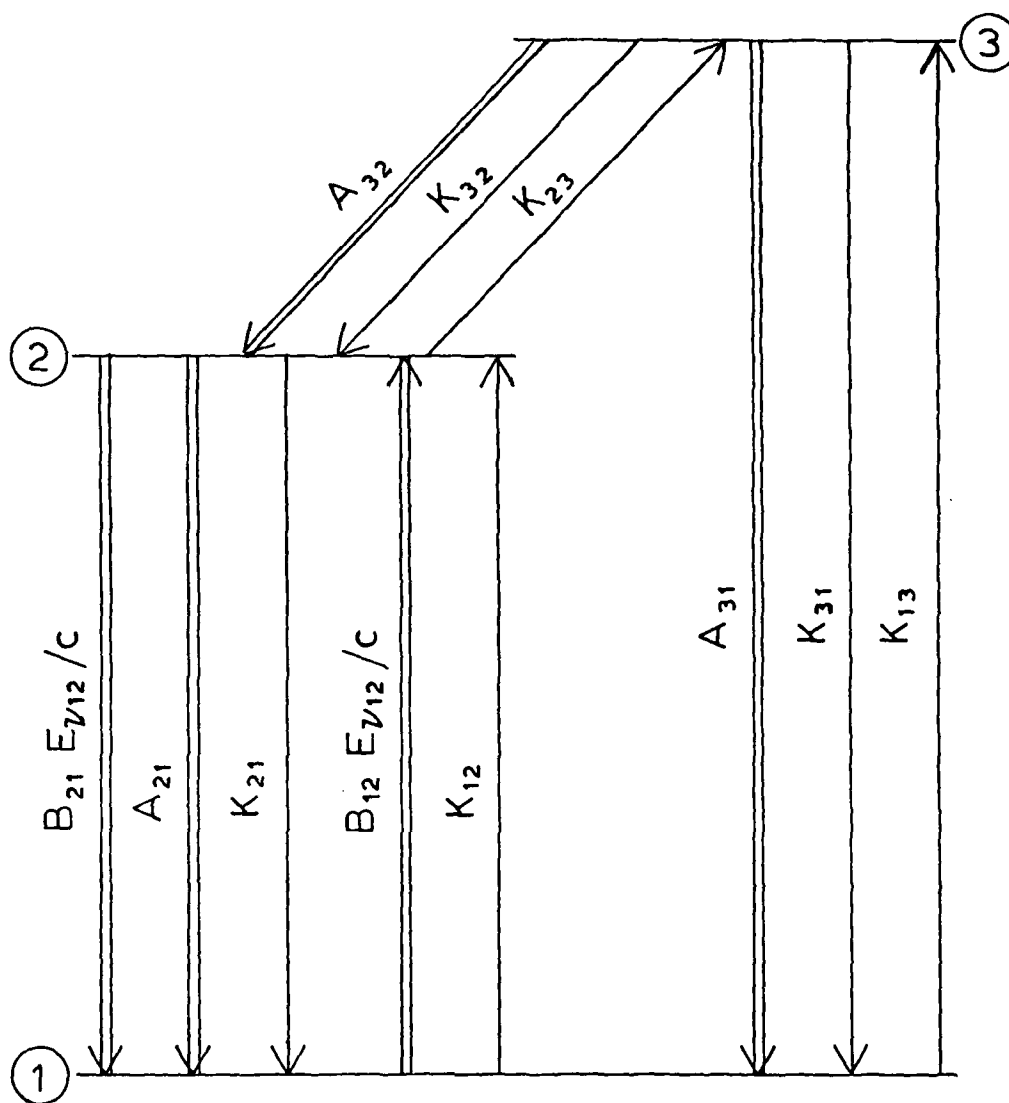


Figure 2C. Three-Level System Under Spectral Irradiances $E_{\nu_{12}}$ and $E_{\nu_{13}}$ and Collisional Excitation of the 3rd Level. Radiative and Collisional Rate Constants Are Shown.

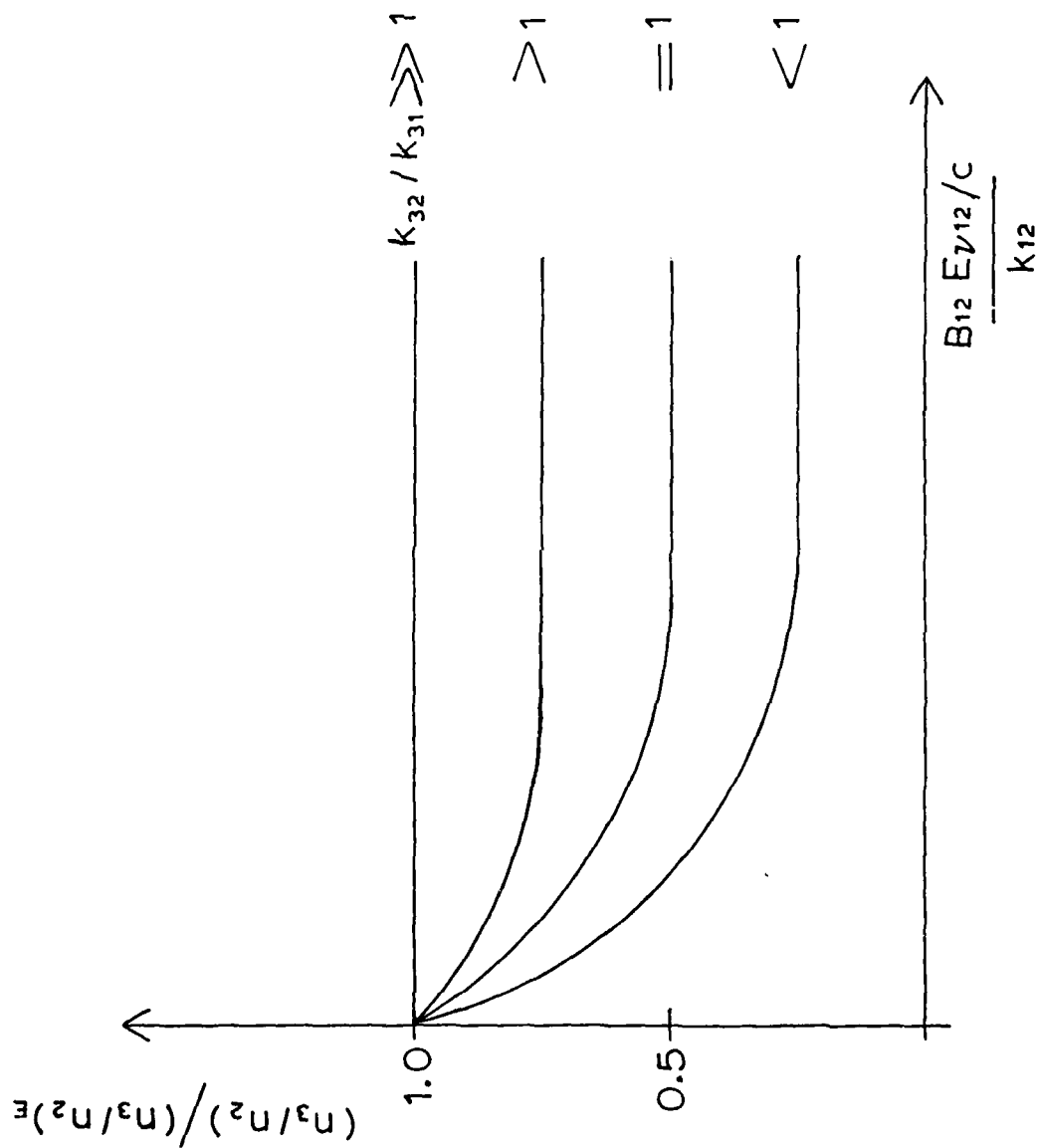


Figure 3C. The Population Ratio n_3/n_2 of a 3. Level System as Function of the Ratio Between Radiative and Collisional Excitation of the Level 2. k_{12}/k_{31} is the Significant Parameter Governing the Deviation from the Equilibrium Value $(n_3/n_2)_E$ as Given By Equation (9).

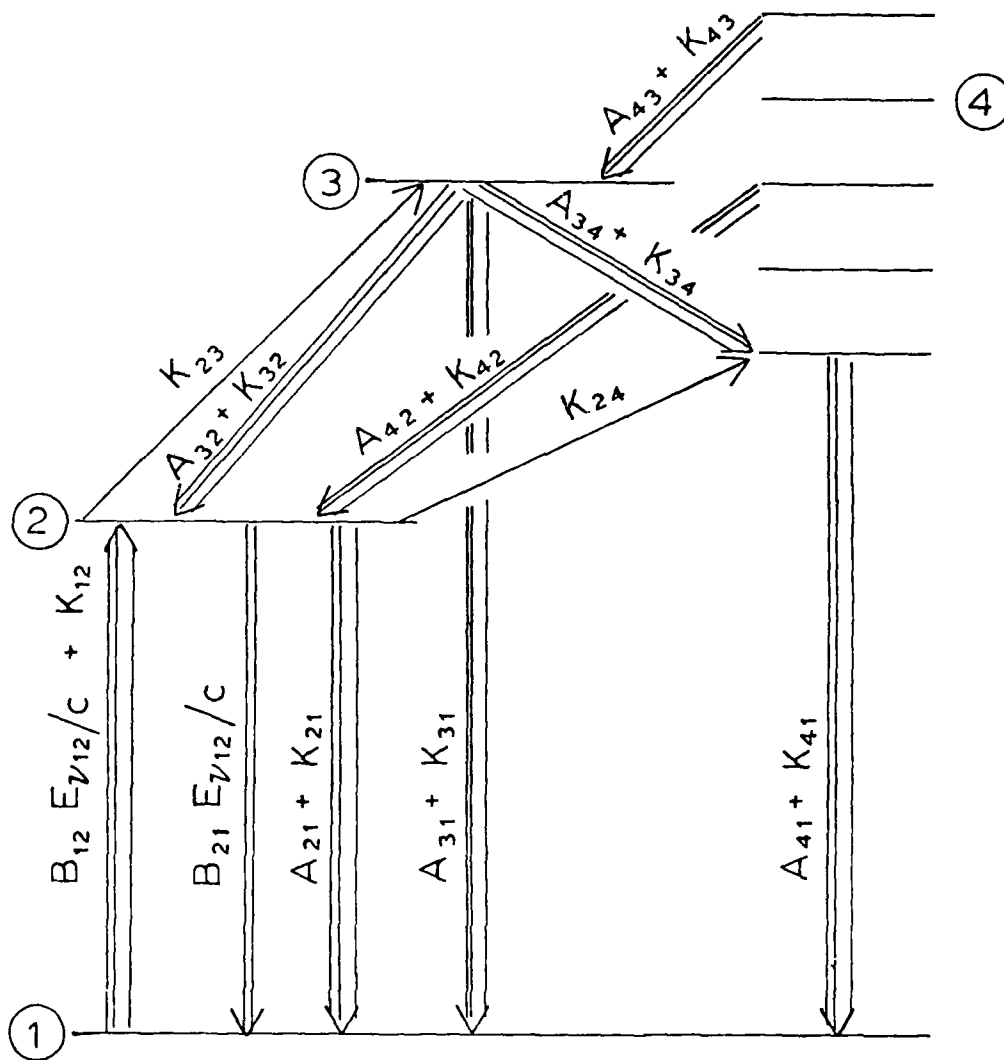


Figure 4C. Four-Level System Under Spectral Irradiance $E_{\nu_{12}}$ and with Radiative and Collisional Coupling Among the Levels. Significant Ratios of the Population are Given in the Text.

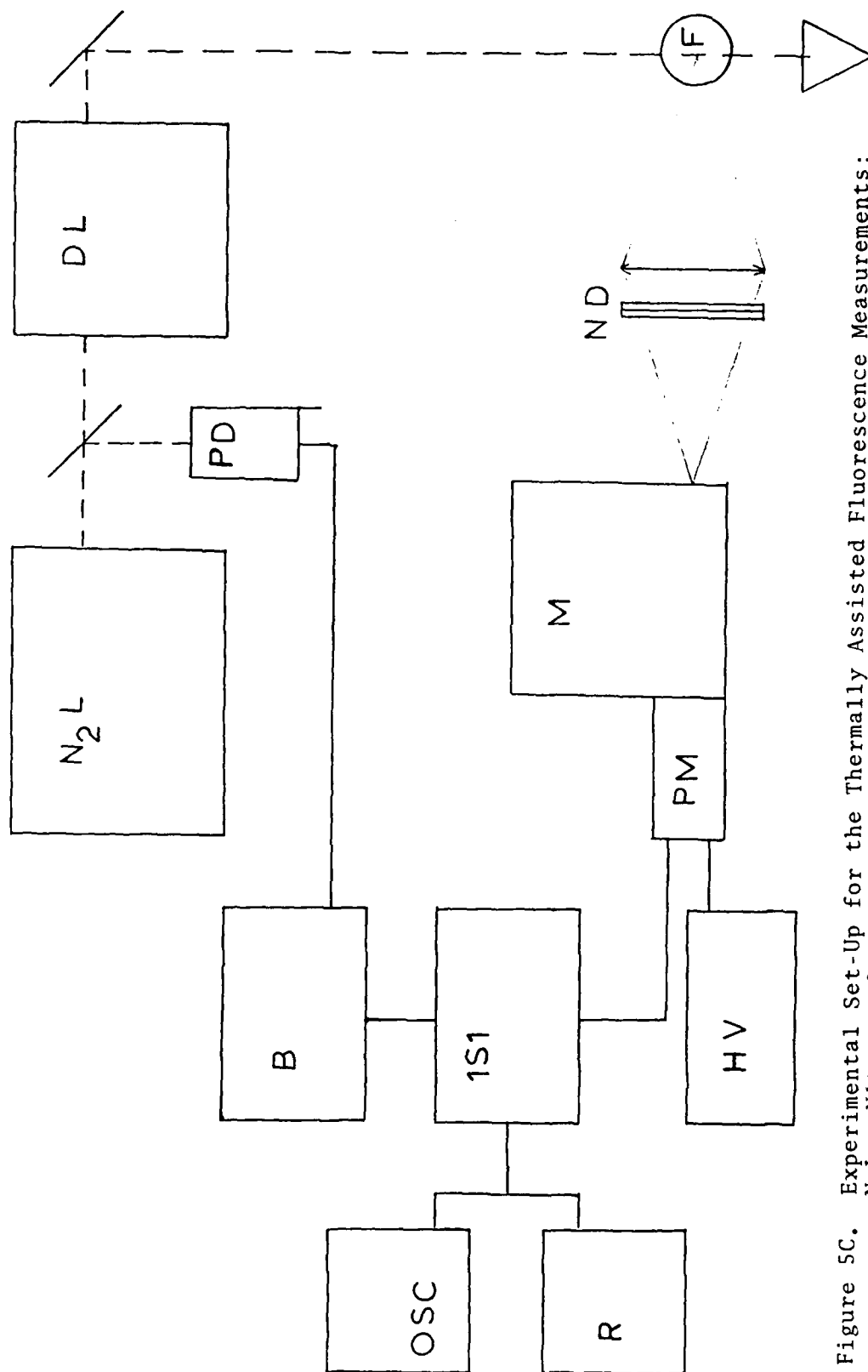


Figure 5C. Experimental Set-Up for the Thermally Assisted Fluorescence Measurements:
 N_2L - Nitrogen Laser; DL - Dye Laser; PD - Photodiode; B - Boxcar;
 F - Flame; ND - Neutral Density; M - Monochromator; PM - Photomultiplier;
 HV - High Voltage Power Supply; 1S1 - Tektronix Sampling Unit; OSC -
 Oscilloscope; R - Recorder.

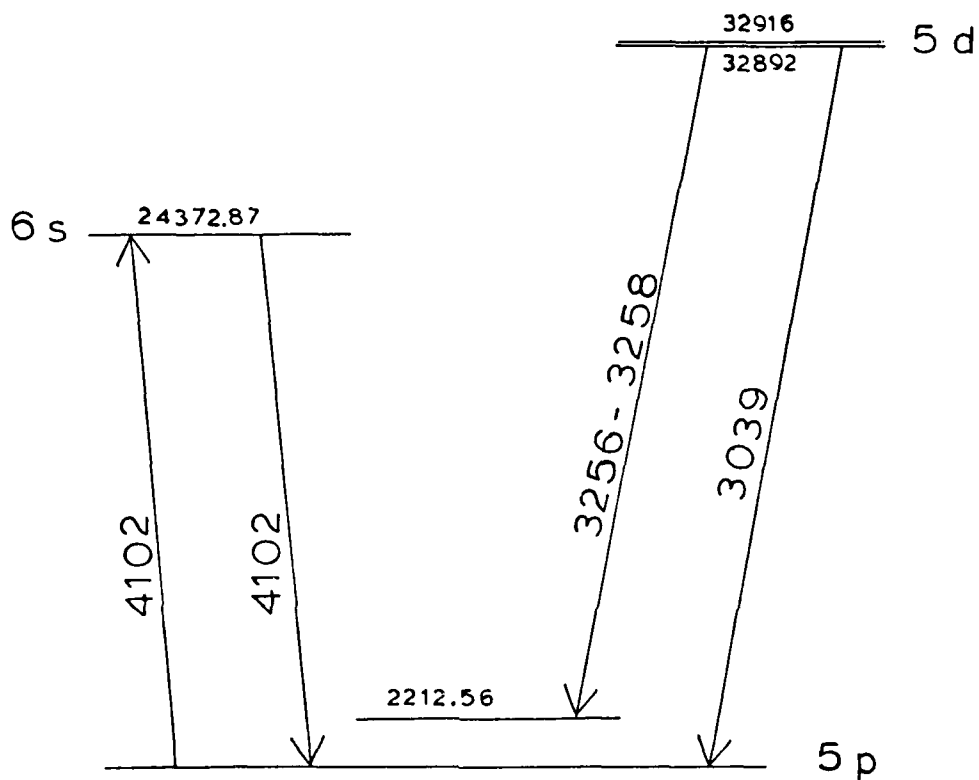


Figure 6C. Temporal Resolved Fluorescence Pulses of Tl. The Thermally Assisted Line (3525 Å) has its Peak Roughly 1 ns After the Fluorescence Maxim from the Radiatively Excited Level (3776 Å).

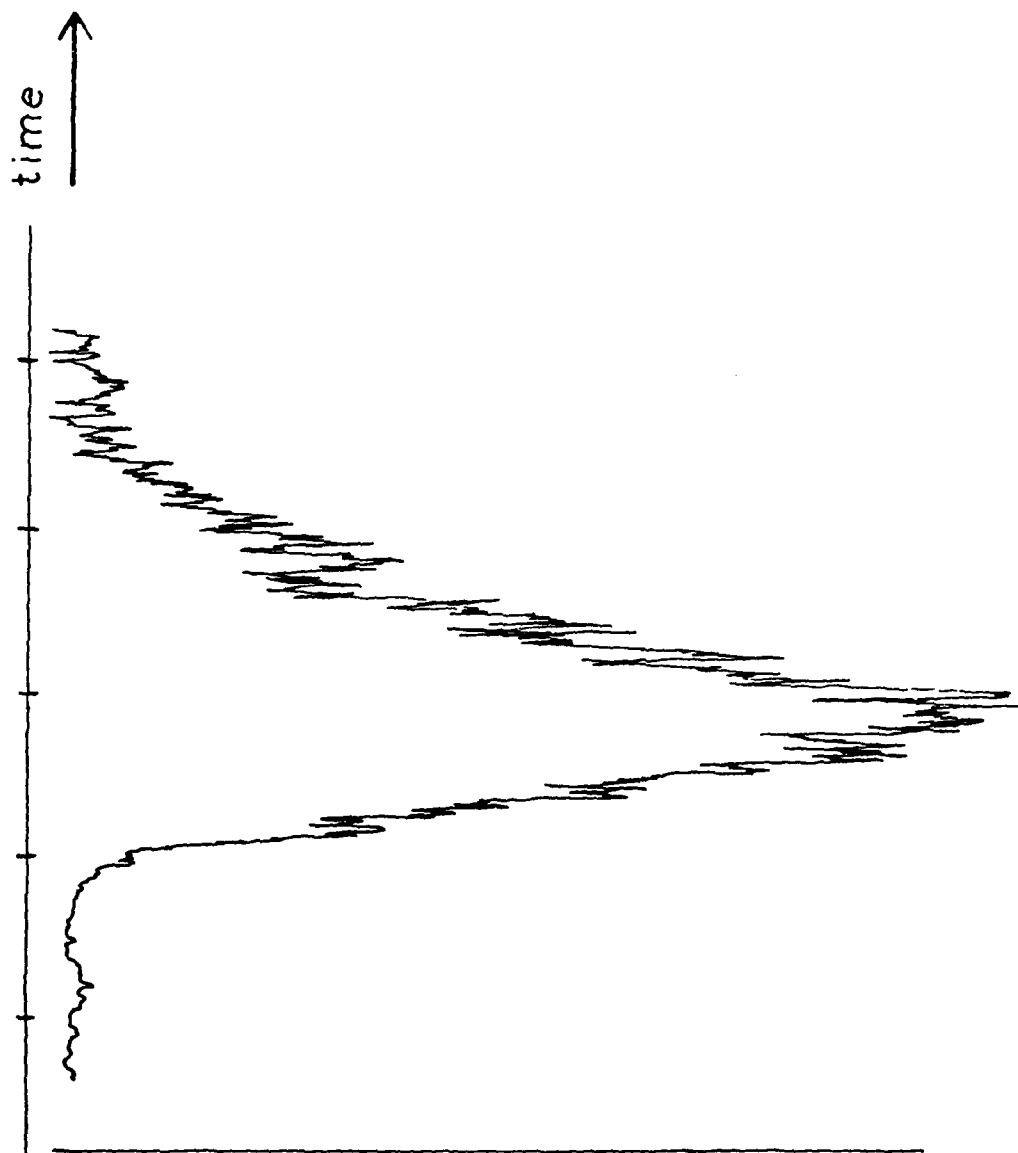


Figure 7C. Energy Scheme of In Showing the Transitions Observed (arrows). The Energy Values of the Levels are in cm^{-1} .

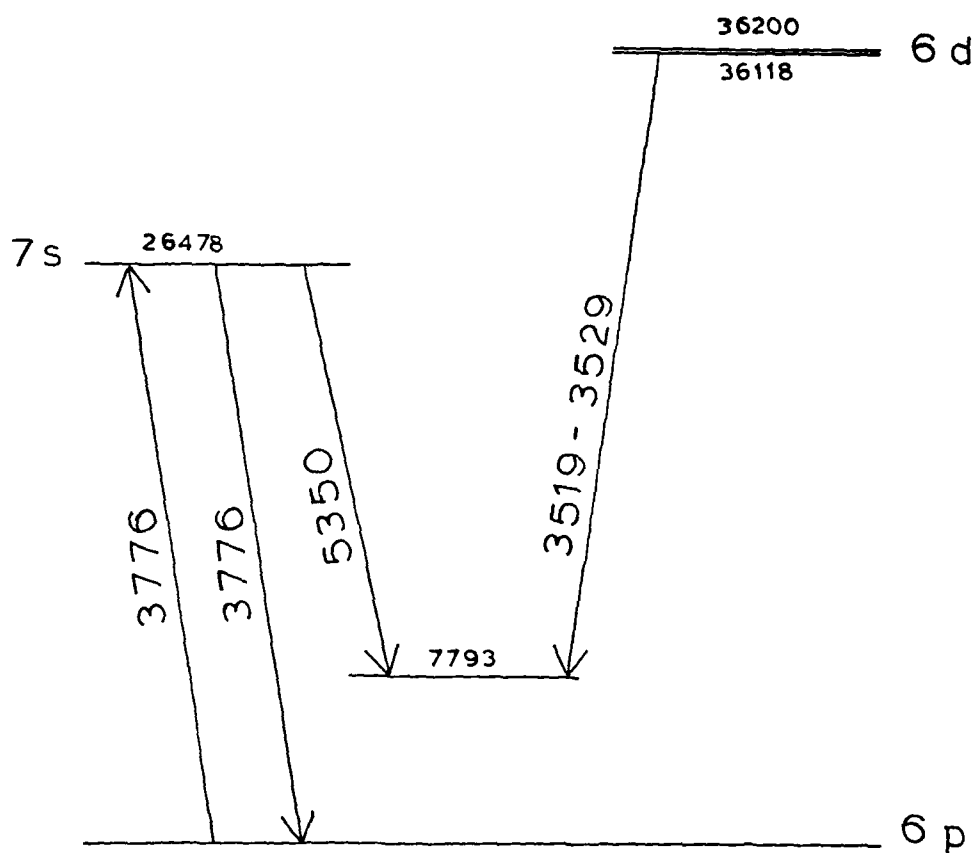


Figure 8C. Typical Thermally Assisted Fluorescence Pulse (3257 \AA) as Recorded with our Apparatus. The Time Scale is 5 ns/div.

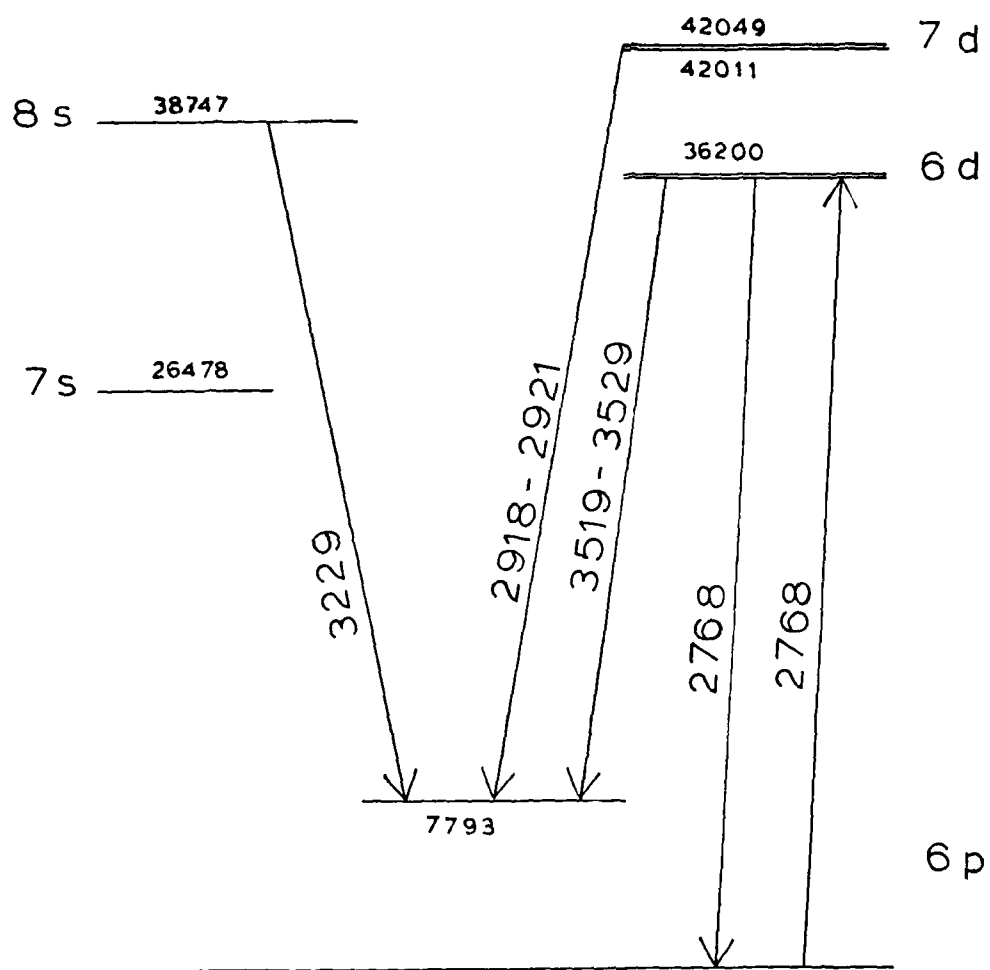


Figure 9C. Energy Scheme of Tl Showing the Transitions Observed (arrows). The Energy Values of the Levels are in cm^{-1} .

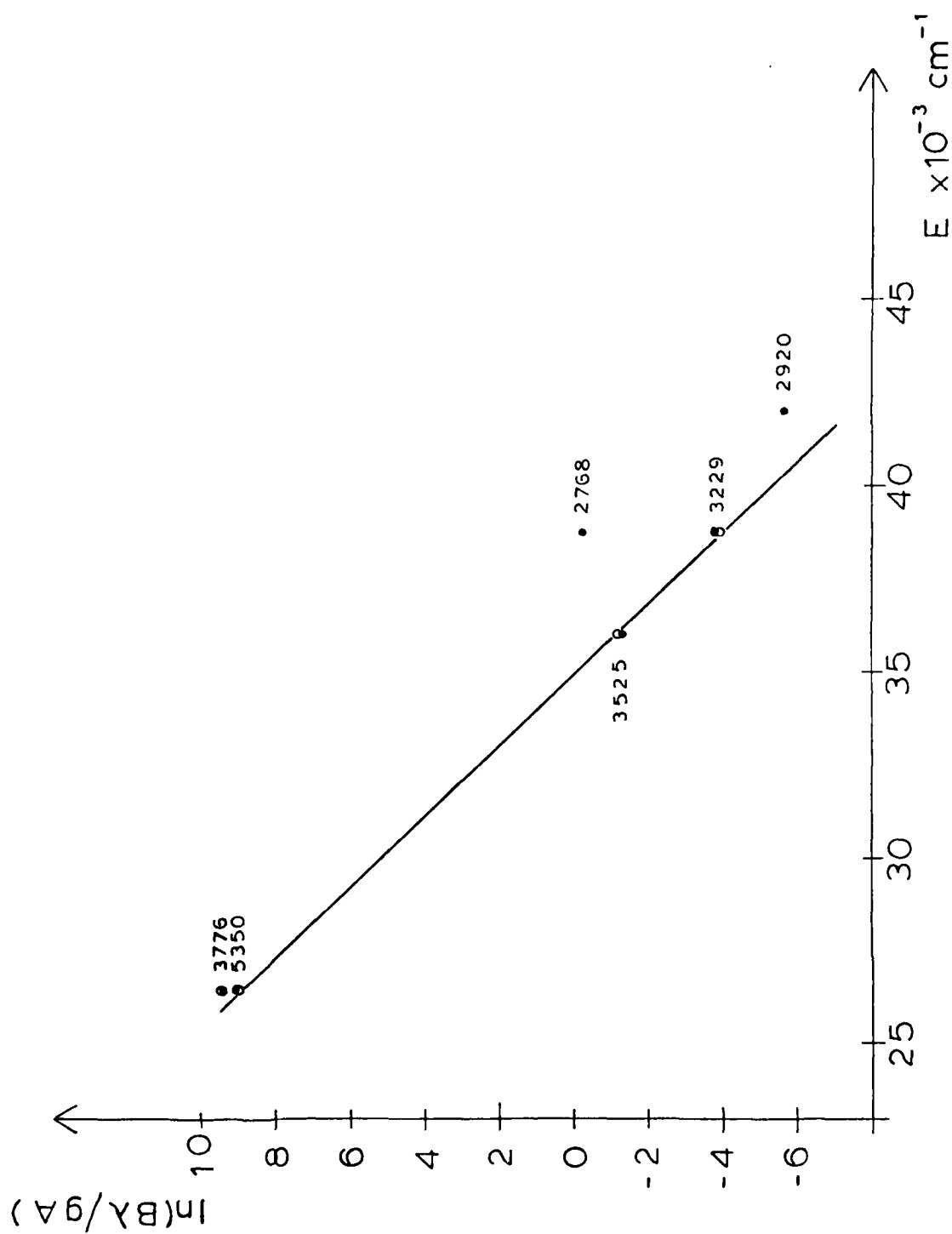


Figure 10C. Energy Scheme of Tl Showing the Transitions Observed (arrows). The Energy Levels of the Levels are in cm^{-1} .

APPENDIX D
(manuscript submitted to J. QUANT.
SPECTROSC. RADIAT. TRANSFER)

"A THEORETICAL AND EXPERIMENTAL APPROACH TO LASER SATURATION BROADENING IN FLAMES"¹

N. Omenetto^{*}, J. Bower, J. Bradshaw, C. A. Van Dijk^{**} and J. D. Winefordner^δ

Department of Chemistry, University of Florida, Gainesville, Florida 32611

^{*} On leave from the Institute of Inorganic and General Chemistry, University of Pavia, Pavia (Italy).

^{**} Post Doctoral Associate, University of Michigan, East Lansing, Michigan.

^δ To whom all correspondence should be addressed.

¹ Work supported by AF-AFOSRF44620-78-C-0005 and by a Wright Patterson Air Force Base Contract AF-33615-78C-2036

KEY WORDS

Broadening, saturation, flames, hydrogen, laser, excitation.

ABSTRACT

The broadening of the absorption profile in hydrogen-based flames diluted with argon and nitrogen is discussed theoretically and demonstrated experimentally with a pulsed tunable dye laser. This broadening is evaluated from the half-width of the profile obtained by scanning the laser beam through the atoms in the flame while monitoring the resulting fluorescence with a high luminosity monochromator, i.e., by observing a fluorescence excitation profile. Results are given for the elements Ca, Sr, Na and In. It is shown that the halfwidth of the atomic profile depends approximately upon the square root of the log of the laser irradiance. This dependence stems from a theoretical treatment based upon the interaction of a gaussian laser profile and a gaussian atomic profile. It is also shown that if the laser spectral bandwidth exceeds by ≈ 5 -10 times the absorption halfwidth, the fluorescence excitation profile provides a simple means of a reliable evaluation of the laser bandwidth.

INTRODUCTION

The high irradiance provided by the pulsed tunable dye laser is capable of saturating both single-photon and 2-photon transitions of atoms in flames at atmospheric pressure.¹⁻⁷ Among other effects, such as the attainment of the maximum fluorescence signal and its relative independence upon the quantum efficiency of the transition, the strong irradiation field is known to be responsible for a broadening of the absorption line profile. This broadening is called saturation broadening. Hosch and Piepmeier,⁸ Van Dijk,⁴ as well as others⁹ reported an experimental verification of saturation broadening by performing both absorption and fluorescence measurements.

The aim of this work is to present a theoretical treatment of the saturation broadening based upon the rate equations approach and for the two cases of a very narrow excitation line laser coupled with a Lorentzian absorption profile and a gaussian laser profile coupled with a gaussian atom profile. The theoretical predictions will be compared with the experimental data obtained by scanning the laser beam throughout the atom profile in different flames while monitoring the fluorescence emitted at right angles, i.e., by obtaining a fluorescence excitation profile.^{10,11}

We realize that our experimental conditions are not applicable to the first case (line source and Lorentzian atom profile). Furthermore, the second case (gaussian laser profile and gaussian atom profile) is certainly an approximation to the real interaction process. Nevertheless, we felt that it was useful to present our experimental data since the saturation broadening was clearly observed in all the cases investigated.

THEORY

The treatment given here follows the basic discussion on saturation which can be found in several books, chapters and articles.¹⁻⁷ Generally, atoms are considered to be dispersed as trace constituents in a gas at atmospheric pressure and characterized by a 2-level system. Coherence effects (cooperative phenomena) are neglected because dephasing, coherence-interrupting collisions are considered to be fast in our atmospheric pressure flames.^{12,13}

Case A. Line source and Lorentzian atom profile

In this case, the laser is assumed to be a very narrow, monochromatic line source and the atomic absorption profile is considered to be homogeneously broadened. The first assumption can be met by tunable dye lasers.^{14,15} Also, the laser beam is assumed to be spatially uniform. The case in which a gaussian spatial profile is assumed for the radial dependence of the laser intensity^{16,17} is discussed in the Appendix.

The atom profile can be considered homogeneous if the following conditions hold: (i) Doppler broadening is negligible compared to collisional broadening; (ii) in the case of combined Doppler and collisional broadening, velocity changing collisions are so fast that atoms cannot be considered to belong to any particular Doppler interval during the time of interaction with the laser beam.

Let the atoms be characterized by levels 1 and 2, with energy difference $h\nu_0$ (J), statistical weights (dimensionless) g_1 and g_2 and number densities (m^{-3}) n_1 and n_2 . The total atomic population in this case is $n_T = n_1 + n_2$. In the steady-state limit, we can obtain from a simple rate equations approach,⁷ the following relationship:

$$\frac{n_2}{n_T} = \frac{B_{12} \{ \rho(\lambda_\ell) / \delta\lambda_{\text{eff}} \} g^a(\lambda_\ell - \lambda_0)}{(1 + \frac{g_1}{g_2}) \left(B_{12} \left(\frac{\rho(\lambda_\ell)}{\delta\lambda_{\text{eff}}} \right) g^a(\lambda_\ell - \lambda_0) + A_{21} + k_{21} \right)}, \quad (1)$$

where

B_{12} = Einstein coefficient of induced absorption, $J^{-1} m^3 s^{-1}$; A_{21} = Einstein coefficient of spontaneous emission, s^{-1} ; k_{21} = collisional (quenching) rate constant, s^{-1} ; $\rho(\lambda_\ell) \equiv \int_{\delta\lambda_\ell} \rho_\lambda(\lambda) d\lambda \equiv \rho_\lambda d\lambda_\ell$, integral energy density of the laser, integrated over the effective width of the laser line, $\delta\lambda_\ell$, in Jm^{-3} ; $g_\lambda^a(\lambda_\ell - \lambda_0)$ = absorption shape function, given by the Lorentzian dispersion formula

$$g_\lambda^a(\lambda_\ell - \lambda_0) = \frac{1}{\pi} \left[\frac{\frac{\delta\lambda_L}{2}}{\left(\frac{\delta\lambda_L}{2} \right)^2 + (\lambda_\ell - \lambda_0)^2} \right], \quad m^{-1}$$

$\delta\lambda_L$ = full width at half maximum of the shape function, m;

$$\frac{1}{\delta\lambda_{\text{eff}}} \equiv g_\lambda^a(\lambda = \lambda_0) = \frac{2}{\pi \delta\lambda_L}, \quad \text{peak value of the shape function, } m^{-1};$$

$\delta\lambda_{\text{eff}}$ = effective width of the absorption profile, m;

$$g_\lambda^a(\lambda_\ell - \lambda_0) = \frac{g_\lambda^a(\lambda_\ell - \lambda_0)}{g_\lambda^a(\lambda = \lambda_0)} = g_\lambda^a(\lambda_\ell - \lambda_0) \left(\frac{\pi \delta\lambda_L}{2} \right), \quad \text{dimensionless.}$$

Equation (1) can be rewritten in terms of the effective lifetime, $\tau (A_{21} + k_{21})^{-1}$ of the excited level as

$$\frac{n_2}{n_T} = \frac{B_{12} \{ \rho(\lambda_\ell) / \delta\lambda_{\text{eff}} \} g^a(\lambda_\ell - \lambda_0) \tau}{(1 + \frac{g_1}{g_2}) B_{12} \{ \rho(\lambda_\ell) / \delta\lambda_{\text{eff}} \} g^a(\lambda_\ell - \lambda_0) \tau + 1} \quad (1a)$$

If the atomic density is low, then n_2 can be expressed in terms of the fluorescence radiance, B_F ($J s^{-1} m^{-2} sr^{-1}$), as

$$B_F = n_2 \left(\frac{\ell}{4\pi} \right) A_{21} h\nu_0 \quad (2)$$

where ℓ (m) is the homogeneous depth of the fluorescence volume in the direction of observation.

We now define the saturation energy density¹⁻⁷ as

$$\frac{\rho^s(\lambda_\ell)}{\delta\lambda_{eff}} \equiv \frac{A_{21} + k_{21}}{\left(1 + \frac{g_1}{g_2}\right) B_{12}} \equiv \frac{1}{\left(1 + \frac{g_1}{g_2}\right) B_{12} \tau} \equiv \frac{A_{21}}{\left(1 + \frac{g_1}{g_2}\right) B_{12} Y_{21}} \quad (3)$$

where $Y_{21} = \{A_{21}/(A_{21} + k_{21})\}$ is the quantum efficiency of the transition.

By rearranging Eq. (1) and making use of Eqs. (2) and (3), we obtain the atomic fluorescence radiance the following expression:

$$B_F = C n_T \frac{\rho(\lambda_\ell)}{\rho^s(\lambda_\ell)} \left(\frac{g_2}{g_1 + g_2} \right) \left\{ \frac{g^a(\lambda_\ell - \lambda_0)}{1 + \left(\frac{\rho(\lambda_\ell)}{\rho^s(\lambda_\ell)} \right) g^a(\lambda_\ell - \lambda_0)} \right\} \quad (4)$$

where $C \equiv h\nu_0 (\ell/4\pi) A_{21}$.

This equation shows the theoretical dependence of the wavelength integrated fluorescence radiance upon the laser energy density and the detuning between the peak of the laser profile, acting here as a delta function, and the peak of the Lorentzian atom absorption profile. It can be easily shown that this equation, in the low intensity limit, reduces to the well known linear dependence of the fluorescence radiance upon $\rho(\lambda_\ell)$ and Y_{21} while, in the high-intensity limit, n_2 becomes half of the total atomic population if the statistical weights are

the same. This particular outcome holds, of course, irrespective of the line shape.

The ratio between braces in Eq. (4) is a modified Lorentzian function, which takes into account the effect of the laser field upon the spectral profile. The low intensity Lorentzian function can be written as

$$g^a(\lambda_\ell - \lambda_0) = \left(\frac{\pi \delta\lambda_L}{2} \right) \left(\frac{1}{\pi} \frac{\frac{\delta\lambda_L}{2}}{\left(\frac{\delta\lambda_L}{2} \right)^2 + (\lambda - \lambda_0)^2} \right) \quad (5)$$

while the modified Lorentzian function in Eq. (4) can be written as a function of the laser density ρ and the detuning $\delta \equiv (\lambda_\ell - \lambda_0)$ as follows:

$$g^a(\delta, \rho) = \left(\frac{\pi \delta\lambda_L}{2} \right) \left\{ \frac{1}{\pi} \frac{\frac{\delta\lambda_L}{2}}{\left(\frac{\delta\lambda_L}{2} \right)^2 \left(1 + \frac{\rho(\lambda_\ell)}{\rho^s(\lambda_\ell)} \right) + \delta^2} \right\} \quad (6)$$

In both equations, $\delta\lambda_L$ is full width at half maximum (FWHM) of the unperturbed Lorentzian function. Inspection of Eqs. (5) and (6) shows that the FWHM of the modified function, here called $\delta\lambda_{\text{excitation}}$, is given by

$$(\delta\lambda_{\text{exc}})^2 = (\delta\lambda_L)^2 + (\delta\lambda_L)^2 \left(\frac{\rho(\lambda_\ell)}{\rho^s(\lambda_\ell)} \right) \quad (7a)$$

or

$$\delta\lambda_{\text{exc}} = \delta\lambda_L \sqrt{1 + \frac{\rho(\lambda_\ell)}{\rho^s(\lambda_\ell)}} \quad (7b)$$

This equation shows that the width of the absorption profile increases with the square root of the laser density.

Several conclusions can be derived from Eq. (7).

- (i) Since $\rho^S(\lambda_\ell)$ depends upon the quantum efficiency of the transition, the broadening effect at a fixed laser density will be greater in high quantum efficiency flames as compared to that observed in low quantum efficiency flames.
- (ii) As indicated by Eq. (7a), a plot of the experimentally observed $(\delta\lambda_{\text{exc}})^2$ vs. the laser density measured at the flame should result in a straight line. From the slope of this line, one can calculate the saturation density for that particular transition while from the intercept one can calculate the low intensity Lorentzian linewidth.
- (iii) At the limit of $\rho(\lambda_\ell) = 0$, $\delta\lambda_{\text{exc}} = \delta\lambda_L$, as it should be.
- (iv) Since the second term in the square root involves a ratio between the densities, one needs only to measure the laser power Φ , at the flame.
- Equation (7) can also be derived from Eqs. (4) and (6) in the following manner. When the detuning is zero, the fluorescence signal is peaked at a value given by the following expression:

$$B_F(\delta=0) = Cn_T \left(\frac{\rho(\lambda_\ell)}{\rho^S(\lambda_\ell)} \right) \left(\frac{g_2}{g_1 + g_2} \right) \left(\frac{1}{1 + \frac{\rho(\lambda_\ell)}{\rho^S(\lambda_\ell)}} \right) ; \quad (8)$$

when the detuning is very large, the fluorescence signal approaches zero. Therefore, we can find the detuning, $\delta_{\frac{1}{2}}^+$, at which the peak value of the function is halved, for both positive and negative detunings. We then have

$$\begin{aligned} \frac{1}{2} \left\{ Cn_T \left(\frac{\rho(\lambda_\ell)}{\rho^S(\lambda_\ell)} \right) \left(\frac{g_2}{g_1 + g_2} \right) \left(\frac{1}{1 + \frac{\rho(\lambda_\ell)}{\rho^S(\lambda_\ell)}} \right) \right\} = \\ = Cn_T \left(\frac{\rho(\lambda_\ell)}{\rho^S(\lambda_\ell)} \right) \left(\frac{g_2}{g_1 + g_2} \right) \left\{ \frac{\left(\frac{\delta\lambda_L}{2} \right)^2}{\left(\frac{\delta\lambda_L}{2} \right)^2 + \left(-\frac{\delta\lambda_L}{2} \right)^2 \left(\frac{\rho(\lambda_\ell)}{\rho^S(\lambda_\ell)} \right) + (\delta_{\frac{1}{2}}^+)^2} \right\} \end{aligned} \quad (9)$$

which gives

$$\delta\lambda_{\text{exc}} = (\delta)_{\frac{1}{2}}^{+} + (\delta)_{\frac{1}{2}}^{-} = \delta\lambda_L \sqrt{1 + \frac{\rho(\lambda_L)}{\rho^S(\lambda_L)}} \quad (10)$$

and is seen to be identical with Eq. (7).

Case b. Gaussian laser profile and gaussian atom profile

This case can be considered to be closer to our experimental set-up when the pulsed laser beam is not very narrow and the atom profile in the flame is described by a Voigt profile. Here, the laser is assumed to be gaussian so that its spectral energy density ($\text{J m}^{-3} \text{ m}^{-1}$) is given by the following expression:

$$\rho_{\lambda}(\lambda) = \rho \frac{2\sqrt{\ln 2}}{\sqrt{\pi} \delta\lambda_L} \exp \left\{ -\frac{2\sqrt{\ln 2}}{\delta\lambda_L} (\lambda - \lambda_L)^2 \right\} \quad (11)$$

where ρ is the integrated energy density (J m^{-3}) and $\delta\lambda_L (\text{m})$ is the FWHM of the laser spectral profile. Accordingly, the atom profile is given by the following dimensional (m^{-1}) shape function:

$$g_{\lambda}^a(\lambda - \lambda_0) = \frac{2\sqrt{\ln 2}}{\sqrt{\pi} \delta\lambda_a} \exp \left\{ -\frac{2\sqrt{\ln 2}}{\delta\lambda_a} (\lambda - \lambda_0)^2 \right\} \quad (12)$$

where $\delta\lambda_a$ is now the FWHM of the atom spectral profile. As stated before, the atoms here are not considered to be grouped in Doppler intervals (which would cause hole burning for a spectrally narrow, saturating laser beam) because of the very effective cross-relaxation taking place in the flame. The interaction of the laser and the atoms in Eq. (1) is now given by the convolution integral of both profiles. Since the convolution of two gaussian functions is still a gaussian function, we obtain

$$\int \rho_{\lambda}(\lambda) g_{\lambda}^a (\lambda - \lambda_0) d\lambda = \rho \frac{2\sqrt{\ln 2}}{\sqrt{\pi} \delta\lambda'} \exp \left\{ - \frac{2\sqrt{\ln 2}}{\delta\lambda'} (\lambda_{\ell} - \lambda_0)^2 \right\} \quad (13)$$

where $(\lambda_{\ell} - \lambda_0)$ is the detuning between the centers of both profiles and $\delta\lambda'$ represents the convolution of the laser and the atom halfwidths, i.e.,

$$\delta\lambda' \equiv \sqrt{(\delta\lambda_{\ell})^2 + (\delta\lambda_a)^2} \quad (14)$$

Proceedings as before and defining now the saturation spectral density as

$$\rho^s = \frac{\delta\lambda' \sqrt{\pi}}{\left(1 + \frac{g_1}{g_2}\right) B_{12} \tau 2\sqrt{\ln 2}} \quad (15)$$

we obtain for the halfwidth of the fluorescence excitation profile

$$\delta\lambda_{\text{exc}} = (\delta\lambda)_{\frac{1}{2}}^+ + (\delta\lambda)_{\frac{1}{2}}^- = \frac{\delta\lambda'}{\sqrt{\ln 2}} \sqrt{\ln \left(2 + \frac{\rho}{\rho^s}\right)} \quad (16)$$

where all of the terms have been previously defined.

Several conclusions can be drawn from Eq. (15):

- (i) High quantum efficiency flames will be more sensitive for the observation of the broadening effect, exactly as in the preceding case.
- (ii) In this case, saturation broadening sets in at a lower rate as compared to the previous case (narrow line and Lorentzian atom profile).
- (iii) At the limit, when $\rho \rightarrow 0$, $\delta\lambda_{\text{exc}} \rightarrow \delta\lambda'$, as it should be.
- (iv) If the value of the laser density greatly exceeds the saturation energy density for that particular transition, the 2 can be neglected in the argument of the logarithm and Eq. (16) can be written as

$$\delta\lambda_{\text{exc}} = \frac{\delta\lambda'}{\sqrt{\ln 2}} \sqrt{\ln \frac{\phi}{\phi^s}} \quad (17)$$

or

$$(\delta\lambda_{\text{exc}})^2 = \frac{(\delta\lambda')^2}{\ln 2} \{ \ln \phi - \ln \phi^s \} \quad (18)$$

where ϕ and ϕ^S correspond to ρ and ρ^S but are fluxes, in $J\ s^{-1}\ m^{-2}$.

From Eq. (18), one can see that, by plotting $(\delta\lambda_{exc})^2$ vs. $\ln\phi$, a straight line is obtained. The slope of this line gives $\delta\lambda$, while the intercept gives ϕ^S .

EXPERIMENTAL

The experimental set-up used is described in detail elsewhere.¹⁸ The tunable dye laser (DL-400, Molelectron, Sunnivale, CA.) pumped by a nitrogen laser (UV-14, Molelectron, Sunnivale, CA) is directed into the flame by means of two plane mirrors after passing through two spatial filters consisting of shielded iris diaphragms (Edmund Scientific, Barrington, N. J.). These filters passed only the central portion of the beam so to improve its uniformity. No lenses were placed between the iris and the flame. The flame used was an oxygen-hydrogen mixture diluted with argon or nitrogen, and supported by a capillary burner. For these measurements, the flame was surrounded by a gas sheath (Ar or N₂) but was not protected by a similar analyte-free flame burning at the same composition and temperature. All measurements were taken at approximately 1 cm above the primary reaction zone. The standard solutions for all elements (Ca, Sr, Na and In) were made from reagent grade chemicals. The concentration was chosen to be very low (in most cases 1 $\mu g/mL$) to avoid any self-absorption, pre-filter or post-filter effects.

The fluorescence was collected at right angle by an optical system consisting of two spherical quartz lenses and a rectangular aperture. The flame was imaged at unit magnification onto this aperture and after that, with the same magnification, onto the entrance slit of a high luminosity monochromator (Jobin Yvon, model H-10, 10-cm focal length, f-3.6) whose slit width was set for all elements at 0.5 mm. The signal from a photomultiplier wired for fast pulse high current work and operated at -1000 V was processed by a dual channel boxcar integrator (model 162-164, PAR, Princeton, N. J.). In order to sample only a small portion

of the fluorescence waveform, which in our case is the result of the saturation process and by the photomultiplier temporal characteristics,¹⁸ we have used a 75-ps risetime sampling head (PAR Model 163 sampled integrator). The monochromator was centered at the peak of the fluorescence line and the laser output was slowly scanned across the absorption profile. These measurements were then repeated by decreasing the laser irradiance with calibrated neutral density filters. Particular care was taken to minimize spurious reflections and scatter of the laser into the monochromator.

The peak power of the laser at the particular transition used was measured with a calibrated photodiode (Model F4000, ITT, Fort Wayne, Indiana) coupled directly to a scope (Type 454, Tektronix, Portland, Oregon).

The laser spectral bandwidth was measured directly with a good resolution grating monochromator (Jobin Yvon, Model HR-1000, 1-m focal length, $f = 5.4$). The spectral slit function of such monochromator, evaluated by scanning a very low pressure mercury pen light in front of it, was found to be 0.12 \AA .

RESULTS AND DISCUSSION

Figures 1-4 show clearly the broadening effect on the line profile as the laser irradiance on the atoms increases. The broadening in the halfwidth ranges from a factor of 1.3 for In to 5.4 for Sr. Obviously, as expected and stated before, this broadening cannot be accounted for by Eq. (7b) which was derived with the assumption of a monochromatic laser and a Lorentzian atom profile. Indeed, since in some cases (Sr and Ca), the laser power exceeded the saturation power by approximately a factor of 100, Eq. (7b) would have predicted a 10-fold broadening of the profile. Except for the case of indium (Fig. 1) for which a 15 ns boxcar gate width was used to average the signal, the profiles have been obtained with the 75 ps risetime sampling head. This explains the different noise levels shown in the figures.

Irrespective of the theoretical assumptions made, both Eq. (7) and, (16) predict a larger broadening effect with high quantum efficiency flames as compared with that observed with low quantum efficiency flames. Despite the fact that our flames are not shielded (apart from an outer gas sheath), the replacement of argon as diluent by nitrogen should change considerably the quantum efficiency. Thus, different broadenings are expected for the same laser power but for the two flames. The experimental results, collected in Table I, do indeed show the correct trend, with the exception of strontium. These values are therefore indicative of the different quantum efficiency and, in turn, of the different saturation powers in the two flames. This matter is discussed in greater details in another paper.¹⁹

In an attempt to compare the experimental data with the theoretical predictions given by Eq. (16), we have calculated for both flames the ratio between the maximum value of $\delta\lambda_{\text{exc}}$ (corresponding to that obtained at full laser power) and the minimum value of $\delta\lambda_{\text{exc}}$ (corresponding to that obtained at $\rho \ll \rho^S$, i.e., when $\delta\lambda_{\text{exc}} \approx \delta\lambda'$). The saturation power was evaluated for each element from the experimental saturation curve.¹⁹ In Table II, we compare this ratio with those obtained experimentally, where the values for $(\delta\lambda_{\text{exc}})_{\text{min}}$ are those obtained at very low laser powers (see also Table III). Apart from some unexplained discrepancies outside the range of the experimental errors (such as the experimental value for strontium in the nitrogen-diluted flame), the agreement between the theory and the experiment can be considered fairly satisfactory, when all the assumptions made at the beginning are properly and critically considered.

In the flames used in this work, the halfwidth of the atom profile is expected to be of the order of 0.05 \AA for all the elements considered. Therefore,

the convolution obtained by scanning the laser through the absorption profile at low laser powers can be practically entirely attributed to the laser spectral halfwidth. For our theory to be consistent, the values so obtained (fluorescence excitation profile) should be the same as those given by the slope of the plot of Eq. (16), as explained before. Table III shows the different values obtained with these two methods. In addition, the values obtained by measuring directly the laser profile with a medium resolution monochromator are also shown. Again, apart from some differences, the average value for the two flames obtained with both techniques (fluorescence excitation profile and saturation broadening) closely agrees with that measured directly. We therefore feel that, whenever the laser bandwidth exceeds by approximately 5 to 10 times the atom profile, the halfwidth obtained from the low intensity fluorescence excitation profile provides a reliable estimate of the laser spectral bandwidth. Obviously, this method fails when the laser bandwidth is much narrower than the atom profile (since in this case the convolution will be essentially given by the atom profile) and loses its significance when the laser bandwidth is much larger (> 20 times) than the atom profile. In this last case, it would be indeed much simpler to scan the laser directly through a small-medium resolution monochromator.

CONCLUSIONS

As stated at the beginning, it was not the purpose of this work to find a theoretical treatment of the saturation broadening that would perfectly fit our experimental conditions. In fact, in order to do this, the exact spectral shape of the laser pulse and the atom profile have to be known. Nevertheless, we feel that the results obtained are useful and can, at least qualitatively, be explained by our theoretical approach.

The main results of this work may be summarized as follows:

- (i) As has been known theoretically and shown experimentally before,¹⁻⁹ the atomic profile broadens when the laser irradiance is such that saturation can be approached.
- (ii) The broadening effect is larger for higher quantum efficiency flames.
- (iii) For a pulsed, tunable dye laser (without spectral narrowing elements in the cavity), pumped by a nitrogen laser and a flame at atmospheric pressure, the broadening depends approximately upon the square root of the log of the laser irradiance.
- (iv) The halfwidth of the fluorescence excitation profile obtained at low laser powers can indeed be taken as a measurement of the laser spectral bandwidth if this bandwidth is approximately 5-10 times larger than the atom profile.

REFERENCES

1. R.H. Pantell and H.E. Putoff, "Fundamental of Quantum Electronics", Wiley, N.Y. 1969.
2. N. Omenetto, Editor: "Analytical Laser Spectroscopy", Wiley, N.Y. 1979.
- 2a. C.Th.J. Alkemade, Plenary Lecture given at the 3rd International Conference on Atomic Spectroscopy, Toronto, 1973.
- 2b. C.Th.J. Alkemade, Plenary Lecture given at the 5th International Conference on Atomic Spectroscopy, Prague, 1977.
3. E.H. Piepmeier, Spectrochim. Acta 27B, 431 (1972).
- 3a. E.H. Piepmeier, Spectrochim. Acta 27B, 445 (1972).
4. C.A. Van Dijk, Ph.D. Dissertation, Utrecht 1978.
5. N. Omenetto, P. Benetti, L.P. Hart, J.D. Winefordner, and C.Th.J. Alkemade, Spectrochim. Acta 28B, 289 (1973).
6. R.A. Van Calcar, M.J.M. Van de Ven, B.K. Van Uitert, K.J. Biewenga, Tj. Hollander, and C.Th.J. Alkemade, JQSRT 21, 11 (1979).
7. M. Omenetto and J.D. Winefordner, Progress in Analytical Atomic Spectroscopy, Vol. 2 (1,2), Pergamon 1979.
8. J.W. Hosch and E.H. Piepmeier, Appl. Spectroscopy 32, 444 (1978).
9. S. Ezekiel and F.Y. Wu, in "Multiphoton Processes", J.H. Eberly and P. Lambropoulos, Editors, Wiley, N.Y. 1978.
10. C.Th.J. Alkemade and T. Wijchers, Anal. Chem. 49, 2111 (1977).
11. R.A. Keller and J.C. Travis, Chapter 8 in N. Omenetto, Ed., "Analytical Laser Spectroscopy", Wiley, N.Y. 1979.
12. H.P. Hooymayers and C.Th.J. Alkemade, JQSRT 6, 847 (1966).
13. J.W. Dailey, Appl. Optics 18, 360 (1979).
14. H. Walther, in "Multiphoton Processes", J.H. Eberly and P. Lambropoulos, Editors, Wiley, N.Y. 1978.

15. F.Y. Wu, R.E. Grove and S. Ezekiel, Phys. Rev. Lett. 35, 1426 (1975).
16. A.B. Rodrigo and R.M. Measures, IEEE QE 9, 972 (1973).
17. J.W. Daily, Appl. Optics 17, 225 (1978).
18. J.D. Bradshaw, N. Omenetto, J.N. Bower, and J.D. Winefordner, Spectrochim. Acta B, submitted.
19. J.N. Bower, N. Omenetto, J.D. Bradshaw, and J.D. Winefordner, Spectrochim. Acta B, submitted.

APPENDIX

Derivation of Equation 16 by taking into account some spatial inhomogeneity of the laser beam.

If the laser beam is not uniform, as assumed in our derivation, its spatial energy density profile can be represented again by a gaussian expression as

$$\rho = \rho_0 \exp \left(- \frac{2 \sqrt{\ln 2}}{\delta_r} r \right)^2 \quad (A1)$$

where ρ_0 is now the integrated energy density at the peak of both the wavelength profile and the radial profile, r ($0 \leq r \leq \infty$) is the radial coordinate and δ_r is the spatial full width at half maximum of the beam. In this case, the interaction of the laser and the atoms, as given by Eq. (13), has to be modified to include the spatial dependence of the laser density.^{16,17} We therefore find for the ratio of the atom densities the following expression:

$$\frac{n_2}{n_T} = \frac{B_{12} \tau \frac{2\sqrt{\ln 2}}{\sqrt{\pi} \delta \lambda'} \exp \left[- \frac{2\sqrt{\ln 2}}{\delta \lambda'} (\lambda_\ell - \lambda_0) \right]^2 \rho_0 \exp \left(- \frac{2\sqrt{\ln 2}}{\delta_r} r \right)^2}{\left(1 + \frac{g_1}{g_2} \right) B_{12} \tau \frac{2\sqrt{\ln 2}}{\sqrt{\pi} \delta \lambda'} \exp \left[- \frac{2\sqrt{\ln 2}}{\delta \lambda'} (\lambda_\ell - \lambda_0) \right]^2 \rho_0 \exp \left(- \frac{2\sqrt{\ln 2}}{\delta_r} r \right)^2 + 1} \quad (A2)$$

which can be written in a simplified form as

$$\frac{n_2}{n_T} = \frac{B_{12} \tau g(\delta \lambda) \rho_0 \exp(-cr)^2}{\left(1 + \frac{g_1}{g_2} \right) B_{12} \tau g(\delta \lambda) \rho_0 \exp(-cr)^2 + 1} \quad (A3)$$

where

$$g(\delta \lambda) \equiv \frac{2\sqrt{\ln 2}}{\sqrt{\pi} \delta \lambda'} \exp \left[- \frac{2\sqrt{\ln 2}}{\delta \lambda'} (\lambda_\ell - \lambda_0) \right]^2, \quad c \equiv \frac{2\sqrt{\ln 2}}{\delta_r}$$

If we now proceed as in the text, introducing the saturation spectral energy density given by Eq. (15), we obtain

$$\frac{n_2}{n_T} = \left(\frac{g_2}{g_1 + g_2} \right) \left(\frac{\exp(-cr)^2}{\exp(-cr)^2 + R(\delta\lambda)} \right) \quad (A4)$$

where $R(\delta\lambda) \equiv \frac{\rho^s}{\rho_0}$.

Assuming the usual vertical monochromator slit arrangement (cylindrical volume) and a proportional variation of n_2 versus r according to the laser variation, the ratio in Eq. (A4) can be integrated over r as follows:¹⁷

$$\frac{n_2}{n_T} = \int_0^\infty \frac{\exp(-cr)^2}{\exp(-cr)^2 + R(\delta\lambda)} 2\pi r \, dr \quad (A5)$$

where the integration limit is extended to infinity since the slit height is much larger than the beam diameter. By solving the integral, we obtain

$$\frac{n_2}{n_T} = \frac{\pi}{c^2} \ln \left[1 + \frac{1}{R(\delta\lambda)} \right] \quad (A6)$$

Evaluating $\delta\lambda_{exc}$ according to the procedure adopted in the main text, we obtain

$$\delta\lambda_{exc} = (\delta)_{\frac{1}{2}}^+ + (\delta)_{\frac{1}{2}}^- = \frac{\delta\lambda'}{\sqrt{\ln 2}} \sqrt{\ln \left[\frac{\rho_0}{\rho^s \left(\sqrt{1 + \frac{\rho_0}{\rho^s}} - 1 \right)} \right]} \quad (A7)$$

which can be written as

$$\delta\lambda_{exc} = \frac{\delta\lambda'}{\sqrt{\ln 2}} \sqrt{\ln \frac{\chi}{(\sqrt{1+\chi} - 1)}} \quad (A8)$$

where $\chi \equiv (\rho_0/\rho^s)$.

In conclusion, if we compare Eq. (A8) with Eq. (16), we can see that the spatial averaging effects, if present, tend to lessen the dependence of the broadening of the spectral atom profile upon the laser power. The effect will of course be more pronounced if the laser beam is focused in the flame so to reach high irradiances. However, even in the presence of such effect, the value of $\delta\lambda'$ as obtained from Eq. (A8), is the same as that given by Eq. (16).

Table I. Experimental values of the saturation-broadened half-widths obtained for Ar-O₂-H₂ and the N₂-O₂-H₂ flames. (*)

Element	$\delta\lambda$ (A°)	
	Ar/O ₂ /H ₂	N ₂ /O ₂ /H ₂
Ca	0.61	0.44
Sr	1.24	1.25
Na	0.99	0.63
In	0.44	0.36

(*) All values are within $\pm 10\%$. Laser power: Ca, 5kw; Sr, 14kw; Na, 17kW; In, 7kW.

Table II. Comparison between the theoretical and the experimental values of the fluorescence excitation profile half-widths for Ar/O₂/H₂ and N₂/O₂/H₂ flames. (a)

Element	$[(\delta\lambda_{\text{exc}})_{\text{max}} / (\delta\lambda_{\text{exc}})_{\text{min}}]^{(b)}$			
	Theoretical (c)		Experimental	
	Ar/O ₂ /H ₂	N ₂ /O ₂ /H ₂	Ar/O ₂ /H ₂	N ₂ /O ₂ /H ₂
Ca	2.5	2.4	3.0	2.2
Sr	2.8	2.8	2.9	5.4
Na	2.4	2.0	4.3	1.6
In	1.7	1.4	2.3	1.3

(a) values are considered to be within $\pm 10\%$.

(b) $(\delta\lambda)_{\text{max}}$ refers to the value obtained with the laser at full power while $(\delta\lambda)_{\text{min}}$ refers to that obtained when the laser is attenuated with neutral density filters until the fluorescence signal is linearly related to the laser irradiance (see values reported in Table III).

(c) calculated according to Equation 16 in the text.

Table III. Comparison between the values of the laser spectral bandwidth as obtained by different methods ^(a)

Element	Direct ^(b) Measurement	Fluorescence ^(c) Excitation Profile		Saturation ^(d) Broadening	
		Ar/O ₂ /H ₂	N ₂ /O ₂ /H ₂	Ar/O ₂ /H ₂	N ₂ /O ₂ /H ₂
Ca	0.23	0.20	0.20	0.26	0.21
Sr	0.23	0.42	0.23	0.46	0.51
Na	0.36	0.23	0.40	0.30	0.35
In	0.24	0.19	0.28	0.26	0.21

(a) values are within $\pm 10\%$.

(b) values obtained by scanning the laser beam through a 1-m grating monochromator ($\Delta\lambda$ resolution = 0.12 \AA). Values are not corrected for the instrumental profile.

(c) values obtained by scanning the attenuated laser beam through the atomic vapor in the flame.

(d) values calculated from the slope of the plot obtained from Equation 16 in the text.

1

ACKNOWLEDGEMENTS

N. Omenetto would like to thank the Committee for the International Exchange of Scholars for the grant of a Fulbright travel fellowship.

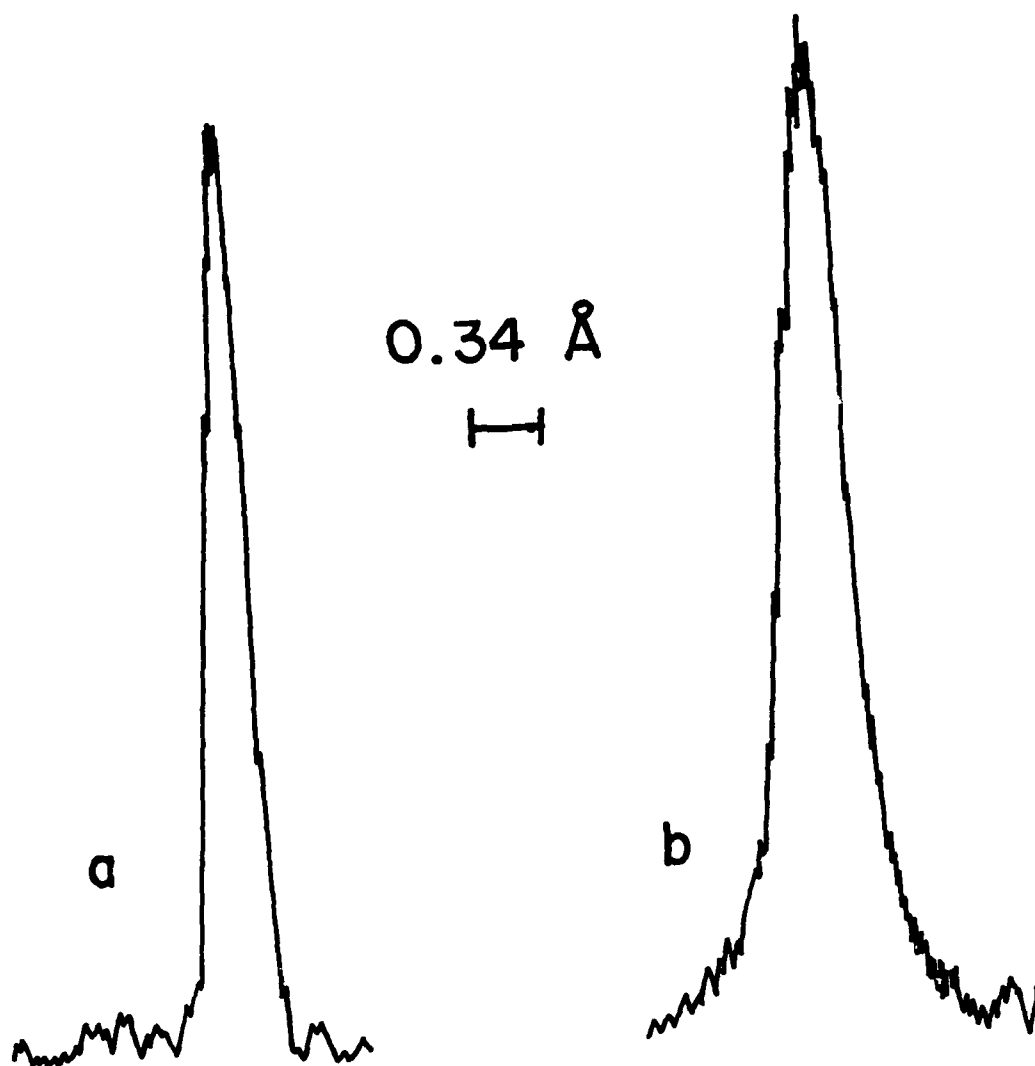


Figure 1D. Fluorescence excitation profiles for indium in the $\text{Ar/O}_2/\text{H}_2$ flame. Resonance fluorescence at 4101 \AA ; abscissa: \AA ; indium concentration in $100 \text{ }\mu\text{g/mL}$; (a) 0.37 kW ; $\delta\lambda_{\text{exc}} = 0.19 \text{ \AA}$; (b) laser power: 3.7 kW ; $\delta\lambda_{\text{exc}} = 0.37 \text{ \AA}$.

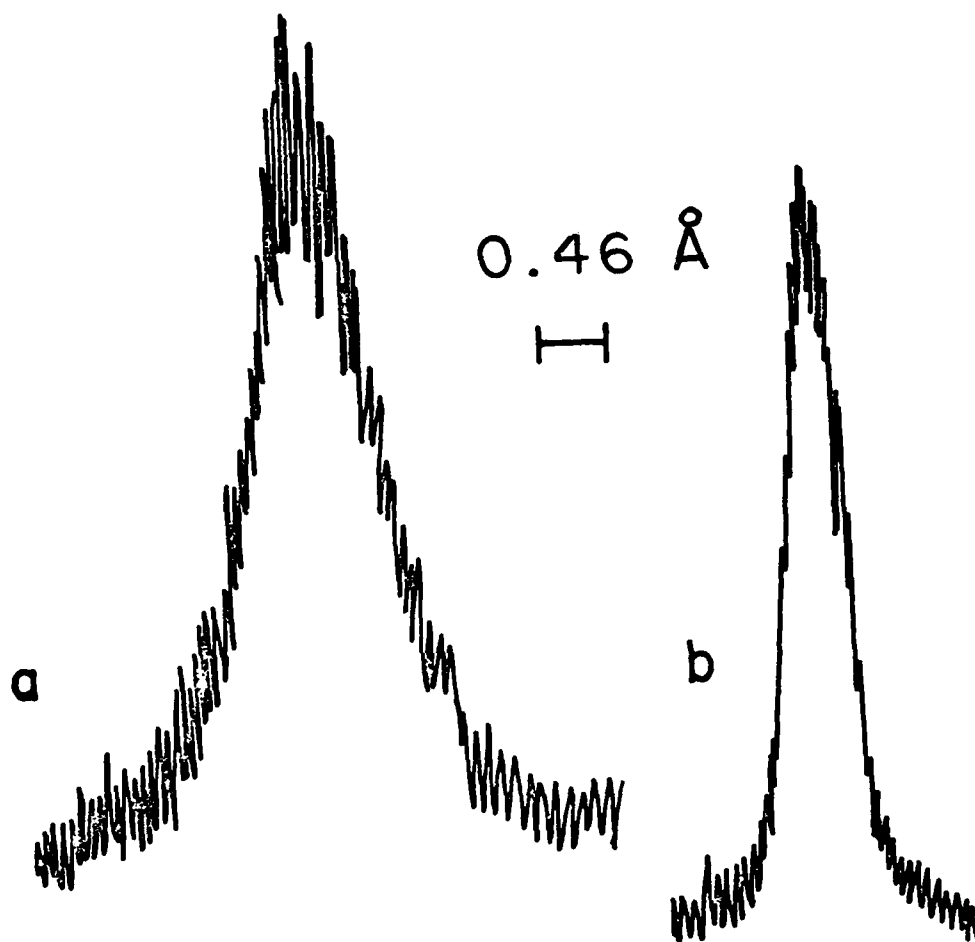


Figure 2D. Fluorescence excitation profiles for sodium in the $\text{Ar/O}_2/\text{H}_2$ flame; the resonance fluorescence is shown

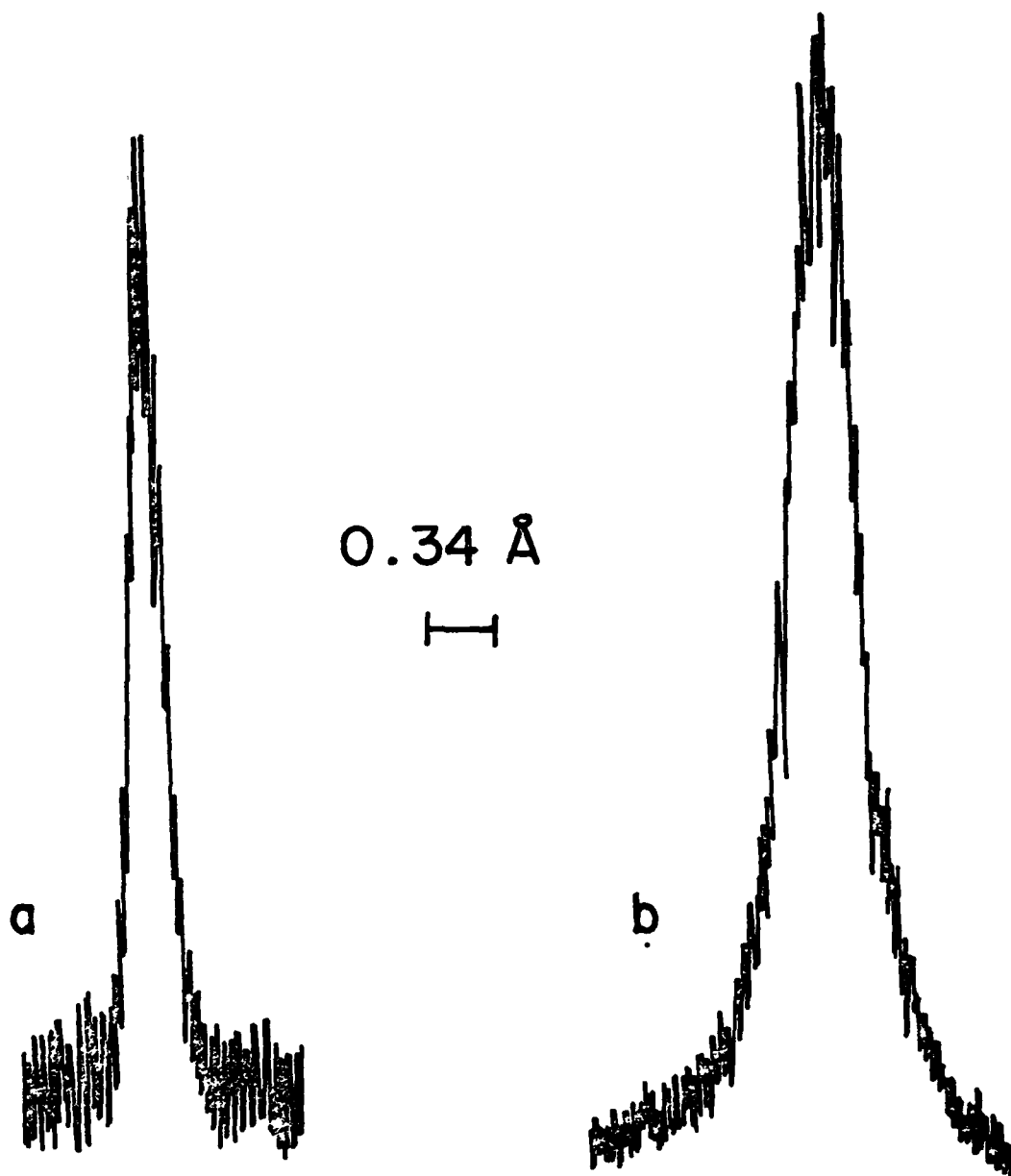


Figure 3D. Fluorescence excitation profiles for calcium in the $\text{N}_2/\text{O}_2/\text{H}_2$ flame; resonance fluorescence at 4227 Å ; abscissa: calcium concentration in $10 \text{ } \mu\text{g/mL}$; (2) laser power: 50W ; $\delta\lambda_{\text{exc}} = 0.20 \text{ Å}$; (b) laser power: 5 kW ; $\delta\lambda_{\text{exc}} = 0.44 \text{ Å}$.

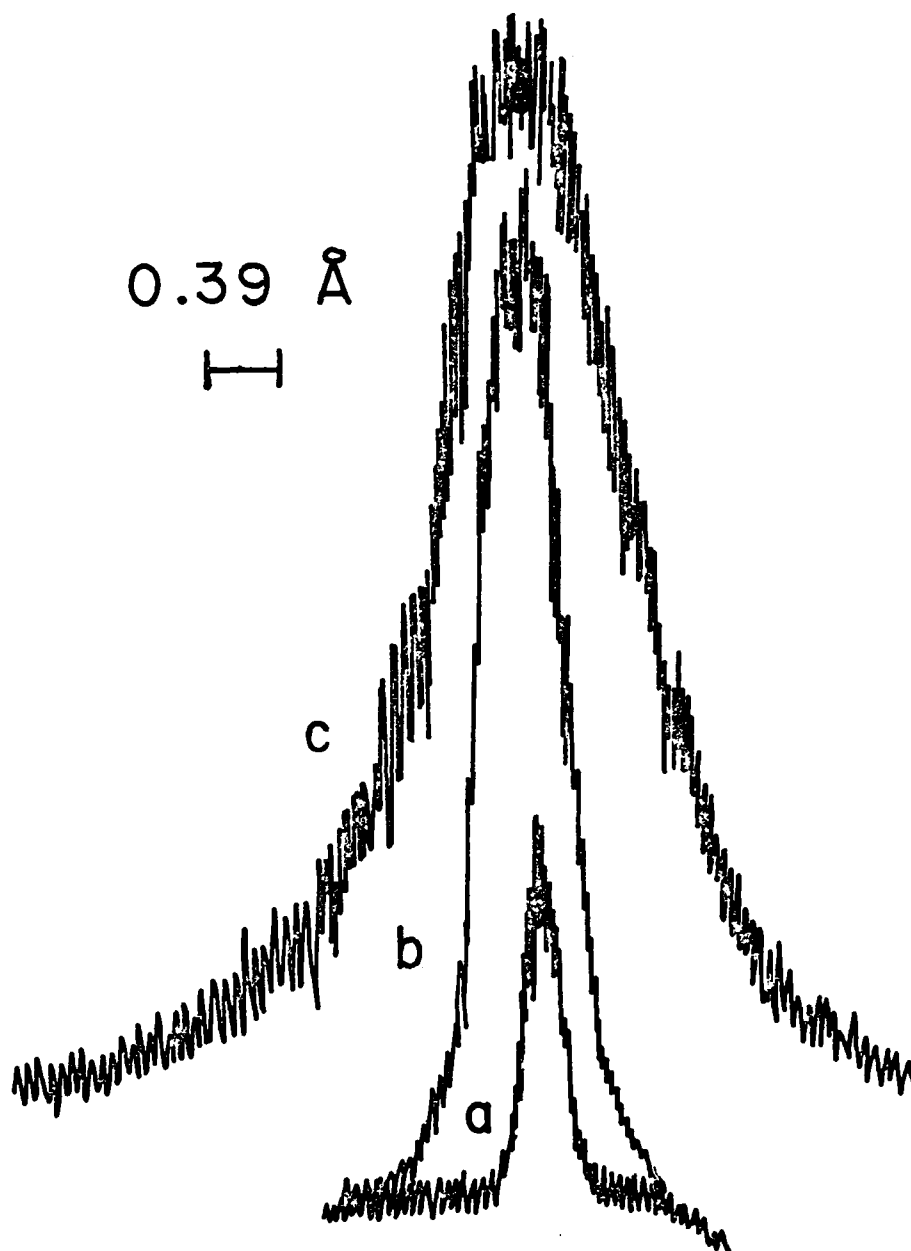


Figure 4D. Fluorescence excitation profiles for strontium in the $N_2/O_2/H_2$ flame; resonance fluorescence at 4607 \AA ; strontium concentration in $1 \mu\text{g/mL}$; (a) laser power: 14W ; $\delta\lambda_{\text{exc}} = 0.23 \text{ \AA}$; (b) laser power: 1.4 kW ; $\delta\lambda_{\text{exc}} = 0.55 \text{ \AA}$; (c) 14 kW ; $\delta\lambda_{\text{exc}} = 1.25 \text{ \AA}$.

